Developing process simulation models for red wine fermentation: Anthocyanin mass transfer and extraction

Patrick Charles Setford, BE (Chem) Hons

A thesis submitted for the degree of Doctor of Philosophy

School of Agriculture, Food and Wine

Faculty of Sciences

May 2019

TABLE OF CONTENTS

THESIS SUMMARY i

DECLARATION iii

PUBLICATIONS iv

CONFERENCES v

PANEL OF SUPERVISORS vi

ACKNOWLEDGEMENTS vii

Chapter 1. Literature Review 1

Factors affecting extraction and evolution of objective quality compounds during red wine maceration and the role of process modelling 2

Summary of research aims 17

Chapter 2. Modelling the Mass Transfer Process of Malvidin-3-Glucoside during Simulated Extraction from Fresh Grape Solids under Wine-Like Conditions 19

Chapter 3. Mass Transfer of Anthocyanins during Extraction from Pre-Fermentative Grape Solids under Simulated Fermentation Conditions: Effect of Convective Conditions 42

Chapter 4. Mathematical modelling of anthocyanin mass transfer to predict extraction in simulated red wine fermentation scenarios 61

Chapter 5. A new method for predicting the extraction of anthocyanins during red wine fermentation 76

Chapter 6. Concluding remarks and future perspectives 109

6. Concluding remarks and future perspectives 110

6.1. Summary and conclusions 110

6.1.1. Factors affecting extraction and evolution of objective quality compounds during red wine maceration and the role of process modelling 110

6.1.2. Modelling the mass transfer process of malvidin-3-glucoside during simulated extraction from fresh grape solids under wine-like conditions 111

6.1.3. Mass Transfer of anthocyanins during extraction from pre-fermentative grape solids under simulated fermentation conditions: Effect of convective conditions .. 112

6.1.4. Mathematical modelling of anthocyanin mass transfer to predict extraction in simulated red wine fermentation scenarios 113

6.1.5. A new method for predicting the extraction of anthocyanins during red wine fermentation 114

6.2. Future perspectives 115

6.2.1. Extension of mass transfer model to include other red grape phenolic compounds 115

6.2.2. Introducing post-extraction mathematical models for reactions of anthocyanins and other phenolic compounds 115

6.2.3. Rederivation and application of model for other non-grape extraction processes in winemaking 116

6.2.4. Incorporation of mass transfer model with online process control 116

6.2.5. Further developments for the current mathematical model 117

THESIS SUMMARY

Phenolic compounds extracted from grape solids during maceration are critical components responsible for the overall quality of red wine. Among these compounds are anthocyanins, which account for the red and purple pigments in young red wine that are crucial to the long-term colour stability for aging red wine. As such, understanding the variables that impact the extraction of these compounds and the mechanisms in which this process takes place are vital to the informed manipulation of red wine phenolic composition for the purposes of improving the quality or consistency of the finished product. A review of the literature presented in Chapter 1 revealed that anthocyanin extraction rate and extractability is influenced greatly by liquid phase properties (composition and temperature) as well as the available solid-liquid contact area and liquid phase velocity. This review also identified the limitations of previously developed phenolic extraction models for predicting the outcome of future extraction scenarios and explored the potential of other well-established mathematical models that could be applied to anthocyanin mass transfer during red wine maceration.

This thesis sought to establish new methods for modelling the extraction and mass transfer of anthocyanins during red wine maceration for the purposes of predicting and controlling the outcome of future winemaking scenarios. To this end, Chapter 2 describes the development of a mathematical model based on solutions to Fick's second law of diffusion, utilising mass transfer variables in both the solid and liquid phases to model the extraction of malvidin-3-glucoside (M3G), the predominant anthocyanin across all red/black grape varieties, from pre-fermentative grape solids. This model was then applied to experimental extraction curves of M3G under forced convection at liquid-phase conditions simulating various stages of red wine maceration and fermentation in order to solve for relevant mass transfer parameters. Response surface methodology was applied to the internal diffusion coefficient and distribution constants solved using this method, allowing the estimation of these parameters at varying temperature, sugar and ethanol conditions within the design of the experiment. Analysis of variance showed that both temperature and ethanol as well as their combined interaction have a significant effect on the internal diffusion rate of M3G, while all individual factors (sugar, ethanol and temperature) as well as their combined interactions significantly influenced the systems distribution constant.

Chapter 3 explores the impact of liquid-phase convection (forced and natural) on M3G extraction under simulated red wine fermentation conditions. This allowed for the calculation of the external (liquid-phase) mass transfer rate of M3G at various stages of red wine fermentation under convective conditions that more closely resemble liquid-phase conditions that occur during the

majority of a red wine maceration regime, excluding mixing operations. Calculated rates of external mass transfer under natural convective conditions showed that both internal (solid-phase) and external (liquid-phase) mass transfer limited the overall extraction rate. By combining these calculated external mass transfer coefficients with the response surface models generated in Chapter 2, predictive simulations of M3G extraction in dynamic liquid phase conditions (fermenting must) were conducted at various rates of external mass transfer. These simulations yielded previously observed but as yet undescribed extraction patterns, whereby during active fermentation the extraction rate and maximum extractability is limited by the extent of fermentation. This new insight provides a rationale for previous studies monitoring the effect of pre-fermentative maceration techniques, whereby no significant increase in anthocyanin concentration could be observed despite having a prolonged maceration period. Chapter 4 further explores the impact of liquid phase conditions on total anthocyanin extraction from a different grape variety, Pinot noir (notorious for its difficulty in achieving a high level of extracted colour), using similar methods for modelling and simulation of fermentation scenarios. Predictive simulations of fermentation scenarios were explored, highlighting the impact of controllable process conditions that can be manipulated by winemakers, including nutrient concentration and fermentation temperature.

Finally in Chapter 5, the mathematical model and mass transfer parameters determined throughout Chapters 2-4 were applied to real world fermentations under both laboratory and industry scale conditions in order to validate the models' predictive capabilities under various conditions. Predictive simulations of anthocyanin extraction in this study showed good agreement with commercial red wine fermentations indicating the models robust ability to predict extraction profiles using a relatively small amount of fermentation data. These simulations represent a significant step forward towards the ultimate goal of process control of red wine phenolic extraction during fermentation.

Collectively, this thesis enhances the understanding of the extractive behaviour of anthocyanins during red wine production, quantifying the impact of process variables that can be manipulated by winemakers and those that change as a result of fermentation. The mathematical models developed in this study could be used to predict the anthocyanin extraction potential in future red wine maceration scenarios based on fruit composition, providing new opportunities for real-time process control, equipment design, optimisation of product quality, and efficient use of fermentation infrastructure.

DECLARATION

I certify that this work contains no material which has been accepted for the award of any other degree or diploma in my name, in any university or other tertiary institution and, to the best of my knowledge and belief, contains no material previously published or written by another person, except where due reference has been made in the text. In addition, I certify that no part of this work will, in the future, be used in a submission in my name, for any other degree or diploma in any university or other tertiary institution without the prior approval of the University of Adelaide and where applicable, any partner institution responsible for the joint-award of this degree.

I acknowledge that copyright of published works contained within this thesis resides with the copyright holder(s) of those works.

I also give permission for the digital version of my thesis to be made available on the web, via the University's digital research repository, the Library Search and also through web search engines, unless permission has been granted by the University to restrict access for a period of time.

I acknowledge the support I have received for my research through the provision of an Australian Government Research Training Program Scholarship.

21/05/2019

Patrick C. Setford — Date

PUBLICATIONS

This thesis is comprised of a series of manuscripts that were published in *Trends in Food Science & technology*, *Molecules* and *Food Research International* during candidature, as well as a manuscript submitted to *Food and Bioprocess Technology* prior to thesis submission for examination. The impact factor of *Trends in Food Science & Technology* was 6.609 in 2017 and the 5 year impact factor was 7.819. The impact factor of *Molecules* was 3.098 in 2017 and the 5 year impact factor was 3.268. The impact factor for *Food Research International* was 3.520 in 2017 and the 5 year impact factor was 4.196.

The text in chapters 1 to 5 appear in a different format due to the specific requirements of each journal. A statement of authorship for each manuscript, published or otherwise, is included at the start of each chapter outlining individual author contributions to the work.

The following peer reviewed publications form the basis of this thesis:

Chapter 1. Setford, P. C., Jeffery, D. W., Grbin, P. R., Muhlack, R. A. (2017). Factors affecting extraction and evolution of phenolic compounds during red wine maceration and the role of process modelling. *Trends in Food Science & Technology*, 69, Part A, 106-117

Chapter 2. Setford, P. C., Jeffery, D. W., Grbin, P. R., Muhlack, R. A. (2018). Modelling the Mass Transfer Process of Malvidin-3-Glucoside during Simulated Extraction from Fresh Grape Solids under Wine-Like Conditions. *Molecules*, 23, 2159

Chapter 3. Setford, P. C., Jeffery, D. W., Grbin, P. R., Muhlack, R. A. (2019). Mass Transfer of Anthocyanins during Extraction from Pre-Fermentative Grape Solids under Simulated Fermentation Conditions: Effect of Convective Conditions. *Molecules*, 24, 73

Chapter 4. Setford, P. C., Jeffery, D. W., Grbin, P. R., Muhlack, R. A. (2019). Mathematical Modelling of Anthocyanin Mass Transfer to Predict Extraction in Simulated Red Wine Fermentation Scenarios. *Food Research International*, 121, 705-713.

Chapter 5. Setford, P. C., Jeffery, D. W., Grbin, P. R., Muhlack, R. A. (2019). A new method for predicting the extraction of anthocyanins during red wine fermentation.; submitted to *Food and Bioprocess Technology*.

CONFERENCES

American Society for Enology and Viticulture Conference 2018, Monterey, California

Presented a flash talk and poster titled “Mathematical modelling of anthocyanin mass transfer to predict extraction in simulated red wine fermentation scenarios”.

CRUSH – The grape and wine science symposium 2017, Adelaide, SA

Presented a talk titled “Developing process simulation models for objective red wine quality parameters during fermentation”.

The Bioprocess Network Annual Conference 2017, Adelaide, SA

Presented a talk titled “Developing process simulation models for objective red wine quality parameters during fermentation” and received the “Early Career Researcher Award” (sponsored by St. Gobain).

The University of Adelaide School of Agriculture, Food and Wine Postgraduate Symposium 2016, Adelaide, SA

Presented a talk titled “Developing process simulation models for objective red wine quality parameters during fermentation”.

PANEL OF SUPERVISORS

Principal supervisor:

Associate Professor David Jeffery

School of Agriculture, Food and Wine

The University of Adelaide

Co-supervisor:

Dr Richard Muhlack

School of Agriculture, Food and Wine

The University of Adelaide

Co-Supervisor:

Associate Professor Paul Grbin

School of Agriculture, Food and Wine

The University of Adelaide

Independent adviser:

Professor Roger Boulton

Department of Chemical Engineering

University of California

ACKNOWLEDGEMENTS

I would first like to thank my supervisor Dr. Richard Muhlack, without whom I would never have had the opportunity to undertake a PhD. Thank you for your unwavering support, guidance, enthusiasm, hard work and patience throughout this project. I'm genuinely honoured to have had you as a mentor and friend and am forever grateful for everything you've done – I couldn't have asked for a better supervisor to have guided me through this journey.

My sincerest thanks go also to Associate Professor David Jeffery whose good humour made coming into Uni each day all the easier and whose critical analysis and academic guidance ensured the quality of each and every aspect of this project. Thank you for acting as my principal supervisor and for teaching me the value of hard work.

To my co-supervisor Associate Professor Paul Grbin, thank you for your time, expertise and invaluable advice throughout this project. Your input during discussions on experimental design and feedback during writing are very greatly appreciated and significantly improved the quality of the work.

I would like also to thank Professor Roger Boulton from the Department of Chemical Engineering, University of California, Davis for acting as the independent advisor on this project and for sharing your knowledge with me. Your dedication enthusiasm for research is truly inspirational and I'm so grateful to have had the opportunity to learn from you.

I would like to acknowledge also the financial support of Wine Australia and The University of Adelaide for providing funding for project which allowed me to pursue this opportunity and opened up many doors for the future. Thank you also to the staff at Pernod Ricard Winemakers for providing fermentation samples, allowing for the validation of mathematical models developed in this project.

I'm extremely grateful also to my friends and colleagues for their encouragement throughout this project. In particular, I would especially like to thank Liang Chen for his assistance picking grapes, helping in the lab and for enduring seemingly endless brewery visits in California – it was a once in a lifetime experience.

To my Mum, Susan Setford, and Dad, Lyndon Setford – I can't thank you enough for everything you've done for me. For your unconditional love, support and encouragement and for always providing me a home. You have made me the person I am today, and I'm forever grateful for everything you've ever done for me. To my sister and brother in law, Meghan and Michael Douglass, thank you for your encouragement throughout this process.

My final thankyou goes to my beautiful partner, Jacinta Uznik. For all the lunches and coffees, for all the hours staying awake with me when sleep was impossible, for coming into Uni with me in the middle of the night to collect samples and for making me a better person from your love, I'm eternally grateful. You're the reason I've made it this far and no words will ever do justice how much you mean to me, I love you forever.

This thesis is dedicated to my grandfather, Geoffrey Frank Wilsdon,

who always told me I could be an Engineer…

CHAPTER 1

LITERATURE REVIEW

The literature review for this thesis is covered in a review article on the factors affecting extraction and evolution of phenolic compounds during red wine maceration and the role of process modelling. This article was prepared in the first 18 months of candidature and covers literature relevant to the project up to June 2017. Relevant literature beyond this date has been included in the introductions of Chapters 2 to 5. A summary of the research aims and objectives is included at the end of this chapter.

Factors affecting extraction and evolution of objective quality compounds during red wine maceration and the role of process modelling

Patrick C. Setford[1], David W. Jeffery[1,2], Paul R. Grbin[1], Richard A. Muhlack[1,*]

[1] Department of Wine and Food Science, School of Agriculture, Food and Wine, The University of Adelaide (UA), PMB 1 Glen Osmond SA 5064, Australia

[2] The Australian Research Council Training Centre for Innovative Wine Production, The University of Adelaide, PMB 1 Glen Osmond SA 5064, Australia

Trends in Food Science & Technology - **2017**, 69, 106-117

Statement of Authorship

Title of Paper	Factors affecting extraction and evolution of phenolic compounds during red wine maceration and the role of process modelling
Publication Status	☑ Published ☐ Accepted for Publication ☐ Submitted for Publication ☐ Unpublished and Unsubmitted work written in manuscript style
Publication Details	Setford, P. C., Jeffery, D. W., Grbin, P. R., & Muhlack, R. A. (2017). Factors affecting extraction and evolution of phenolic compounds during red wine maceration and the role of process modelling. Trends in Food Science & Technology, vol. 69, Part A, pp. 106-117.

Principal Author

Name of Principal Author (Candidate)	Patrick C. Setford		
Contribution to the Paper	Read and reviewed all relevant literature to this article, prepared entire first draft of the manuscript and helped address reviewer comments.		
Overall percentage (%)	70%		
Certification:	This paper is a review on original research that was conducted during the period of my Higher Degree by Research candidature and is not subject to any obligations or contractual agreements with a third party that would constrain its inclusion in this thesis. I am the primary author of this paper.		
Signature		Date	7/5/19

Co-Author Contributions

By signing the Statement of Authorship, each author certifies that:

i. the candidate's stated contribution to the publication is accurate (as detailed above);

ii. permission is granted for the candidate in include the publication in the thesis; and

iii. the sum of all co-author contributions is equal to 100% less the candidate's stated contribution.

Name of Co-Author	David W. Jeffery		
Contribution to the Paper	Contributed to the conception of the article, critically reviewed and edited the manuscript and helped address reviewer comments.		
Signature		Date	7/5/19

Name of Co-Author	Paul R. Grbin		
Contribution to the Paper	Contributed to the conception of the article, critically reviewed and edited the manuscript and helped address reviewer comments.		
Signature		Date	13/5/19

Name of Co-Author	Richard A. Muhlack		
Contribution to the Paper	Contributed to the conception of the article, supervised the work, helped prepare, edit and critically review the manuscript and helped address reviewer comments. Acted as the corresponding author.		
Signature		Date	7·5·2019

Please cut and paste additional co-author panels here as required.

Trends in Food Science & Technology 69 (2017) 106–117

Contents lists available at ScienceDirect

Trends in Food Science & Technology

journal homepage: http://www.journals.elsevier.com/trends-in-food-science-and-technology

Review

Factors affecting extraction and evolution of phenolic compounds during red wine maceration and the role of process modelling

Patrick C. Setford [a], David W. Jeffery [a, b], Paul R. Grbin [a], Richard A. Muhlack [a, *]

[a] Department of Wine and Food Science, School of Agriculture, Food and Wine, The University of Adelaide (UA), PMB 1 Glen Osmond, SA 5064, Australia
[b] The Australian Research Council Training Centre for Innovative Wine Production, The University of Adelaide, PMB 1 Glen Osmond, SA 5064, Australia

ARTICLE INFO

Article history:
Received 12 September 2016
Received in revised form
20 August 2017
Accepted 19 September 2017
Available online 21 September 2017

Keywords:
Phenolic extraction
Mass transfer
Diffusion
Anthocyanin
Tannin

ABSTRACT

Background: The overall quality of red wine is well known to be influenced markedly by various phenolic compounds that are extracted from the grape solids during maceration. The concentration and composition of phenolics then impact the flavour and mouthfeel of wines.
Scope and Approach: This review analyses the available literature on specific process variables that influence the diffusive mass transfer and evolution of phenolic compounds during red wine maceration. These variables are discussed in terms of techniques and strategies used by winemakers to influence the extractive behaviour of phenolic compounds and control their concentration in the finished wine. Mathematical models used to describe extraction and evolution phenomena in wine are also examined and the potential for future models to predict phenolic behaviour is discussed.
Key Findings and Conclusions: The impact of various winemaking techniques aimed at improving the extraction of phenolic compounds during red winemaking, as well as the subsequent reactions that take place following extraction, are qualitatively well understood. Mathematically, many of these techniques can be described in terms of their changing process variables such as temperature, solvent conditions and sold-liquid contact. Despite this, non-steady state models for mass transport or reaction kinetics of phenolic compounds in wine fermentation are currently unavailable in published literature. Further research into the production of global models capable of accurately describing this behaviour would be a significant advancement for industry and would aid in the development of adaptive process control technologies for red wine phenolic composition.

1. Introduction

Fermentation is the most critical value adding activity in the winemaking process, with significant technical, equipment and human resource demands associated with the process (Muhlack, Scrimgeour, Wilkes, Godden, & Johnson, 2013). Although ethanol is the main product of wine fermentation, the concentration and composition of phenolic compounds such as tannins and anthocyanins, as well as aroma and flavour components specific to grape varieties and those introduced by yeast, wood contact, and aging processes, have the greatest influence on the overall sensorial quality of the finished wine (Bisson & Karpel, 2010; Cheynier et al., 2006; Garde-Cerdán & Ancín-Azpilicueta, 2006; González-Barreiro, Rial-Otero, Cancho-Grande, & Simal-Gándara, 2015; Somers & Evans, 1974). As such, understanding the impact of parameters that affect the concentration of these compounds during winemaking is vital to producing a final product of desired quality and composition. Although each grape variety has specific phenolic compounds that can drastically change the characteristics of the resulting wine, anthocyanins and proanthocyanidins are two of the most important classes of phenolic compounds that affect red wine quality (Cheynier et al., 2006) and as such will be the focus of this review.

1.1. Anthocyanins

Anthocyanins are the chemical components of red grapes and wines that predominantly account for red and purple pigments (Bindon, Kassara, Hayasaka, Schulkin, & Smith, 2014; Gómez-Plaza, Gil-Muñoz, López-Roca, Martínez-Cutillas, & Fernández-Fernández, 2001). For the majority of red grape varieties, the synthesis of these molecules occurs exclusively in the grape skins beginning at véraison (the onset of ripening) and continues to

* Corresponding author.
E-mail address: richard.muhlack@adelaide.edu.au (R.A. Muhlack).

https://doi.org/10.1016/j.tifs.2017.09.005
0924-2244/

accumulate throughout the ripening process (Bindon, Kassara, et al., 2014; Canals, Llaudy, Valls, Canals, & Zamora, 2005) (Fig. 1). Although the proportion of different anthocyanins varies depending on many factors including the grape variety and growing region, there are five central anthocyanidins (aglycones) – malvidin, cyanidin, peonidin, petunidin and delphinidin – that act as the chromophores of their associated anthocyanins (i.e., the 3-*O*-β-D-glucosides) in wine (Cheynier et al., 2006; Gao, Girard, Mazza, & Reynolds, 1997; Gómez-Plaza et al., 2001). Despite the varying concentrations of these compounds among grape varieties, malvidin-3-glucoside is generally the most abundant anthocyanin, accounting for greater than 40% of the total anthocyanin concentration (He et al., 2012).

During the maceration phase of red winemaking, where the grape solids remain in contact with the juice, anthocyanins are extracted from the skins through a diffusive process and their concentrations decrease after several days of contact when the rate of anthocyanins undergoing various reactions (described later) exceeds the extraction rate. This process can be well described by a two-term extraction model with an initial fast extraction followed by a slower decrease to its final value (Boulton, Singleton, Bisson, & Kunkee, 1996; Somers & Evans, 1979) as shown in Fig. 2a and described by Equation (1).

$$\frac{d[A]}{dt} = k_1[A_1 - A] - k_2[A - A_2] \quad (1)$$

where $[A]$ is the concentration of anthocyanins in the wine at time t, A_1 and k_1 are the maximum value and rate constant for the initial irreversible extraction and A_2 and k_2 are the equilibrium value and rate constant for the second equilibrium stage resulting from a series of physical and chemical reactions (discussed later). A similar model was used by Zanoni, Siliani, Canuti, Rosi, and Bertuccioli (2010), however the initial anthocyanin concentration was included in the model and the degradation step was modelled as continuously decreasing during maceration without reaching a final value, described by Equation (2).

$$\frac{d[A]}{dt} = k_1[A_1 - A] - k_2 \quad (2)$$

Whereas ripeness is the main factor that affects anthocyanin accumulation in grape skin, poor extraction can result in wines lacking in colour even if skin anthocyanin concentrations are relatively high (Canals et al., 2005). Once extracted, reactions involving anthocyanins are important to red wine colour and studies undertaken to determine the main factors responsible for the decrease in anthocyanin concentration that occurs during red wine fermentation, will be discussed in this review.

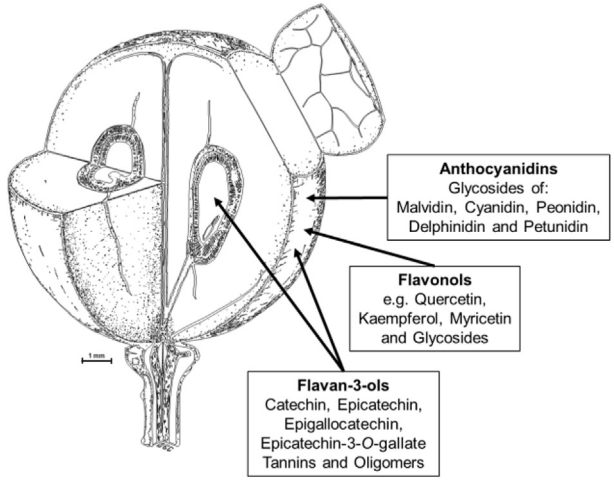

Fig. 1. Location of objective quality compounds in red grapes, adapted from Coombe (1987) ©1987 American Society for Enology and Viticulture. AJEV 38:120–127.

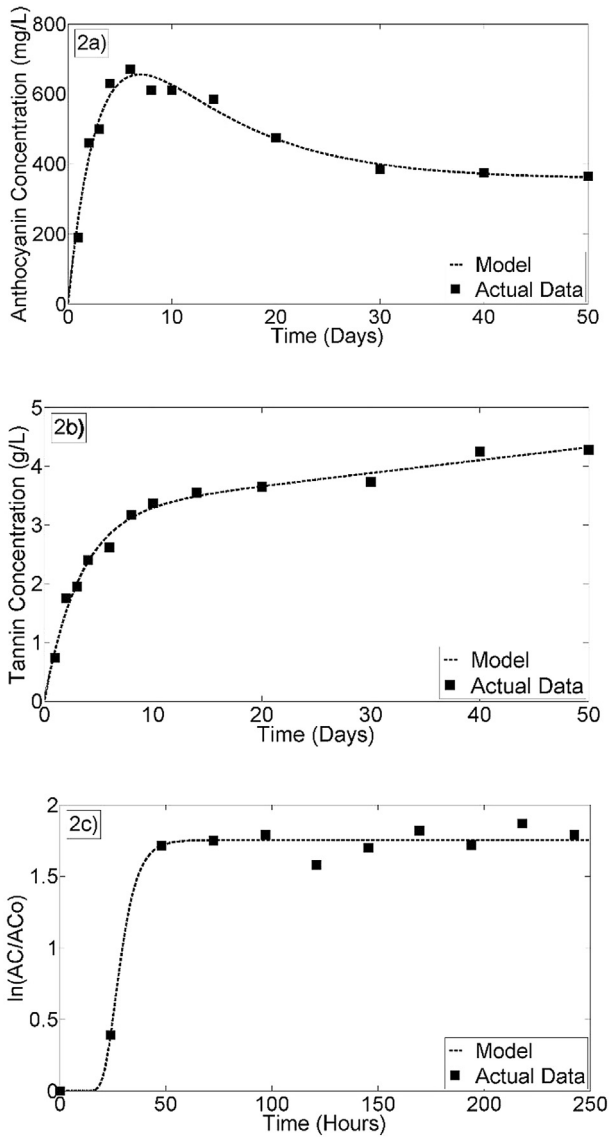

Fig. 2. Examples of commonly used regression models to fit red wine maceration data for the evolution of (a) anthocyanins, (b) proanthocyanidins and (c) polymeric pigments. Data from Ribéreau-Gayon (1964) (a, b) and Zanoni et al. (2010) (c).

1.2. Proanthocyanidins

Proanthocyanidins, also known as condensed tannins include procyanidins and prodelphinidins which are polymers of monomeric flavan-3-ol (catechin) subunits. The concentrations of these molecules in wine have a significant impact on sensory attributes directly associated with quality, such as astringency and mouthfeel (Busse-Valverde, Bautista-Ortín, Gómez-Plaza, Fernández-Fernández, & Gil-Muñoz, 2012; McRae & Kennedy, 2011) due to their ability to precipitate proteins of saliva (Cheynier et al., 2006; Vidal et al., 2003). In addition to their sensorial impact in wine, the potential nutraceutical properties of proanthocyanidins and

their monomers in areas including immunomodulatory, anticancer, antioxidant, anti-inflammatory, antithrombotic and cardio-protective effect have led to an increase in research attention being paid (Smeriglio, Barreca, Bellocco, & Trombetta, 2017). Unlike anthocyanins, which are synthesised and located exclusively in the skin, proanthocyanidins are found in the vacuoles of skin cells as well as the inner and outer integuments of the seeds (Hernández-Jiménez, Kennedy, Bautista-Ortín, & Gómez-Plaza, 2012) (Fig. 1). The size and structure of proanthocyanidins in wine is heavily dependent on the location from which they originate within the grape. Proanthocyanidins extracted from the skins of grapes contain higher levels of epigallocatechin and are less rich in (-)-epicatechin-3-*O*-gallate (Bindon & Kennedy, 2011). In addition, the average molecular mass of skin tannins is substantially higher than that of seed tannins, meaning they exhibit a higher mean degree of polymerisation (Bindon, Kassara, et al., 2014). These structural differences are important from both an analytical and sensory point of view, as they allow for estimating the proportion of proanthocyanidins extracted from the skins and seeds (Busse-Valverde, Gómez-Plaza, López-Roca, Gil-Munoz, & Bautista-Ortín, 2011), which in turn impacts on astringent sub-qualities of wine (Gawel, Francis, & Waters, 2007; Vidal et al., 2003).

As with anthocyanins, proanthocyanidins are extracted from the grape solids into the must (crushed solids and grape juice) during the maceration process, however the kinetics of their evolution in wine differ significantly. Modelling of proanthocyanidin concentration during extraction indicates there is a diffusion process dependent on the concentration of tannin already in the wine as well as a dissolution process that is independent of concentration. A two-term extraction model with first and zero order terms can be used to accurately fit experimental data for both tannin extraction during red wine maceration (Boulton et al., 1996) and the total phenolic index (Zanoni et al., 2010). Mathematically, this two-term extraction model can be represented by Equation (3) and the general shape is shown by Fig. 2b.

$$\frac{d[T]}{dt} = k_3[T_1 - T] + k_4 \tag{3}$$

where $[T]$ is the concentration of tannin in the wine at time t, T_1 is the equilibrium concentration of the diffusion extraction step and k_3 and k_4 are the rate constants for the diffusion and dissolution steps, respectively.

The apparent existence of two separate extraction processes has been attributed to tannin being extracted from both the grape skins and the seeds (Boulton et al., 1996). A newer analytical technique known as phlorogluconolysis (whereby the condensed tannins are cleaved via acid-catalysis in the presence of phloroglucinol and the product is analysed using HPLC) allowed this to be verified, with the diffusive term attributed to extraction from the skins and the dissolution term attributed to extraction from the seeds (Cerpa-Calderón & Kennedy, 2008). González-Manzano, Rivas-Gonzalo, and Santos-Buelga (2004) found a similar pattern when extracting flavan-3-ols from grape skin and seeds into a 12.5% ethanol solution. Their results did not, however, show the apparent lag phase described by Cerpa-Calderón and Kennedy (2008). This difference is likely due to the ethanol concentration being constant throughout the extraction, whereas the ethanol concentration gradually increases over time during fermentation. The reason for seed tannin extraction presenting itself as a dissolution process (or one which exhibits an initial lag phase) is likely due to the required disorganisation of the outer lipidic cuticle surrounding the seeds, which is assisted by higher alcohol concentrations (Hernández-Jiménez et al., 2012).

1.3. Derived pigments

Unlike anthocyanins and proanthocyanidins, the evolution of derived pigments during fermentation is not the direct result of solid-liquid extraction. As one type of derived wine pigment, polymeric pigments begin forming during fermentation as a condensation reaction between anthocyanins and wine components, especially tannins (Cheynier et al., 2006; Levengood & Boulton, 2004; Singleton & Trousdale, 1992). Although anthocyanin-tannin reactions are thought to be the largest contributors to polymeric pigments (Fig. 3), reactions with other co-factors have been shown to result in other wine pigments. Anthocyanin polymers and pyranoanthocyanins result from the condensation of yeast metabolites with anthocyanins, and caftaric acid-anthocyanin adducts are formed through enzymatic oxidation reactions (Bautista-Ortín, Martínez-Hernández, Ruiz-García, Gil-Muñoz, & Gómez-Plaza, 2016; Boulton, 2001). These “new” pigments play an important role in wine from a quality standpoint, helping to maintain wine colour in the long term after bottling. During aging, the colour of young red wines with a purple tint (due primarily to monomeric grape anthocyanins) changes to that of a tawny or brick-red tint (as a result of incorporation of anthocyanins into derived pigments). As well as this colour change, the decreasing astringency that occurs during aging has also been attributed to the formation of polymeric pigments (Cheynier et al., 2006).

Zanoni et al. (2010) found that the reaction to form polymeric pigments can be well characterised as having three separate phases: a lag phase, an exponential formation phase and a stationary phase; the kinetics of this reaction can be mathematically described by a sigmoidal kinetic model described by Equation (4) and displayed in Fig. 2c.

$$ln\frac{AC_t}{AC_0} = AC_\infty \exp\left(- exp\left(\frac{k_{AC} \times 2.718}{AC_\infty}\left(t_{lag} - t\right) + 1\right)\right) \tag{4}$$

where AC_t is the instantaneous pigmented polymer concentration, AC_0 is the initial pigmented polymer content, AC_∞ is the potential maximum pigmented polymer concentration, k_{AC} is the first-order rate constant for the exponential pigmented polymer formation phase and t_{lag} is the lag time before the exponential formation phase.

These forms of kinetic models are very effective at fitting experimental data and can be used to give a great deal of insight into the effect of changing process conditions by comparing with one another the extraction and transformation kinetics between a series of ferments. However, they are limited in their ability to quantitatively predict the effect that changing process conditions such as temperature, solvent concentration, mixing operations and subsequent reactions post-extraction would have on the extraction and transformation kinetics of phenolic compounds and their final concentrations in a future ferment. Fig. 4 presents a summary of the main factors affecting phenolic concentration that will be discussed. Overall, this review aims to compare and evaluate findings reported for the impact of specific process variables on the extractive behaviour of phenolic compounds in wine, with particular attention being paid to mathematical models used to describe these processes. Various techniques employed by winemakers to alter the extraction of phenolic compounds are also compared and related to the specific process variables that they directly impact.

2. Physical factors affecting phenolic extraction

During the winemaking process, phenolic compounds are extracted from the berry solids (the skins and seeds) into the must

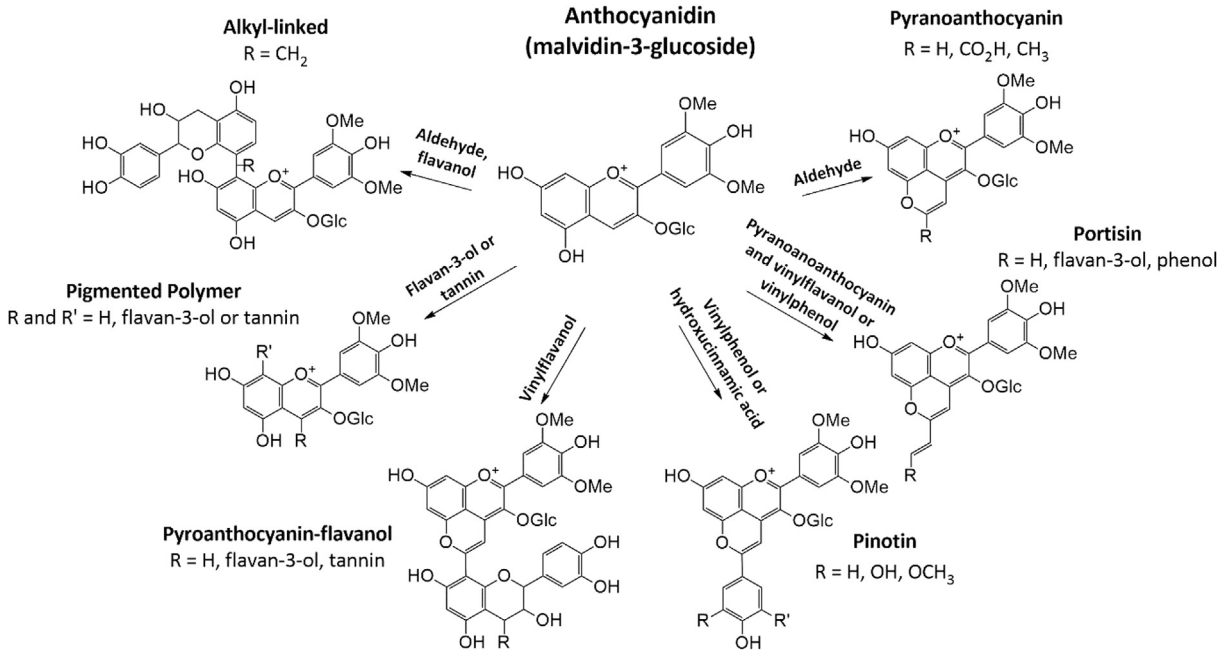

Fig. 3. Anthocyanin reactions occurring during the winemaking process.

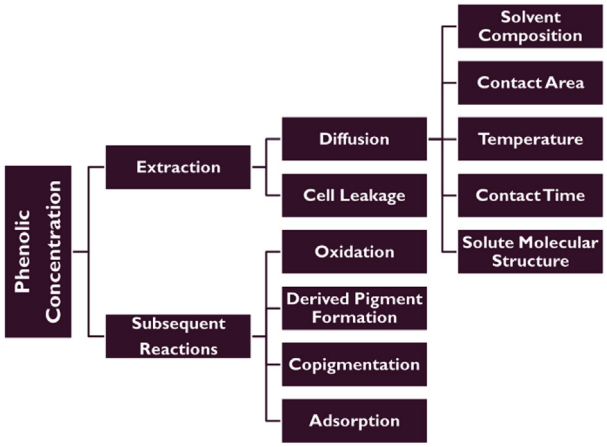

Fig. 4. Summary of factors affecting phenolic concentration.

via two main mechanisms: a semi-instantaneous initial leakage from the edges of broken skin cells that occurs at crushing, and a slower concentration-driven diffusion across the solid layers that occurs throughout the maceration period (Cerpa-Calderón & Kennedy, 2008; Sparrow, Smart, Dambergs, & Close, 2015). In general, the extraction of a solute from porous botanical particles to the bulk of the solvent during a concentration-driven diffusion process involves four steps (Gertenbach, 2001):

1. Solvent diffusion into the porous solid
2. Solute dissolution into the solvent
3. Dissolved solute diffusion to the particle surface
4. Dissolved solute diffusion from the particle surface to the surrounding solvent

As shown in Fig. 5, Steps 1, 2 and 3 encapsulate internal diffusion, which occurs independently of mixing. In general, steps 1 and 3 are rate limiting for the majority of phenolic compounds during the diffusion stage of extraction due to the physical structure of plant materials, which give a natural resistance to liquid penetration and dissolved solute movement within the plant (Cissé et al., 2012; Gertenbach, 2001).

This extraction process can be well described by Fick's second law of diffusion where the rate of diffusion is a function of the solute concentration gradient and the internal diffusion coefficient. For a system where the internal diffusivity remains constant and obeys Fick's second law, the one-dimensional extraction for planar and radial extraction of spherical particles is represented as:

$$\frac{\partial C}{\partial t} = D\frac{\partial^2 C}{\partial x^2} \tag{5}$$

where C is the instantaneous solute concentration, D is the diffusion coefficient and x is the distance of internal diffusion. In a diffusion controlled process where the phenolic compounds move from a region of high concentration to that of a lower concentration within the solid, there are several process variables that are likely to have an impact on the overall rate of extraction by influencing the internal and external rates of diffusion. These factors include solvent composition, temperature, and available surface area (Cerpa-Calderón & Kennedy, 2008).

2.1. Solvent composition

At increased concentrations of ethanol and sulfur dioxide (SO_2) in water, the relative permittivity (dielectric constant) of the solvent is decreased, which lowers the solvation of molecules (Cacace & Mazza, 2003; Karacabey & Mazza, 2008). Therefore, an increase in the concentration of these molecules in the solvent would be expected to lessen their interactions with solute molecules and increase the rate of internal diffusion. Previous kinetic models such as those proposed by Amendola, De Faveri, and Spigno (2010), Andrich, Zinnai, Venturi, and Fiorentini (2005), Bucić-Kojić, Planinić, Tomas, Bilić, and Velić (2007) and Zanoni et al. (2010) have used a fixed value for the extraction rate constant when modelling phenolic extraction. However, because the solid grape

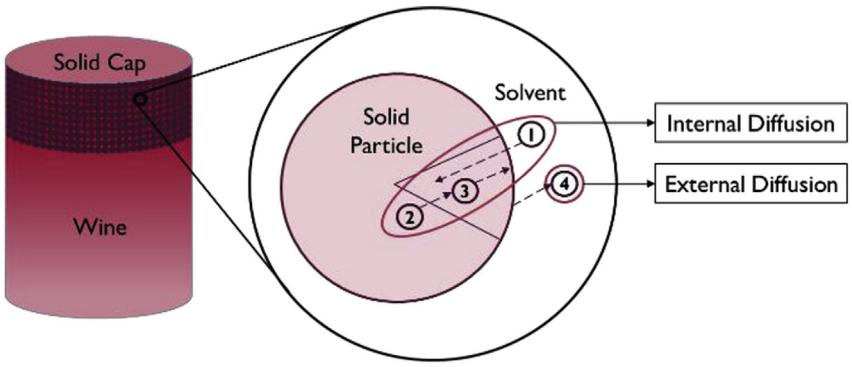

Fig. 5. Mechanisms of internal and external diffusion during fermentative maceration, depicted for a red wine fermentation in a stainless steel tank. Step 1: Solvent diffusion into the porous solid, Step 2: Solute dissolution into the solvent, Step 3: Dissolved solute diffusion to the particle surface, Step 4: Dissolved solute diffusion from the particle surface to the surrounding solvent. (For interpretation of the references to colour in this figure legend, the reader is referred to the web version of this article.)

pomace is in a solvent that has a continuously increasing ethanol concentration, the internal diffusion coefficient would not be expected to remain the same during fermentation (González-Manzano et al., 2004).

González-Manzano et al. (2004) studied the extraction of flavon-3-ols of white grape pomace using simulated maceration of grape skin and seeds at varying ethanol concentrations (0%, 5% and 12.5% ethanol by volume) and showed a clear positive trend of flavanol extraction rate with increasing ethanol concentration. However because the time of maceration was limited to five hours, it was unclear whether ethanol concentration impacted the final equilibrium concentration of flavanols or simply the rate of extraction. In a similar study, Canals et al. (2005) observed the extraction behaviour of phenolic compounds from grape skin and seed during maceration in liquid media of differing ethanol concentrations as well as at different stages of berry ripening. Their results showed a clear increase in the extent of anthocyanin and proanthocyanidin extraction at ethanol concentrations similar to wine (13% by volume) compared to that of unfermented grape juice (0% by volume).

Whereas ethanol concentration has a significant impact on both the rate and extent of phenolic extraction, SO_2 at levels normally associated with red wine fermentation appear to have a much lower effect (Sacchi, Bisson, & Adams, 2005). Watson, Price, and Valladao (1995) found that there were no significant differences in anthocyanin concentration at initial SO_2 concentrations of 0, 50 and 100 mg/L. In a similar study, Bakker et al. (1998) reported that SO_2 had only a minor effect on the extraction of anthocyanins and total phenolics at concentrations of 0, 75 and 150 mg/L.

2.2. Temperature

Temperature plays a significant role in the extraction of phenolic compounds during fermentative maceration as it influences the permeability of the cell membranes in the grape solids (Koyama, Goto-Yamamoto, & Hashizume, 2007) and enhances the solubility of phenolic compounds, thus affecting the internal diffusion coefficient (Cacace & Mazza, 2003). Because the temperature of the system impacts heavily on the rate of fermentation (and thus the rate of ethanol production) (Boulton, 2001; Coleman, Fish, & Block, 2007; Cramer, Vlassides, & Block, 2002; O'Neill, van Heeswijck, & Muhlack, 2011), it also has a secondary effect on phenolic extraction due its influence on the viscosity and density of the solvent – two parameters which are often used to correlate the rate of external diffusion and mass transfer in similar systems (Cacace & Mazza, 2003; Guerrero, Torres, & Nunez, 2008; Mantell, Rodríguez, & Martínez de la Ossa, 2002; Rodríguez-Jimenes et al., 2013).

In addition to the fermentation temperature, which itself can vary significantly depending on the winery and style of wine to be produced (generally 7–15 °C for white and 20–30 °C for red wines), as well as the cap (containing grape skins and seeds) temperature which can differ from the fermenting juice below by up to 8–14 °C (Schmid, Schadt, Jiranek, & Block, 2009), there are several methods employed by winemakers that involve the use of more extreme temperatures to promote the extraction of phenolic compounds from the grape solids. Thermovinification, a process where the grape juice is heated to 50–70 °C with skin contact for 10–30 min prior to the commencement of fermentation, is one such vinification process that has been widely studied for its influence on phenolic extraction (Aguilar et al., 2015; El Darra, Grimi, Maroun, Louka, & Vorobiev, 2013; El Darra et al., 2016; Gao et al., 1997). Since thermovinification generally involves pressing the marc (grape skins and seeds) after heating (thus resulting in no solid-liquid contact during fermentation) it would be expected that this would have a profound effect on the phenolic composition of the resulting wine and since the solid-liquid contacting phase of winemaking using thermovinification occurs prior to fermentation, it would be expected to reduce the total tannin concentration due to the requirement of ethanol to break down grape seed cuticles before extraction (Boulton et al., 1996).

A related technique prior to fermentation, microwave maceration, whereby musts are irradiated with microwaves to achieve 70 °C, has been studied with regards to its impact on phenolic extraction. When comparing this method to a submerged cap control, Carew, Sparrow, Curtin, Close, and Dambergs (2014) found that the microwave macerated replicates produced wines with double the anthocyanin concentration and triple the tannin concentration after 6 months bottle age. Although this study did not monitor the phenolic levels at different stages of extraction, the authors acknowledged that investigating the effectiveness of existing heat and mass transfer models (such as those based on Fick's second law) could be a useful tool for explaining the observed heating and extraction patterns that occur as a result of microwave maceration and aid in the development of technologies that use this technique (Carew, Sparrow, et al., 2014). In a similar study, Carew, Gill, Close, and Dambergs (2014) compared the effects of microwave maceration of musts (with early press-off) of Pinot Noir grapes to a regular thermovinification process in two separate trials (A and B). At 216 days post-inoculation, the microwave macerated and heat treated samples were found to have significantly higher levels of phenolic compounds, with anthocyanin and pigment

levels between 20 and 50% higher in both cases across the trials and more than double the tannin concentration in all trials except thermovinification in trial A where the concentration was similar to the control. As with the previous study, the specific concentrations of phenolic compounds (anthocyanins and tannins) were not monitored throughout fermentation, hence the kinetics of extraction were not evaluated.

Another heating process used by winemakers to assist phenolic extraction known as flash release has also been reported to have a significant impact on the extraction kinetics and the phenolic composition at the end of the maceration period. This process involves heating the must at atmospheric pressure to around 95 °C before applying a strong vacuum, which results in rapid cooling of the berry skin cell walls as well as making them more fragile (Doco, Williams, & Cheynier, 2007; Morel-Salmi, Souquet, Bes, & Cheynier, 2006; Smith, McRae, & Bindon, 2015). Morel-Salmi et al. (2006) showed that flash release resulted in a fast initial concentration of anthocyanins, which lowered slightly during the 5-day maceration period to reach comparable levels to the control in the finished wine. The proanthocyanidins similarly showed a higher initial concentration immediately following flash release treatment, but continued to increase during maceration. This difference can be attributed to the presence of increased ethanol concentrations in the must, which is known to aid in the extraction of skin and seed proanthocyanidins (Canals et al., 2005; González-Manzano et al., 2004).

Must-freezing is a low temperature technique less commonly used by winemakers to facilitate enhanced extraction. This process differs from other temperature related processes as the extraction occurs after the freezing process and is caused by damage to the cell membranes rather than changes to the physical parameters of the solvent and solute (Sacchi et al., 2005). Busse-Valverde et al. (2011) found that must freezing with dry ice resulted in musts with only a slightly higher total anthocyanin content (1–2% higher) throughout the 10-day maceration period compared with cold soaked and enzyme treated trials (6% higher). Another extraction method used by winemakers to promote phenolic extraction involves cool temperature maceration prior to fermentation (also known as cold soaking), where the grapes are crushed and the solids allowed to soak in the juice for several days (Gil-Muñoz et al., 2009; Koyama et al., 2007). During this process, the must is usually cooled to 10–15 °C in order to slow the rate of natural fermentation that could occur prior to inoculation (Sacchi et al., 2005). In a study by Koyama et al. (2007), who followed the extraction of several classes of phenolic compounds during cold maceration of red wine, it was found that cold soaking resulted in a slower initial extraction rate of anthocyanins and proanthocyanidins, but had no effect on the maximum concentrations of these phenolics at the end of the 10-day maceration period relative to the control. In addition, it was also found that cold maceration significantly slowed the rate of seed-derived flavan-3-ol monomer extraction (determined using phloroglucinolysis) likely due to the decreased ethanol concentrations in the early stages of this maceration period – a phenomenon also noted by other authors (Canals et al., 2005; González-Manzano et al., 2004).

Although many studies have sought to identify the role of temperature in the extraction of phenolics during wine must maceration (Burns et al., 2001; Busse-Valverde et al., 2011; El Darra et al., 2013; El Darra et al., 2016; Gil-Muñoz et al., 2009; Koyama et al., 2007; Lerno et al., 2015), few have followed phenolic concentrations throughout the maceration period, and to the authors' knowledge, none have attempted to derive temperature-dependent kinetics for this process. However, the impact of temperature on extraction kinetics was studied in a comparable process by Cacace and Mazza (2003), who investigated the mass transfer of anthocyanins from black currants under different solvent conditions and at different temperatures and solid/solvent ratios. Their results showed a quadratic relationship of temperature at constant solvent concentrations, with this effect being independent of the solid/solvent ratios for temperatures up to 35 °C. Beyond this temperature, the concentration of anthocyanins decreased due to their instability at higher temperatures (Cacace & Mazza, 2003). In addition, the study showed that temperature affected the diffusion coefficients of phenolic compounds according to an Arrhenius relationship (Equation (6)) at constant solvent conditions – an observation supported by Bucić-Kojić et al. (2007), who noted that the total extraction rate of phenolic compounds from grape seeds into 50% ethanol solution could also be accurately modelled by the Arrhenius equation.

$$D = Aexp\left(\frac{-E_a}{RT}\right) \tag{6}$$

where D is the overall diffusion coefficient, A is the pre exponential factor, E_a is the activation energy, T is the absolute temperature and R is the universal gas constant. At different temperatures, the diffusivity can be calculated with respect to both a reference temperature and diffusivity as shown in Equation (7) (Chan, Yusoff, & Ngoh, 2014).

$$\frac{D}{D_{ref}} = \frac{Aexp(-E_a/RT)}{Aexp\left(-E_a/RT_{ref}\right)} = exp\left[\frac{E_a}{R}\left(\frac{1}{T_{ref}} - \frac{1}{T}\right)\right] \tag{7}$$

where D_{ref} and T_{ref} are the reference diffusivity and temperature, respectively. This method was used by Xu, Huang, and He (2008), who modelled the extraction of isoflavones from *Pueraria lobate* (a common herb in Chinese medicine), which could be applied to phenolic extraction during red wine maceration to estimate the effect of changing temperature conditions.

2.3. Contact area

During fermentative maceration, the grape solids (skins, seeds and stems) rise to the top of the fermenting vessel and form a cap as a result of the upward force of evolving carbon dioxide (Weber, Nelson, & Gay, 2002). In addition to helping insulate the system (which causes the must temperature to rise), the production of a cap results in less contact between the solid and liquid components of the must (Sacchi et al., 2005). In order to increase the solid-liquid contact area and help maintain a constant temperature while simultaneously limiting the potential for contamination by aerobic spoilage microorganisms (Carew, Sparrow, et al., 2014), winemakers generally adopt one of several methods to "manage" the cap (Fig. 6): pumping liquid from the bottom of the tank and spraying it over the solids cap (Fig. 6a); mechanically punching down the solids into the liquid (Fig. 6b); or using a baffled rotary tank that assists in submerging the grape solids back into the liquid (Fig. 6c).

Fischer, Strasser, and Gutzler (2000) investigated the impact of different solid-liquid contacting methods on the extraction of a wide range of phenolic compounds, including total anthocyanin concentration and proanthocyanidin constituents (catechin and epicatechin). Three grape varieties were used in this study investigating manual punch-down, mechanical punch-down, pump-over and fermentation in a spiral rotor tank. Interestingly, the impact that the fermentation technology had on the phenolic composition of the wine was seemingly dependent on the grape variety. For example, the total monomeric anthocyanin extraction was greater for mechanical punch-down than mechanical pump-

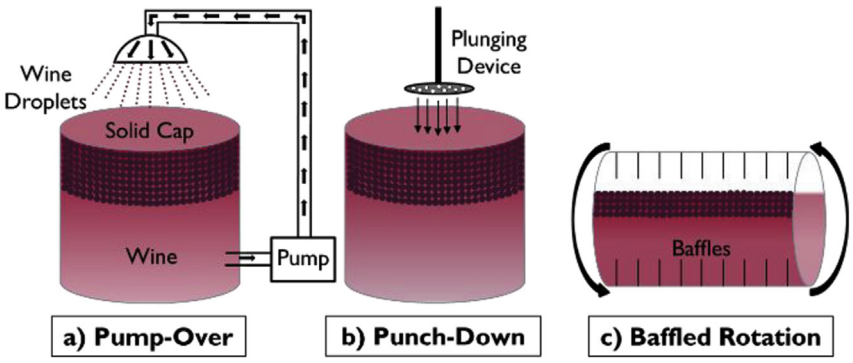

Fig. 6. Examples of cap management techniques employed by winemakers (a) pumping-over the liquid over the cap, (b) punching-down the cap into the liquid, and (c) using a rotating, baffled tank to submerge the cap.

over for Pinot Noir and Dornfelder grapes, but the opposite was found for Portugieser grapes. A variety-dependent effect on phenolic composition was also found by Leone, La Notte, and Antonacci (1983). It has been suggested by Boulton et al. (1996) that the method of solid-liquid contacting will have less of an impact on the extent of phenolic extraction but will have an effect on the extraction rate.

Although studies have been conducted on the differences in phenolic extraction when comparing cap management techniques, it does not appear that any studies have compared different times for each contact method, for example, varying the length of time taken for pump-over or punch-down and evaluating phenolic concentration and composition. After a pump-over operation has been completed, the solid cap remains in contact with the liquid for approximately half an hour (Fischer et al., 2000; Schmid et al., 2009) and as such it would be expected that an increased pump-over time would yield higher phenol concentrations due to an increased total contact time. Although methods of enhancing contact between the solid and liquid phases of grape must have been qualitatively compared for different grape varieties and methods (Fischer et al., 2000; Leone et al., 1983), there appears to be few attempts to model these systems and calculate their external diffusion and mass transfer rates for the purpose of optimising the extraction potential of wines during these mixing operations. Empirical correlations in the form of modifications of the Stokes-Einstein equation, in conjunction with a series of dimensionless numbers describing the fluid flow, have been widely used to estimate the external diffusion coefficient of phenolic compounds in both batch (Cacace & Mazza, 2003; Espinoza-Pérez, Vargas, Robles-Olvera, Rodrı, & Garcı, 2007; Rodríguez-Jimenes et al., 2013) and semi-batch (Guerrero et al., 2008; Mantell et al., 2002) extraction systems to calculate the rate of mass transfer. These correlations can be used with the aid of experimental results of instantaneous phenolic concentration in the liquid solvent to calculate the internal diffusion coefficient and overall mass transfer rate. A summary of internal diffusion coefficients of various compounds in differing systems solved using this method is presented in Table 1 and shows the range of values that could be expected for a similar system of phenolic compounds under different process conditions. Many authors have used this method to model the internal and external mass transfer rates and diffusion coefficients of phenolic compounds in various systems but it has not been used to model phenolic extraction in active fermentations of red wine or at lab scale using pre-fermentative grape solids (skins and seeds) in model wine solutions. Mantell et al. (2002) and Guerrero et al. (2008) have, however, investigated the continuous solvent extraction of various phenolic compounds in post-fermentation red and white grape marc. In each instance, the external diffusion coefficient was estimated by one modification of the Stokes-Einstein equation proposed by Wilke and Chang (1955):

$$D_{AB} = \frac{7.4 \times 10^{-8} (\varphi M_B)^{1/2} T}{\mu V_A^{0.6}} \tag{8}$$

where D_{AB} is the external diffusion coefficient of solute A in solvent B, M_B is the solvent molecular mass, T is the absolute temperature of the system, φ is the solvent association factor (1.5 for ethanol and 2.26 for water), μ is the solvent dynamic viscosity, and V_A is the molar volume of the solute at its normal boiling point and can be calculated as a function of its critical volume (Reid, Prausnitz, & Poling, 1987). This value can then be used to solve for the external mass transfer coefficient (k_e) through a dimensionless system of equations typically of the form:

$$Sh = Sh_0 + CRe^m Sc^{1/3} \tag{9}$$

where C and m are constants determined by the characteristics of the system and where:

$$Re = \frac{\rho v d}{\mu}, \quad Sh = \frac{k_e l}{D_{AB}}, \quad Sc = \frac{\mu}{\rho D_{AB}}$$

In this way, it would be possible to calculate and compare the external mass transfer coefficients of active red wine fermentations where different mixing technologies are applied based on the diffusion characteristics of specific phenolic compounds in the liquid phase, the particle diameter (d), distance for diffusion (l), the physical properties of the liquid (such as the density (ρ), viscosity (μ) and the relative velocity (v)) of the liquid phase. In turn, this process could be used to model various mixing operations employed by winemakers and allow for direct quantitative comparisons of their effectiveness.

As well as mixing methods that improve the surface contact between the solid and liquid, another technique aimed at enhancing the available contact area has recently been investigated for commercial use. This method uses a mechanism known as accentuated cut edges (ACE), which decreases the solid particle size by physically cutting the skins into smaller pieces, thereby increasing the perimeter to surface area ratio to facilitate increased cell leakage at these sites (Sparrow et al., 2015). Early studies into this technique have found that ACE maceration resulted in higher levels of tannin (approximately 3 times greater) and stable pigment (approximately 60% higher) during fermentation (Sparrow, Holt, Pearson, Dambergs, & Close, 2016) as well as in the resulting wine six months after the onset of fermentation (Sparrow et al., 2015, 2016). During the fermentative maceration stage using ACE,

Table 1
Internal diffusion coefficients of phenolic compounds under various extraction condition.

Product	Solute	Solvent (units provided where available)	T (°C)	Internal Diffusion Coefficient (m^2/ s)	Reference
Black Currants	Anthocyanins	67% Ethanol	40	1.23×10^{-10}	Cacace and Mazza (2003)
	Anthocyanins	700 mg/L Sulfured Water	40	2.43×10^{-10}	
	Total Phenolics	67% Ethanol	40	1.03×10^{-10}	
	Total Phenolics	700 mg/L Sulfured Water	40	5.05×10^{-10}	
Grape Marc	Anthocyanins	Methanol	40	3.53×10^{-10}	Mantell et al. (2002)
	Anthocyanins	Methanol	50	3.85×10^{-10}	
	Anthocyanins	Methanol	60	5.02×10^{-10}	
Milled Grape Seeds	Total Phenolics	50% Ethanol	25	7.2×10^{-13}	Bucić-Kojić, Sovová, Planinić, and Tomas (2013)
	Total Phenolics	50% Ethanol	50	9.2×10^{-13}	
	Total Phenolics	50% Ethanol	70	1.23×10^{-12}	
Roselle Calyces	Anthocyanins	Water	25	3.6×10^{-11}	Cissé et al. (2012)
	Anthocyanins	Water	50	6.8×10^{-11}	
	Anthocyanins	Water	70	9.9×10^{-11}	
Coffee Beans	Caffeine	Water	90	3.21×10^{-10}	Espinoza-Pérez et al. (2007)
Vanilla Pods	Vanillin	60% (w/w) Ethanol	50	1.91×10^{-11}	Rodríguez-Jimenes et al. (2013)
	p-Hydroxybenzaldehyde	60% (w/w) Ethanol	50	1.30×10^{-11}	
	p-Hydroxybenzoic acid	60% (w/w) Ethanol	50	1.55×10^{-11}	

free anthocyanin content was found to differ only slightly from that of the periodically punched-down control and the submerged cap control (Sparrow et al., 2016). This observation is possibly due to the significantly enhanced extraction of tannins, which occur in greater concentrations than anthocyanins and are known to have a substantial impact on the formation of polymeric pigments (Bindon, Kassara, et al., 2014). Due to the recentness of this research, it does not appear that any literature exists on directly correlating skin particle size with the extraction kinetics of anthocyanins and tannins during fermentative maceration.

Other techniques aimed at improving solid-liquid mass transfer such as ultrasound-assisted extraction (UAE), pulsed-electric field (PEF) and macerating enzymes, are also being investigated for their application in the winery. In the case of UAE, the application of sound waves causes cavitation near the surface of the solid and decreases the effect of the boundary layer through micro-stirring, effectively improving the contact area (Hagenson & Doraiswamy, 1998; Tao, Zhang, & Sun, 2014). On the other hand, PEF uses an external electric field between two electrodes surrounding the material (López, Puértolas, Condón, Álvarez, & Raso, 2008). This non-thermal process causes an electrical breakdown of the cell membranes, allowing for easier mass transfer of phenolic compounds (López et al., 2008). The application of these technologies during red wine maceration has been shown to positively influence extraction (El Darra et al., 2013; El Darra et al., 2016; Ghafoor, Choi, Jeon, & Jo, 2009; López et al., 2008; Puértolas, Saldaña, Condón, Álvarez, & Raso, 2009; Tao, Zhang, et al., 2014), however, modelling their impact on cell degradation as a function of their power consumption would help winemakers improve and more accurately predict the phenolic potential of their wines. Pectolytic macerating enzymes are another method often used by winemakers that improve the available surface for mass transfer and aid in cell leakage by breaking down the grape berry cell walls (Ducasse et al., 2010; Sacchi et al., 2005; Smith, McRae, et al., 2015). Although enzymes have generally been shown to improve the extraction of phenolic compounds during the maceration stage of red wine production (Bautista-Ortín, Fernández-Fernández, López-Roca, & Gómez-Plaza, 2007; Ducasse et al., 2010), conflicting results for effects on anthocyanin and tannin concentration have been reported (Bautista-Ortín et al., 2007; Puértolas et al., 2009). Because these processes directly affect the integrity of the skin walls, the application of Fick's second law as a way of modelling the extractive behaviour of ferments that use these technologies would not be appropriate. Research into other mathematical methods that can be used to quantify their impact on cell integrity for the purposes of predictive modelling would be of significant benefit to the field.

3. Reactions of extracted phenolics

3.1. Oxidation

Beyond understanding the extraction of grape constituents and the impact of winemaking technologies in modelling these processes, aspects of phenolic reactivity need to also be considered. Despite the complex array of reactions that can potentially occur (Fig. 3), oxidation of anthocyanins with dissolved oxygen has been investigated by several authors under the hypothesis that it is the main reaction leading to the decreasing concentration of anthocyanins during winemaking. Increased oxygenation during the prefermentative stage of winemaking has a strong influence on both the anthocyanin and total phenolic evolution (Castellari, Arfelli, Riponi, & Amati, 1998). Musts supplied with additional oxygen prior to fermentation (75 and 375 mg/L) showed a 15 and 20% lower concentration of total anthocyanins at the end of the 72 h maceration period, respectively, and 11 and 12% lower concentration of total phenolics, respectively (Castellari et al., 1998).

Although not measured quantitatively, Zanoni et al. (2010) noted that the rate of malvidin degradation was lower for industrial vinifications compared to micro-vinifications, leading them to conclude that this discrepancy was likely due to a higher level of protection provided to the must by carbon dioxide. Andrich et al. (2005) attempted to model the evolution of anthocyanins throughout maceration using Fick's second law of diffusion as a basis for the extraction phase and the oxidation reaction with oxygen as a basis for the subsequent decrease. When the rate of anthocyanin oxidation was considered directly proportional to the concentration of anthocyanins and dissolved oxygen, a system of five differential equations was obtained and rate constants of between 2.4×10^{-3} and 12.8×10^{-3} for anthocyanin oxidation were found, depending on grape variety and contacting method used in each trial. These differences indicate that there are likely to be other factors influencing the must concentration of anthocyanins.

3.2. Copigmentation

In addition to the derived pigments formed from condensation reactions, anthocyanins can also undergo a non-covalent physiochemical association with a colourless cofactor or through self-

association in a process known as copigmentation (Boulton, 2001; Lambert, Asenstorfer, Williamson, Iland, & Jones, 2011). This phenomenon helps stabilise the structure of the anthocyanin and generally enhances the absorbance of the wine at 520 nm, accounting for up to 50% of the colour observed in young red wines. Additionally, this process can result in a shift to the wavelength of maximum absorbance of up to 20 nm (Bimpilas, Panagopoulou, Tsimogiannis, & Oreopoulou, 2016; Boulton, 2001).

In a study on the anthocyanin copigmentation with the flavan-3-ol catechin in model wine solutions González-Manzano, Mateus, De Freitas, and Santos-Buelga (2008) observed that the hyperchromatic shift (increased absorbance) caused by copigmentation was more pronounced after 30 min following the preparation of the solutions, indicating that this process is thermodynamically driven rather than kinetically driven. Using this observation as a basis, Lambert et al. (2011) studied the copigmentation of malvidin-3-glucoside with various phenolic compounds in order to derive the thermodynamic parameters for the reactions, using an existing equation (Brouillard, Mazza, Saad, Albrecht-Gary, & Cheminat, 1989).

$$ln\left(\frac{(A-A_0)}{A_o}\right) = ln(K_1 r_1) + n \times ln[CP]_0 \quad (10)$$

where A_0 is the maximum absorbance of malvidin-3-glucoside only at 530 nm, A is the sample's absorbance in the presence of the copigment, $[CP]_0$ is the copigment concentration in the sample, r_1 is the molar extinction ratio of the coefficients of the copigmented flavylium ion to that of the unassociated flavylium ion (the ion which is generally considered to be the predominant species participating in copigmentation), n is the stoichiometric constant and K_1 is the stability constant. Lambert et al. (2011) also found that the flavonol quercetin (present in grape skin, Fig. 1) appeared to be the most effective copigment at wine pH and room temperature, with a stability constant of 2900 ± 1300, compared to caffeic acid and catechin, which both proved to be poor copigments, with stability constants of 70 ± 20 and 90 ± 20, respectively. The self-association of malvidin-3-glucoside resulted in a stability constant of 3300 ± 300, and was the only copigmentation reaction to exhibit a higher level of stability than quercetin (Lambert et al., 2011).

3.3. Adsorption by yeast

Because phenolic compounds (such as tannins and anthocyanins) generally contain both hydrophobic aromatic rings and hydrophilic hydroxyl groups (i.e., they are amphiphilic), they are able to simultaneously bind at several sites on surfaces of other molecules (Hanlin, Hrmova, Harbertson, & Downey, 2010). The sensation of oral astringency due to red wine is the result of tannins precipitating proteins in saliva through both hydrogen bonding and hydrophobic interactions (Busse-Valverde et al., 2011; Canals et al., 2005; Cheynier et al., 2006; Hanlin et al., 2010; Vidal et al., 2003). Tannins are also able to bind with other molecules with hydroxyl and aromatic (or aliphatic) groups, such as cell wall polysaccharides (Hanlin et al., 2010). *Saccharomyces cerevisiae* yeast cell walls are composed of exposed mannoproteins bound to oligopolysaccharides (with different polarities depending on the strain), allowing them to adsorb molecules such as tannins, anthocyanins and other volatile compounds that are released during the maceration stage of winemaking (Morata et al., 2003).

In addition to studies conducted on the adsorption of components responsible for quality attributes (anthocyanins and tannins) by different yeast strains (Lubbers, Charpentier, Feuillat, & Voilley, 1994; Morata et al., 2003; Razmkhab et al., 2002) and grape cell walls (Bautista-Ortín et al., 2016; Bindon, Smith, Holt, & Kennedy, 2010; Bindon, Smith, & Kennedy, 2010), some investigation has been undertaken by Vasserot, Caillet, and Maujean (1997) on modelling the rate of decolouration at different anthocyanin concentrations. This study demonstrated that the majority of anthocyanin adsorption takes place within the first five minutes of contact and also that strong linear correlations exist between absorbed anthocyanins and the initial anthocyanin concentration at yeast levels ranging from 3 to 30 g/L. The study also revealed that temperature and ethanol concentration strongly affected the adsorption of anthocyanins by yeast lees, with higher temperatures increasing anthocyanin adsorption and higher ethanol concentrations having the opposite effect.

4. Conclusion

4.1. Potential applications

Chemical mechanisms and pathways for formation and/or extraction of phenolic compounds (Bindon, Madani, Pendleton, Smith, & Kennedy, 2014; Cerpa-Calderón & Kennedy, 2008) along with flavour and aroma constituents (Black, Parker, Siebert, Capone, & Francis, 2015; Mouret et al., 2014; Pogorzelski & Wilkowska, 2007; Polášková, Herszage, & Ebeler, 2008; Robinson et al., 2014; Smith, Bekker, Smith, & Wilkes, 2015; Styger, Prior, & Bauer, 2011; Sumby, Grbin, & Jiranek, 2010; Ugliano, 2013) have been described previously, however non-steady state models for mass transport or reaction kinetics of these species in wine fermentation are not available in published literature. A global model describing kinetics of components responsible for wine quality parameters as well as more basic parameters such as sugar or ethanol would be a significant advancement. As a starting point, predictive mathematical models for ethanol, sugar and macronutrients have been previously developed (Coleman et al., 2007; Cramer et al., 2002; O'Neill et al., 2011) and the effect of mixing operations on external mass transfer of phenolic compounds in different systems is also well established (Cacace & Mazza, 2003; Espinoza-Pérez et al., 2007; Rodríguez-Jimenes et al., 2013). Bringing together these key aspects of wine science with process engineering models could provide new capability for predicting quality potential and wine matrix interactions for each batch of juice, which could be exploited together with real-time process control systems to drive an active ferment to a specified final phenolic concentration, thereby minimising differences due to variation within the berries from vintage to vintage. The ability to achieve this goal would be of great benefit to large-scale wine producers who strive to meet consumer expectations in terms of cost, quality and consistency from year to year.

The development of engineering models to describe synthesis and extraction phenomena associated with wine fermentation would also provide insights into novel fruit and wine process operations that might enhance (or diminish) key wine quality attributes, such as optimising skin extraction while minimising seed extraction. Furthermore, such models may present new opportunities for equipment design, where mixing operations are improved and greater control over the solid-liquid contact area is available. The ability to predict and optimise the rate and extent of phenolic extraction during normal fermentative maceration by manipulating process variables such as temperature and mixing operations could also remove the need for winemakers to use advanced maceration techniques such as cold soaking and thermovinification, thereby decreasing the cost of production and improving the overall efficiency of the winery through optimising tank space and minimising energy consumption. With robust predictive extraction models, winemakers would have the capacity

to realise, prior to fermentation, the theoretical phenolic potential of their fruit (which changes with vintage, variety and terroir), affording the ability to guide the winemaking process towards a particular style – based on changing consumer preferences and demands – using fixed infrastructure.

4.2. Research gaps and future directions

The generation of engineering models to describe extraction phenomena associated with wine fermentation would provide new opportunities for optimised product quality, process control and equipment design. Although there has been a considerable amount of research on the impacts of changing individual process variables, there has been little to no work on attempting to reconcile these effects into a method for predictive modelling of phenolic extraction in wine. As a starting point for future research, knowledge on the rates of internal diffusion as a function of solvent concentration and temperature would aid in estimating extraction rates during active fermentations where these variables are continuously changing, as well as in predicting the effects of other processes employed by winemakers, such as thermovinification and cold soaking. Further research into the external diffusion and mass transfer of phenolic compounds that occurs during mixing operations, and modelling of these processes through empirical methods and computational fluid dynamic analysis, would also expand the current body of literature and further the goal of better controlling extraction during fermentation. Exploring the impact of novel technologies that could be applied to winemaking, such as pulsed-electric field and ultrasound-assisted extraction, and their effects on internal diffusion resulting from grape skin and seed cell degradation, would also be a valuable addition.

The construction and study of process models capable of predicting the phenolic composition of wine musts during the extractive phase would be of benefit to a range of wine research initiatives. It is likely that insights gained from this process would assist in deriving similar diffusion models for other stages of the winemaking process, such as the extraction of phenolic compounds upon the addition of wood chips or during micro-oxygenation and barrel aging – processes that also have a significant impact on the quality and sensory properties of the finished wine (Oberholster et al., 2015; Tao, García, & Sun, 2014). In addition, a robust extraction model capable of predicting phenolic content based on a series of input parameters would be applicable when investigating other areas of winemaking; for example, in the study of low alcohol wine production, where the ability to improve phenolic extraction despite low initial concentrations in the grape solids and lower alcohol concentrations during maceration, would be of great benefit.

Acknowledgements

We acknowledge Vladimir Jiranek for his insightful comments on this manuscript. P.S. is supported through a UA School of Agriculture Food and Wine Scholarship [1606990] and is also a recipient of a Wine Australia supplementary scholarship [AGW Ph1505]. The authors acknowledge the financial support from the School of Agriculture, Food and Wine, UA, and Australian grapegrowers and winemakers through their investment body, Wine Australia, with matching funds from the Australian Government.

References

Aguilar, T., Loyola, C., de Bruijn, J., Bustamante, L., Vergara, C., von Baer, D., et al. (2015). Effect of thermomaceration and enzymatic maceration on phenolic compounds of grape must enriched by grape pomace, vine leaves and canes. *European Food Research and Technology, 242*, 1–10.

Amendola, D., De Faveri, D. M., & Spigno, G. (2010). Grape marc phenolics: Extraction kinetics, quality and stability of extracts. *Journal of Food Engineering, 97*, 384–392.

Andrich, G., Zinnai, A., Venturi, F., & Fiorentini, R. (2005). A tentative mathematical model to describe the evolution of phenolic compounds during the maceration of Sangiovese and Merlot grapes. *Italian Journal of Food Science, 17*, 45–58.

Bakker, J., Bridle, P., Bellworthy, S., Garcia-Viguera, C., Reader, H., & Watkins, S. (1998). Effect of sulphur dioxide and must extraction on colour, phenolic composition and sensory quality of red table wine. *Journal of the Science of Food and Agriculture, 78*, 297–307.

Bautista-Ortín, A., Fernández-Fernández, J., López-Roca, J., & Gómez-Plaza, E. (2007). The effects of enological practices in anthocyanins, phenolic compounds and wine colour and their dependence on grape characteristics. *Journal of Food Composition and Analysis, 20*, 546–552.

Bautista-Ortín, A. B., Martínez-Hernández, A., Ruiz-García, Y., Gil-Muñoz, R., & Gómez-Plaza, E. (2016). Anthocyanins influence tannin–cell wall interactions. *Food Chemistry, 206*, 239–248.

Bimpilas, A., Panagopoulou, M., Tsimogiannis, D., & Oreopoulou, V. (2016). Anthocyanin copigmentation and color of wine: The effect of naturally obtained hydroxycinnamic acids as cofactors. *Food Chemistry, 197*, 39–46.

Bindon, K. A., Kassara, S., Hayasaka, Y., Schulkin, A., & Smith, P. A. (2014). Properties of wine polymeric pigments formed from anthocyanin and tannins differing in size distribution and subunit composition. *Journal of Agricultural and Food Chemistry, 62*, 11582–11593.

Bindon, K. A., & Kennedy, J. A. (2011). Ripening-induced changes in grape skin proanthocyanidins modify their interaction with cell walls. *Journal of Agricultural and Food Chemistry, 59*, 2696–2707.

Bindon, K. A., Madani, S. H., Pendleton, P., Smith, P. A., & Kennedy, J. A. (2014). Factors affecting skin tannin extractability in ripening grapes. *Journal of Agricultural and Food Chemistry, 62*, 1130–1141.

Bindon, K. A., Smith, P. A., Holt, H., & Kennedy, J. A. (2010). Interaction between grape-derived proanthocyanidins and cell wall material. 2. Implications for vinification. *Journal of Agricultural and Food Chemistry, 58*, 10736–10746.

Bindon, K. A., Smith, P. A., & Kennedy, J. A. (2010). Interaction between grape-derived proanthocyanidins and cell wall material. 1. Effect on proanthocyanidin composition and molecular mass. *Journal of Agricultural and Food Chemistry, 58*, 2520–2528.

Bisson, L. F., & Karpel, J. E. (2010). Genetics of yeast impacting wine quality. *Food Science and Technology, 1*, 139–162.

Black, C., Parker, M., Siebert, T., Capone, D., & Francis, I. (2015). Terpenoids and their role in wine flavour: Recent advances. *Australian Journal of Grape and Wine Research, 21*, 582–600.

Boulton, R. (2001). The copigmentation of anthocyanins and its role in the color of red wine: A critical review. *American Journal of Enology and Viticulture, 52*, 67–87.

Boulton, R., Singleton, V., Bisson, L., & Kunkee, R. (1996). *Principles and practices of winemaking*. New York: Chapman and Hall.

Brouillard, R., Mazza, G., Saad, Z., Albrecht-Gary, A., & Cheminat, A. (1989). The copigmentation reaction of anthocyanins: A microprobe for the structural study of aqueous solutions. *Journal of the American Chemical Society, 111*, 2604–2610.

Bucić-Kojić, A., Planinić, M., Tomas, S., Bilić, M., & Velić, D. (2007). Study of solid–liquid extraction kinetics of total polyphenols from grape seeds. *Journal of Food Engineering, 81*, 236–242.

Bucić-Kojić, A., Sovová, H., Planinić, M., & Tomas, S. (2013). Temperature-dependent kinetics of grape seed phenolic compounds extraction: Experiment and model. *Food Chemistry, 136*, 1136–1140.

Burns, J., Gardner, P. T., Matthews, D., Duthie, G. G., Lean, J., & Crozier, A. (2001). Extraction of phenolics and changes in antioxidant activity of red wines during vinification. *Journal of Agricultural and Food Chemistry, 49*, 5797–5808.

Busse-Valverde, N., Bautista-Ortín, A. B., Gómez-Plaza, E., Fernández-Fernández, J. I., & Gil-Muñoz, R. (2012). Influence of skin maceration time on the proanthocyanidin content of red wines. *European Food Research and Technology, 235*, 1117–1123.

Busse-Valverde, N., Gómez-Plaza, E., López-Roca, J. M., Gil-Munoz, R., & Bautista-Ortín, A. B. (2011). The extraction of anthocyanins and proanthocyanidins from grapes to wine during fermentative maceration is affected by the enological technique. *Journal of Agricultural and Food Chemistry, 59*, 5450–5455.

Cacace, J. E., & Mazza, G. (2003). Mass transfer process during extraction of phenolic compounds from milled berries. *Journal of Food Engineering, 59*, 379–389.

Canals, R., Llaudy, M., Valls, J., Canals, J., & Zamora, F. (2005). Influence of ethanol concentration on the extraction of color and phenolic compounds from the skin and seeds of Tempranillo grapes at different stages of ripening. *Journal of Agricultural and Food Chemistry, 53*, 4019–4025.

Carew, A., Gill, W., Close, D., & Dambergs, R. (2014). Microwave maceration with early pressing improves phenolics and fermentation kinetics in Pinot noir. *American Journal of Enology and Viticulture, 65*, 401–406.

Carew, A. L., Sparrow, A. M., Curtin, C. D., Close, D. C., & Dambergs, R. G. (2014). Microwave maceration of Pinot noir grape must: Sanitation and extraction effects and wine phenolics outcomes. *Food and Bioprocess Technology, 7*, 954–963.

Castellari, M., Arfelli, G., Riponi, C., & Amati, A. (1998). Evolution of phenolic compounds in red winemaking as affected by must oxygenation. *American Journal of Enology and Viticulture, 49*, 91–94.

Cerpa-Calderón, F. K., & Kennedy, J. A. (2008). Berry integrity and extraction of skin and seed proanthocyanidins during red wine fermentation. *Journal of*

Agricultural and Food Chemistry, 56, 9006–9014.
Chan, C.-H., Yusoff, R., & Ngoh, G.-C. (2014). Modeling and kinetics study of conventional and assisted batch solvent extraction. *Chemical Engineering Research and Design, 92*, 1169–1186.
Cheynier, V., Dueñas-Paton, M., Salas, E., Maury, C., Souquet, J.-M., Sarni-Manchado, P., et al. (2006). Structure and properties of wine pigments and tannins. *American Journal of Enology and Viticulture, 57*, 298–305.
Cissé, M., Bohuon, P., Sambe, F., Kane, C., Sakho, M., & Dornier, M. (2012). Aqueous extraction of anthocyanins from *Hibiscus sabdariffa*: Experimental kinetics and modeling. *Journal of Food Engineering, 109*, 16–21.
Coleman, M. C., Fish, R., & Block, D. E. (2007). Temperature-dependent kinetic model for nitrogen-limited wine fermentations. *Applied and Environmental Microbiology, 73*, 5875–5884.
Coombe, B. (1987). Distribution of solutes within the developing grape berry in relation to its morphology. *American Journal of Enology and Viticulture, 38*, 120–127.
Cramer, A. C., Vlassides, S., & Block, D. E. (2002). Kinetic model for nitrogen-limited wine fermentations. *Biotechnology and Bioengineering, 77*, 49–60.
Doco, T., Williams, P., & Cheynier, V. (2007). Effect of flash release and pectinolytic enzyme treatments on wine polysaccharide composition. *Journal of Agricultural and Food Chemistry, 55*, 6643–6649.
Ducasse, M.-A., Canal-Llauberes, R.-M., de Lumley, M., Williams, P., Souquet, J.-M., Fulcrand, H., et al. (2010). Effect of macerating enzyme treatment on the polyphenol and polysaccharide composition of red wines. *Food Chemistry, 118*, 369–376.
El Darra, N., Grimi, N., Maroun, R. G., Louka, N., & Vorobiev, E. (2013). Pulsed electric field, ultrasound, and thermal pretreatments for better phenolic extraction during red fermentation. *European Food Research and Technology, 236*, 47–56.
El Darra, N., Turk, M. F., Ducasse, M.-A., Grimi, N., Maroun, R. G., Louka, N., et al. (2016). Changes in polyphenol profiles and color composition of freshly fermented model wine due to pulsed electric field, enzymes and thermovinification pretreatments. *Food Chemistry, 194*, 944–950.
Espinoza-Pérez, J., Vargas, A., Robles-Olvera, V., Rodrı, G., & Garcı, M. (2007). Mathematical modeling of caffeine kinetic during solid–liquid extraction of coffee beans. *Journal of Food Engineering, 81*, 72–78.
Fischer, U., Strasser, M., & Gutzler, K. (2000). Impact of fermentation technology on the phenolic and volatile composition of German red wines. *International Journal of Food Science & Technology, 35*, 81–94.
Gao, L., Girard, B., Mazza, G., & Reynolds, A. (1997). Changes in anthocyanins and color characteristics of Pinot Noir wines during different vinification processes. *Journal of Agricultural and Food Chemistry, 45*, 2003–2008.
Garde-Cerdán, T., & Ancín-Azpilicueta, C. (2006). Review of quality factors on wine ageing in oak barrels. *Trends in Food Science & Technology, 17*, 438–447.
Gawel, R., Francis, L., & Waters, E. J. (2007). Statistical correlations between the in-mouth textural characteristics and the chemical composition of Shiraz wines. *Journal of Agricultural and Food Chemistry, 55*, 2683–2687.
Gertenbach, D. (2001). Solid–liquid extraction technologies for manufacturing nutraceuticals from botanicals. In J. Shi, G. Mazza, & M. Le Maguer (Eds.), *Functional foods biochemical and processing aspects* (Vol. 2, pp. 331–366). Boca Raton: Taylor and Francis Group.
Ghafoor, K., Choi, Y. H., Jeon, J. Y., & Jo, I. H. (2009). Optimization of ultrasound-assisted extraction of phenolic compounds, antioxidants, and anthocyanins from grape *(Vitis vinifera)* seeds. *Journal of Agricultural and Food Chemistry, 57*, 4988–4994.
Gil-Muñoz, R., Moreno-Pérez, A., Vila-López, R., Fernández-Fernández, J. I., Martínez-Cutillas, A., & Gómez-Plaza, E. (2009). Influence of low temperature pre-fermentative techniques on chromatic and phenolic characteristics of Syrah and Cabernet Sauvignon wines. *European Food Research and Technology, 228*, 777–788.
Gómez-Plaza, E., Gil-Muñoz, R., López-Roca, J., Martínez-Cutillas, A., & Fernández-Fernández, J. (2001). Phenolic compounds and color stability of red wines: Effect of skin maceration time. *American Journal of Enology and Viticulture, 52*, 266–270.
González-Barreiro, C., Rial-Otero, R., Cancho-Grande, B., & Simal-Gándara, J. (2015). Wine aroma compounds in grapes: A critical review. *Critical Reviews in Food Science and Nutrition, 55*, 202–218.
González-Manzano, S., Mateus, N., De Freitas, V., & Santos-Buelga, C. (2008). Influence of the degree of polymerisation in the ability of catechins to act as anthocyanin copigments. *European Food Research and Technology, 227*, 83–92.
González-Manzano, S., Rivas-Gonzalo, J. C., & Santos-Buelga, C. (2004). Extraction of flavan-3-ols from grape seed and skin into wine using simulated maceration. *Analytica Chimica Acta, 513*, 283–289.
Guerrero, M. S., Torres, J. S., & Nunez, M. J. (2008). Extraction of polyphenols from white distilled grape pomace: Optimization and modelling. *Bioresource Technology, 99*, 1311–1318.
Hagenson, L. C., & Doraiswamy, L. K. (1998). Comparison of the effects of ultrasound and mechanical agitation on a reacting solid-liquid system. *Chemical Engineering Science, 53*, 131–148.
Hanlin, R., Hrmova, M., Harbertson, J., & Downey, M. (2010). Review: Condensed tannin and grape cell wall interactions and their impact on tannin extractability into wine. *Australian Journal of Grape and Wine Research, 16*, 173–188.
He, F., Liang, N.-N., Mu, L., Pan, Q.-H., Wang, J., Reeves, M. J., et al. (2012). Anthocyanins and their variation in red wines I. Monomeric anthocyanins and their color expression. *Molecules, 17*, 1571–1601.
Hernández-Jiménez, A., Kennedy, J. A., Bautista-Ortín, A. B., & Gómez-Plaza, E. (2012). Effect of ethanol on grape seed proanthocyanidin extraction. *American Journal of Enology and Viticulture, 63*, 57–61.
Karacabey, E., & Mazza, G. (2008). Optimization of solid–liquid extraction of resveratrol and other phenolic compounds from milled grape canes *(Vitis vinifera)*. *Journal of Agricultural and Food Chemistry, 56*, 6318–6325.
Koyama, K., Goto-Yamamoto, N., & Hashizume, K. (2007). Influence of maceration temperature in red wine vinification on extraction of phenolics from berry skins and seeds of grape *(Vitis vinifera)*. *Bioscience, Biotechnology, and Biochemistry, 71*, 958–965.
Lambert, S. G., Asenstorfer, R. E., Williamson, N. M., Iland, P. G., & Jones, G. P. (2011). Copigmentation between malvidin-3-glucoside and some wine constituents and its importance to colour expression in red wine. *Food Chemistry, 125*, 106–115.
Leone, A., La Notte, E., & Antonacci, D. (1983). Some characteristics of polyphenolic substances in red wines obtained by different processes of maceration. In C. Peri, & C. Cantarelli (Eds.), *Progress in Food engineering* (pp. 267–277). Switzerland: Forster-Verlag.
Lerno, L., Reichwage, M., Ponangi, R., Hearne, L., Block, D. E., & Oberholster, A. (2015). Effects of cap and overall fermentation temperature on phenolic extraction in cabernet sauvignon fermentations. *American Journal of Enology and Viticulture, 66*, 444–453.
Levengood, J., & Boulton, R. (2004). The variation in the color due to copigmentation in young Cabernet Sauvignon wines. In *ACS symposium series* (Vol. 886, pp. 35–52). Oxford University Press.
López, N., Puértolas, E., Condón, S., Álvarez, I., & Raso, J. (2008). Application of pulsed electric fields for improving the maceration process during vinification of red wine: Influence of grape variety. *European Food Research and Technology, 227*, 1099–1107.
Lubbers, S., Charpentier, C., Feuillat, M., & Voilley, A. (1994). Influence of yeast walls on the behavior of aroma compounds in a model wine. *American Journal of Enology and Viticulture, 45*, 29–33.
Mantell, C., Rodríguez, M., & Martínez de la Ossa, E. (2002). Semi-batch extraction of anthocyanins from red grape pomace in packed beds: Experimental results and process modelling. *Chemical Engineering Science, 57*, 3831–3838.
McRae, J. M., & Kennedy, J. A. (2011). Wine and grape tannin interactions with salivary proteins and their impact on astringency: A review of current research. *Molecules, 16*, 2348–2364.
Morata, A., Gómez-Cordovés, M., Suberviola, J., Bartolomé, B., Colomo, B., & Suárez, J. (2003). Adsorption of anthocyanins by yeast cell walls during the fermentation of red wines. *Journal of Agricultural and Food Chemistry, 51*, 4084–4088.
Morel-Salmi, C., Souquet, J.-M., Bes, M., & Cheynier, V. (2006). Effect of flash release treatment on phenolic extraction and wine composition. *Journal of Agricultural and Food Chemistry, 54*, 4270–4276.
Mouret, J., Camarasa, C., Angenieux, M., Aguera, E., Perez, M., Farines, V., et al. (2014). Kinetic analysis and gas–liquid balances of the production of fermentative aromas during winemaking fermentations: Effect of assimilable nitrogen and temperature. *Food Research International, 62*, 1–10.
Muhlack, R., Scrimgeour, N., Wilkes, E., Godden, P., & Johnson, D. (2013). Optimising fermentation through simulation. *Wine & Viticulture Journal, 28*, 38–43.
O'Neill, B., van Heeswijck, T., & Muhlack, R. (2011). Models for predicting wine fermentation kinetics. In *CHEMECA* (Sydney).
Oberholster, A., Elmendorf, B., Lerno, L., King, E., Heymann, H., Brenneman, C., et al. (2015). Barrel maturation, oak alternatives and micro-oxygenation: Influence on red wine aging and quality. *Food Chemistry, 173*, 1250–1258.
Pogorzelski, E., & Wilkowska, A. (2007). Flavour enhancement through the enzymatic hydrolysis of glycosidic aroma precursors in juices and wine beverages: A review. *Flavour and Fragrance Journal, 22*, 251–254.
Polášková, P., Herszage, J., & Ebeler, S. E. (2008). Wine flavor: Chemistry in a glass. *Chemical Society Reviews, 37*, 2478–2489.
Puértolas, E., Saldaña, G., Condón, S., Álvarez, I., & Raso, J. (2009). A comparison of the effect of macerating enzymes and pulsed electric fields technology on phenolic content and color of red wine. *Journal of Food Science, 74*, C647–C652.
Razmkhab, S., Lopez-Toledano, A., Ortega, J. M., Mayen, M., Merida, J., & Medina, M. (2002). Adsorption of phenolic compounds and browning products in white wines by yeasts and their cell walls. *Journal of Agricultural and Food Chemistry, 50*, 7432–7437.
Reid, R. C., Prausnitz, J. M., & Poling, B. E. (1987). *The properties of gases and liquids* (5th ed.). New York: McGraw-Hill.
Ribéreau-Gayon, P. (1964). The phenolic composition of grapes and wine. *Annales de Physiologie Végétale, 6*, 119–147.
Robinson, A. L., Boss, P. K., Solomon, P. S., Trengove, R. D., Heymann, H., & Ebeler, S. E. (2014). Origins of grape and wine aroma. Part 1. Chemical components and viticultural impacts. *American Journal of Enology and Viticulture, 65*, 1–24.
Rodríguez-Jimenes, G. C., Vargas-Garcia, A., Espinoza-Pérez, D. J., Salgado-Cervantes, M. A., Robles-Olvera, V. J., & García-Alvarado, M. A. (2013). Mass transfer during vanilla pods solid liquid extraction: Effect of extraction method. *Food and Bioprocess Technology, 6*, 2640–2650.
Sacchi, K. L., Bisson, L. F., & Adams, D. O. (2005). A review of the effect of winemaking techniques on phenolic extraction in red wines. *American Journal of Enology and Viticulture, 56*, 197–206.
Schmid, F., Schadt, J., Jiranek, V., & Block, D. (2009). Formation of temperature gradients in large-and small-scale red wine fermentations during cap management. *Australian Journal of Grape and Wine Research, 15*, 249–255.
Singleton, V. L., & Trousdale, E. K. (1992). Anthocyanin-tannin interactions explaining differences in polymeric phenols between white and red wines.

American Journal of Enology and Viticulture, 43, 63–70.
Smeriglio, A., Barreca, D., Bellocco, E., & Trombetta, D. (2017). Proanthocyanidins and hydrolysable tannins: Occurrence, dietary intake and pharmacological effects. *British Journal of Pharmacology, 174*, 1244–1262.
Smith, M., Bekker, M., Smith, P., & Wilkes, E. (2015). Sources of volatile sulfur compounds in wine. *Australian Journal of Grape and Wine Research, 21*, 705–712.
Smith, P., McRae, J., & Bindon, K. (2015). Impact of winemaking practices on the concentration and composition of tannins in red wine. *Australian Journal of Grape and Wine Research, 21*, 601–614.
Somers, T. C., & Evans, M. E. (1974). Wine quality: Correlations with colour density and anthocyanin equilibria in a group of young red wines. *Journal of the Science of Food and Agriculture, 25*, 1369–1379.
Somers, T. C., & Evans, M. E. (1979). Grape pigment phenomena: Interpretation of major colour losses during vinification. *Journal of the Science of Food and Agriculture, 30*, 623–633.
Sparrow, A. M., Holt, H. E., Pearson, W., Dambergs, R. G., & Close, D. C. (2016). Accentuated Cut Edges (ACE): Effects of skin fragmentation on the composition and sensory attributes of Pinot Noir wines. *American Journal of Enology and Viticulture, 67*, 169–178.
Sparrow, A. M., Smart, R. E., Dambergs, R. G., & Close, D. C. (2015). Skin particle size affects the phenolic attributes of Pinot Noir wine: Proof of concept. *American Journal of Enology and Viticulture, 67*, 29–37.
Styger, G., Prior, B., & Bauer, F. F. (2011). Wine flavor and aroma. *Journal of Industrial Microbiology & Biotechnology, 38*, 1145–1159.
Sumby, K. M., Grbin, P. R., & Jiranek, V. (2010). Microbial modulation of aromatic esters in wine: Current knowledge and future prospects. *Food Chemistry, 121*, 1–16.
Tao, Y., García, J. F., & Sun, D.-W. (2014). Advances in wine aging technologies for enhancing wine quality and accelerating wine aging process. *Critical Reviews in Food Science and Nutrition, 54*, 817–835.
Tao, Y., Zhang, Z., & Sun, D.-W. (2014). Experimental and modeling studies of ultrasound-assisted release of phenolics from oak chips into model wine. *Ultrasonics Sonochemistry, 21*, 1839–1848.
Ugliano, M. (2013). Oxygen contribution to wine aroma evolution during bottle aging. *Journal of Agricultural and Food Chemistry, 61*, 6125–6136.
Vasserot, Y., Caillet, S., & Maujean, A. (1997). Study of anthocyanin adsorption by yeast lees. Effect of some physicochemical parameters. *American Journal of Enology and Viticulture, 48*, 433–437.
Vidal, S., Francis, L., Guyot, S., Marnet, N., Kwiatkowski, M., Gawel, R., et al. (2003). The mouth-feel properties of grape and apple proanthocyanidins in a wine-like medium. *Journal of the Science of Food and Agriculture, 83*, 564–573.
Watson, B., Price, S., & Valladao, M. (1995). Effect of fermentation practices on anthocyanin and phenolic composition of Pinot noir wines. *American Journal of Enology and Viticulture, 46*, 404.
Weber, R., Nelson, M., & Gay, S. (2002). Modelling wine production. In *EMAC* (pp. 237–240). Brisbane: Institution of Engineers Australia.
Wilke, C., & Chang, P. (1955). Correlation of diffusion coefficients in dilute solutions. *AIChE Journal, 1*, 264–270.
Xu, H.-N., Huang, W.-N., & He, C.-H. (2008). Modeling for extraction of isoflavones from stem of *Pueraria lobata* (Willd.) Ohwi using n-butanol/water two-phase solvent system. *Separation and Purification Technology, 62*, 590–595.
Zanoni, B., Siliani, S., Canuti, V., Rosi, I., & Bertuccioli, M. (2010). A kinetic study on extraction and transformation phenomena of phenolic compounds during red wine fermentation. *International Journal of Food Science & Technology, 45*, 2080–2088.

SUMMARY OF RESEARCH AIMS

The ultimate goal of this project was to develop a mathematical model that describes the dynamic non-steady state mass transfer of anthocyanins during red wine maceration and fermentation and which can be used to predict future extraction scenarios. Previous attempts at modelling the extraction of anthocyanins during red wine fermentation have focussed on fitting experimental or commercial extraction data to first and second order kinetic models, whereby a single kinetic parameter was used to describe the extractive phase. Although this approach can be used to quantify the overall anthocyanin extraction rate of a given ferment, it is limited in its ability to quantitatively predict the rate and extent of anthocyanin extraction in future fermentation scenarios where process conditions may vary. To account for this, the specific objectives of the study were:

1. Review the main physical factors that impact the rate and extent of extraction of anthocyanins, tannin and major flavour components during red wine maceration and fermentation.
2. Develop mathematical models describing the mass transfer of anthocyanins during red wine maceration and response models for relevant mass transfer parameters at winemaking process conditions.
3. Develop predictive mathematical models for simulating anthocyanin extraction during active fermentation scenarios.
4. Validate predictive mass transfer models at the commercial scale using extraction data from commercial fermentations.

<u>Objective 1: Review fermentation parameters that impact phenolic extraction</u>

In the past few decades, a significant amount of research has been undertaken on various winemaking parameters that may impact the extraction and subsequent evolution of anthocyanins and other phenolic compounds. As such, the first objective of this project was to determine through literature review which factors are most likely to impact the extraction rate and extractability of phenolic compounds in order to determine which parameters should be included in the development of new mathematical models for this process. A secondary goal here was to also determine the current state of mathematical models that can be used to predict the effect of individual parameters (such as temperature or mixing operations). Results of this undertaking are summarised in Chapter 1.

Objective 2: Develop mass transfer models for anthocyanin extraction and response models for relevant mass transfer parameters

In Chapter 2, a first principles mathematical model for anthocyanin mass transfer was developed for anthocyanin extraction from grape skins into fermenting liquid. A key difference between this model and those previously developed for phenolic extraction in wine is the separation of diffusion and other mass transfer parameters in the solid and liquid phases, allowing for these to be individually studied. Following this, response equations for key mass transfer parameters (temperature, liquid phase ethanol and sugar concentrations) were developed through factorially designed extraction experiments, and the impact of liquid phase convection on anthocyanin mass transfer was also determined. Further detail on these results can be found in Chapters 2 to 4.

Objective 3: Simulate anthocyanin extraction under dynamic fermentation and process conditions

Previous mathematical models of phenolic extraction during red wine fermentation have used single values to describe the overall extraction rate. The response equations for mass transfer parameters developed in Chapters 2 and 4 combined with knowledge on the effect of convective conditions allowed for dynamic simulations of anthocyanin extractions under fermentation conditions to be undertaken. In doing this, the impact of fermentation parameters (such as temperature, initial nutrient and yeast concentration, and rate of mixing) on the overall rate and extent of extraction could be quantitatively compared. These simulations are presented in the latter part of Chapters 3 and 4.

Objective 4: Validate the predictive capabilities of mass transfer models

Because the response equations and mass transfer parameters throughout this project were calculated based on the results of small scale (1.5 L) extractions, it was essential to examine the applicability of the developed mathematical models under scaled up conditions. As an initial approach to this, anthocyanin (specifically malvidin-3-glucoside) extraction curves from large-scale commercial red wine fermentations were compared with extraction simulations using the mathematical model developed in Chapters 2 and 3 for malvidin-3-glucoside, based on fermentation data supplied by the winery. A good agreement was found between the measured extraction curves and the simulations, showing the potential for using the derived mathematical models in predicting extraction during commercial fermentations. These results are presented in Chapter 5.

CHAPTER 2

Modelling the Mass Transfer Process of Malvidin-3-Glucoside during Simulated Extraction from Fresh Grape Solids under Wine-Like Conditions

Patrick C. Setford[1], David W. Jeffery[1,2], Paul R. Grbin[1,2], Richard A. Muhlack[1,2,*]

[1] Department of Wine and Food Science, School of Agriculture, Food and Wine, The University of Adelaide (UA), PMB 1 Glen Osmond SA 5064, Australia

[2] The Australian Research Council Training Centre for Innovative Wine Production, The University of Adelaide, PMB 1 Glen Osmond SA 5064, Australia

Molecules - **2018**, 23, 2159

Statement of Authorship

Title of Paper	Modelling the mass transfer process of malvidin-3-glucoside during simulated extraction from fresh grape solids under wine-like conditions
Publication Status	☑ Published ☐ Accepted for Publication ☐ Submitted for Publication ☐ Unpublished and Unsubmitted w ork w ritten in manuscript style
Publication Details	Setford, P. C., Jeffery, D. W., Grbin, P. R., & Muhlack, R. A. (2018). Modelling the Mass Transfer Process of Malvidin-3-Glucoside during Simulated Extraction from Fresh Grape Solids under Wine-Like Conditions. Molecules, vol. 23, no. 9, p. 2159.

Principal Author

Name of Principal Author (Candidate)	Patrick C. Setford		
Contribution to the Paper	Designed experiments, performed experimental work, performed laboratory analysis of samples (HPLC, viscometer), analysed and interpreted data, performed mathematical modelling, prepared entire first draft of the manuscript and helped address reviewer comments.		
Overall percentage (%)	70%		
Certification:	This paper reports on original research I conducted during the period of my Higher Degree by Research candidature and is not subject to any obligations or contractual agreements with a third party that would constrain its inclusion in this thesis. I am the primary author of this paper.		
Signature		Date	7/5/19

Co-Author Contributions

By signing the Statement of Authorship, each author certifies that:

i. the candidate's stated contribution to the publication is accurate (as detailed above);

ii. permission is granted for the candidate in include the publication in the thesis; and

iii. the sum of all co-author contributions is equal to 100% less the candidate's stated contribution.

Name of Co-Author	David W. Jeffery		
Contribution to the Paper	Contributed to the research idea and experimental design, assisted with laboratory analysis, assisted with interpretation of data, critically reviewed and edited the manuscript and helped address reviewer comments.		
Signature		Date	7/5/19

Name of Co-Author	Paul R. Grbin		
Contribution to the Paper	Contributed to the research idea and experimental design, assisted with interpretation of data, critically reviewed and edited the manuscript and helped address reviewer comments.		
Signature		Date	13/5/19

Name of Co-Author	Richard A. Muhlack		
Contribution to the Paper	Contributed to the conception of the article and experimental design, assisted with mathematical modelling, assisted with experimental setup and supervised the work. Helped prepare, edit and critically review the manuscript and helped address reviewer comments. Acted as the corresponding author.		
Signature		Date	7.5.2019

Please cut and paste additional co-author panels here as required.

molecules

MDPI

Article

Modelling the Mass Transfer Process of Malvidin-3-Glucoside during Simulated Extraction from Fresh Grape Solids under Wine-Like Conditions

Patrick C. Setford [1], David W. Jeffery [1,2], Paul R. Grbin [1,2] and Richard A. Muhlack [1,2,*]

[1] Department of Wine and Food Science, School of Agriculture, Food and Wine, The University of Adelaide, PMB 1, Glen Osmond SA 5064, Australia; patrick.setford@adelaide.edu.au (P.C.S.); david.jeffery@adelaide.edu.au (D.W.J.); paul.grbin@adelaide.edu.au (P.R.G.)

[2] The Australian Research Council Training Centre for Innovative Wine Production, The University of Adelaide, PMB 1, Glen Osmond SA 5064, Australia

* Correspondence: richard.muhlack@adelaide.edu.au; Tel.: +61-8-8313-6771

Received: 27 July 2018; Accepted: 24 August 2018; Published: 27 August 2018

Abstract: Extraction of grape components is a key consideration for red winemaking. The impact of changing process variables on mass transfer properties of anthocyanins from fresh pre-fermentative red grape solids under forced convective conditions was explored using the dominant red grape anthocyanin, malvidin-3-glucoside (M3G) as a model solute. A two level full factorial design was implemented to investigate effects of temperature, sugar and ethanol on mass transfer properties. Factor levels were chosen to simulate conditions found at various points during the maceration and fermentation steps of the red winemaking process. A rigorous mathematical model was developed and applied to experimental extraction curves, allowing the separation of mass transport properties in liquid and solid phases in a wine-like system, for the first time. In all cases, the coefficient of determination exceeded 0.92, indicating good agreement between experimental and mathematically-solved M3G concentrations. For the conditions studied, internal mass transfer was found to limit M3G extraction and changes to the liquid phase composition and temperature influence the distribution constant. Surface response models of mass transfer parameters were developed to allow future simulations of fermentation scenarios aimed at maximising the extraction potential of M3G.

Keywords: phenolic extraction; diffusion; anthocyanin; process modelling; wine colour; mass transfer

1. Introduction

Malvidin-3-*O*-β-D-glucoside (M3G) is frequently the focus of red wine research due to its relatively high importance to colour (including derived pigments) and overall quality. Understanding the effect of physical and chemical parameters on the extraction and subsequent evolution of phenolic compounds, and in particular anthocyanins, is crucial for producing red wine of high quality with desired sensorial characteristics.

In traditional red winemaking the grape solids typically remain in contact with the juice for around one to two weeks, from the time of grape crushing and well into the fermentation period of the must (fermenting juice and solids). During this time, anthocyanins are extracted from the semi-porous skins via the mechanism of solid-liquid diffusion, where the concentration slowly accumulates in the liquid over a period of several days until the rate of accumulation of monomeric anthocyanins is exceeded by the rate of subsequent reactions, including condensation, self-association, co-pigmentation, oxidation and physical adsorption processes with grape solids and yeast lees [1]. As a consequence

of fermentative maceration, the upward force from evolving carbon dioxide raises the grape solids to the top of the fermenting vessel, forming a cap which limits both the solid contact area with the bulk of the liquid and the phenolic potential of the wine. Winemakers typically adopt one of several methods to mix the solids and increase the solid-liquid contact area to help facilitate phenolic (including anthocyanin) extraction. Methods typically include either mechanically punching down the solids into the liquid to break up the cap, pumping over liquid from the bottom of the tank and spraying it over the top to resubmerge the cap, or fermenting in a baffled rotary tank that periodically revolves and submerges the solids into the liquid. Despite this, conflicting results on the method of contacting with respect to phenolic extraction potential have been found [1], indicating that solute diffusion within the solid to the solid-liquid interface may be limiting.

In the past, methods of enhancing contact between the solid and liquid phases of grape must have previously been qualitatively compared for different grape varieties [2,3]. To the authors' knowledge however, there have been no reported attempts at modelling these physical processes and systems to define what is happening at the solid-liquid interface so that the different extraction techniques can be systematically compared. Previously, simple correlations have been derived to model the extraction and subsequent evolution of anthocyanins and other phenolic compounds during red wine maceration and fermentation [4–6]. These forms of kinetic models can be used to provide information and insight into the impact of changing process conditions and are very effective at fitting experimental data. However, there is limited ability to quantitatively predict the effect of mixing (maceration) operations or changing process conditions during fermentation, such as temperature and liquid phase concentrations of ethanol, sugar, and water on the extraction kinetics and final equilibrium concentrations of phenolics. In contrast, empirical correlations in conjunction with systems of dimensionless numbers describing the fluid flow have been widely used in other biological systems to estimate the external diffusion coefficient of phenolic compounds. This method has been used in both semi-batch [7,8] and batch [9–11] solid-liquid extraction systems to determine the effect of mixing on the rate of phenolic extraction. This approach has not hitherto been applied to a red wine fermentation system.

This study sought to evaluate the mass transfer and diffusive properties of M3G as an important model solute during solid-liquid extraction from fresh red grape solids under forced convective conditions at various simulated stages of red wine fermentation with regards to varying solvent and temperature conditions.

2. Results and Discussion

2.1. Extraction Kinetics and Model Analysis

M3G extraction from fresh pre-fermentative Merlot grape pomace was examined using a 2^3 full factorial design under forced convective conditions with solutions differing in temperature, and sugar and ethanol concentrations to simulate fermentative extraction. Although forced convective conditions are usually only present during fermentative maceration during mechanical mixing operations (with the exception of the mixing effect caused by CO_2 evolution and temperature stratification), constant mixing was employed for this experiment so that the liquid phase could be considered a homogenous mixture without an anthocyanin concentration gradient. This allowed for the mass transfer properties of internal and external diffusion to be evaluated independently from one another and to provide an accurate evaluation of the extractive behaviour within the grape solids under the chosen experimental conditions. For all factor combinations, mean values of solid and liquid phase extraction and accumulation of M3G throughout maceration together with the model solution using the method described in Sections 3.2 and 3.3 are presented in Figure 1 and the mid-point is presented in Figure 2. For low- and mid-temperature levels (4.4 °C and 12.2 °C respectively), the concentration of M3G in the liquid phase increased throughout the extraction period, whereas at the high temperature level (23.1 °C) the concentration began to decrease after reaching a maximum. Because this work is concerned with modelling the extraction of M3G and the majority of anthocyanin extraction takes

place within the first days of liquid contacting, experimental data up to and including the maximum concentration in the liquid phase was used for modelling the extraction process according to Fick's second law.

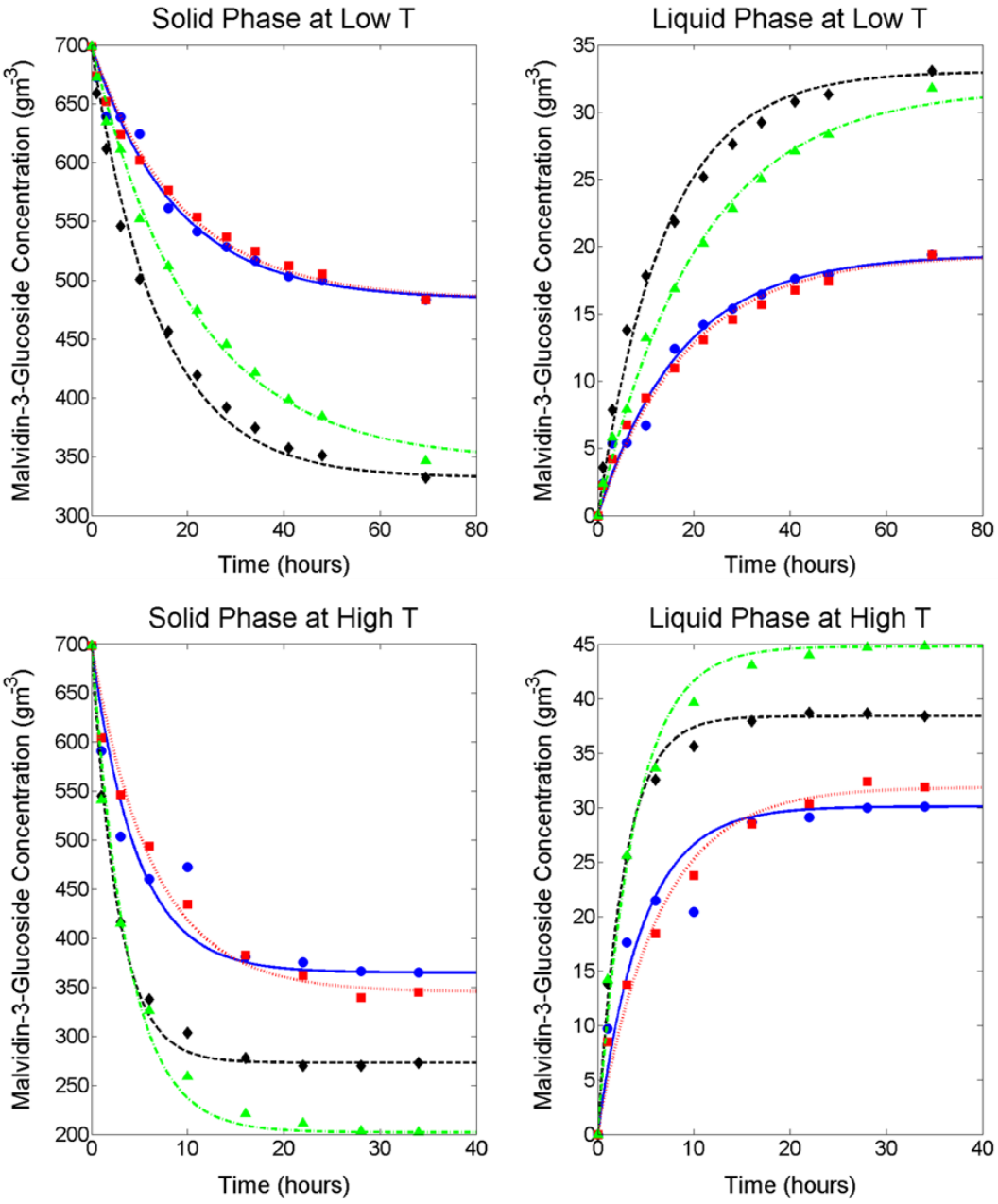

Figure 1. Experimental and fitted models for malvidin-3-glucoside solid phase depletion (**left**) and liquid phase accumulation (**right**) at low temperature (**upper**) and high temperature (**lower**) conditions. ●, water; ■, 266 g/L glucose; ♦, 14% v/v ethanol; ▲, 266 g/L glucose and 14% v/v ethanol.

Molecules **2018**, *23*, 2159

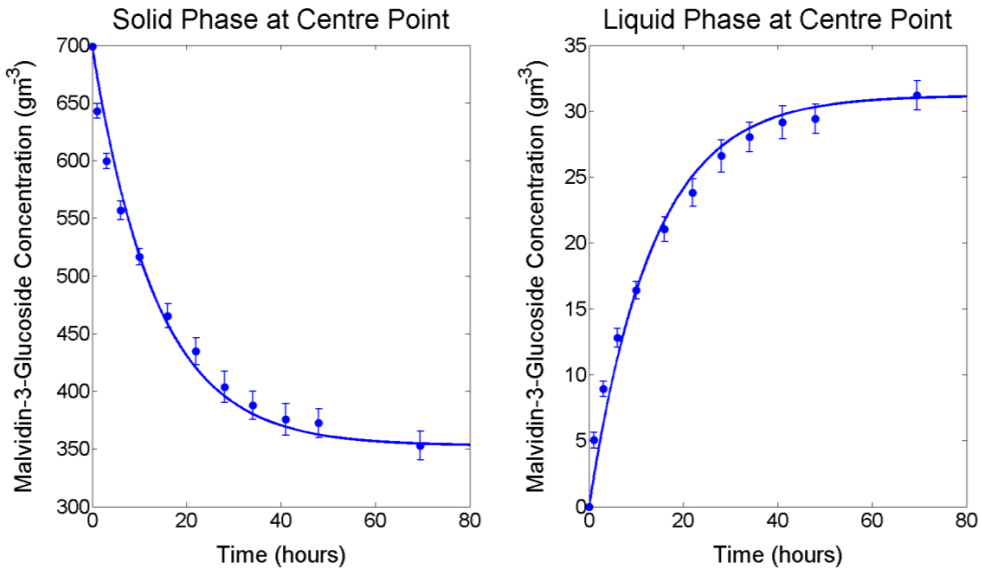

Figure 2. Experimental and fitted model for malvidin-3-glucoside solid phase depletion (**left**) and liquid phase accumulation (**right**) at the factorial centre point conditions (12.2 °C, 133 g/L glucose and 7% ethanol). Error bars represent standard deviation.

A summary of the internal and external diffusion and mass transfer coefficients, as well as several relevant mass transfer properties calculated are presented for each experimental condition in Table 1, together with R^2 and *RMSE* R^2 values were >0.92 and small *RMSE* values were observed in all cases. Inclusion of a replicated centre point within the full factorial design provided an estimate of standard error (ranging from 0.29 to 0.62 g m^{-3}) and repeatability (coefficient of variation (CV) of 0.12 for the initial 1 h extraction sample, followed by CV values ranging from 0.036 to 0.067) throughout the extraction process. Regression residuals are consistent with this standard error range, indicating the model developed and presented in Sections 3.2 and 3.3 can be used to effectively predict M3G extraction rates from fresh grape solids at conditions simulating various stages of the fermentation process.

Complete ANOVA tables for $D_{s\beta}$, $k_{c\beta}$ and K are provided in Tables S1–S3 respectively. As evidenced from the factorial analysis (presented in Table 2) and Figure 1, the inclusion of ethanol in the liquid phase had a positive influence on both the rate of extraction ($k_{c\beta}$) as well as the final concentration of M3G (K) at all temperature conditions ($p < 0.05$), although glucose was not found to significantly affect internal diffusion ($D_{s\beta}$) and mass transfer ($k_{c\beta}$). This may be due to ethanol improving the solvent properties of the penetrating liquid allowing easier dissolution of anthocyanins. The main effect of glucose on K is significant ($p < 0.01$), however the factor effect is approximately 70% smaller than that of either temperature or ethanol. Therefore, at low temperature conditions, it appears that the inclusion of glucose in the liquid phase had only a minor influence on the final concentration of M3G when compared to the pure water extracts and 14% ethanol extracts, respectively. In contrast, at high temperature conditions, the inclusion of both glucose and ethanol resulted in an increase in final concentration of M3G in the liquid phase when compared to the extract containing only 14% ethanol, with factorial analysis confirming temperature, glucose and ethanol effects on K were all significant ($p < 0.05$). This result indicates a previously unobserved phenomenon whereby at higher temperatures, glucose in the presence of ethanol appeared to aid the extraction rate and maximum extractability of M3G. Although interesting, the scenario of high sugar and high ethanol concentrations is unlikely to be observed in a typical red winemaking operation and was necessary only to fulfil the requirements of the experimental design. In agreement with other studies [12,13], increasing the temperature of the system had a large positive impact on both the rate and the final extraction yield of anthocyanins.

Table 1. Summary of mass transfer properties ($D_{s\gamma}$, $k_{c\gamma}$, $D_{s\beta}$, $k_{c\beta}$ and K), Biot numbers (Bi) and statistical parameters ($RMSE$ and R^2) for malvidin-3-glucoside solved using the method outlined in Sections 3.2 and 3.3.

Trial Conditions			Diffusion and Mass Transfer Properties						Model Fit	
Temp.	**Glucose**	**Ethanol**	D_{Sy} (m^2 s^{-1})	K_{cy} (m s^{-1})	$D_{S\beta}$ (m^2 s^{-1})	$K_{c\beta}$ (m s^{-1})	K	Bi	$RMSE$	R^2
Low	Low	Low	4.68×10^{-12}	1.89×10^{-4}	6.04×10^{-14}	7.09×10^{-11}	4.01×10^{-2}	2.18×10^{4}	0.955	0.978
Low	Low	High	2.76×10^{-12}	1.20×10^{-4}	1.29×10^{-13}	1.51×10^{-10}	9.95×10^{-2}	1.62×10^{4}	1.073	0.990
Low	High	Low	2.14×10^{-12}	9.79×10^{-4}	5.67×10^{-14}	6.65×10^{-11}	4.01×10^{-2}	1.20×10^{4}	0.765	0.984
Low	High	High	1.17×10^{-12}	5.84×10^{-4}	8.22×10^{-14}	9.64×10^{-11}	9.17×10^{-2}	1.13×10^{4}	0.748	0.995
Mid	Mid	Mid	3.58×10^{-12}	1.48×10^{-4}	1.26×10^{-13}	1.47×10^{-10}	8.84×10^{-2}	1.81×10^{4}	1.346	0.982
High	Low	Low	8.29×10^{-12}	3.00×10^{-4}	3.51×10^{-13}	4.12×10^{-10}	8.25×10^{-2}	1.23×10^{4}	2.685	0.925
High	Low	High	5.71×10^{-12}	2.18×10^{-4}	7.55×10^{-13}	8.85×10^{-10}	1.41×10^{-1}	7.05×10^{3}	1.062	0.993
High	High	Low	4.26×10^{-12}	1.71×10^{-4}	2.71×10^{-13}	3.18×10^{-10}	9.24×10^{-2}	1.01×10^{4}	1.592	0.978
High	High	High	2.77×10^{-12}	1.18×10^{-4}	6.43×10^{-13}	7.54×10^{-10}	2.22×10^{-1}	7.09×10^{3}	1.674	0.988

Full factorial analysis of variance (ANOVA) was conducted for experimentally determined parameters of solid-phase (internal) diffusivity ($D_{s\beta}$), solid phase (internal) mass transfer coefficient ($k_{c\beta}$), and distribution constant (K), with factor effects and associated statistical significance shown in Table 2.

Table 2. Factor effects and statistical significance of experimentally determined model parameters: solid-phase (internal) diffusivity ($D_{s\beta}$), solid phase (internal) mass transfer coefficient ($k_{c\beta}$) and distribution constant (K)

	$D_{S\beta}$		$K_{c\beta}$		K	
Coefficient	**Factor Effect**	***p* Value**	**Factor Effect**	***p* Value**	**Factor Effect**	***p* Value**
Temp. (A)	4.29×10^{-13}	1.81×10^{-5} ***	5.03×10^{-10}	1.81×10^{-5} ***	6.70×10^{-2}	3.56×10^{-6} ***
Glucose (B)	-6.58×10^{-14}	2.03×10^{-1}	-7.71×10^{-11}	2.03×10^{-1}	2.06×10^{-2}	8.64×10^{-3} **
Ethanol (C)	2.17×10^{-13}	1.84×10^{-3} **	2.54×10^{-10}	1.84×10^{-3} **	7.49×10^{-2}	1.53×10^{-6} ***
AB	-4.09×10^{-14}	4.14×10^{-1}	-4.80×10^{-11}	4.14×10^{-1}	2.45×10^{-2}	3.39×10^{-3} **
AC	1.70×10^{-13}	7.28×10^{-3} **	1.99×10^{-10}	7.28×10^{-3} **	1.93×10^{-2}	1.19×10^{-2} *
BC	-1.77×10^{-14}	7.18×10^{-1}	-2.08×10^{-11}	7.18×10^{-1}	1.58×10^{-2}	2.91×10^{-2} *
ABC	3.35×10^{-15}	9.45×10^{-1}	3.94×10^{-12}	9.45×10^{-1}	1.98×10^{-2}	1.07×10^{-2} *

*, ** and *** represent factors that are statistically significant at the 5%, 1% and 0.1% levels, respectively.

This result could be explained by the increased solubility and diffusivity of M3G at higher temperatures as well as an increased rate of swelling and softening of the solid material [12].

As shown in Table 1, internal solid diffusion rates obtained from the model solution are approximately one to two orders of magnitude smaller than their respective external diffusion rates in the liquid phase. This is expected, as internal diffusion encompasses liquid penetration, solute dissolution and the subsequent diffusion through the solid matrix, which is a tortuous diffusion path [10]. Furthermore, the internal mass transfer coefficients are six to seven times smaller in order of magnitude than the respective external mass transfer coefficients, giving a good indication that the extraction of M3G in this system is heavily dependent on diffusion within the solid. In general, diffusion within the solid is typically the rate-controlling step during solid-liquid extraction of phenolic compounds [13,14]. The extent of control can be numerically indicated as the mass analogue of the Biot number (full nomenclature and equation notation can be found in Appendixs A–D):

$$Bi = \frac{k_{c\gamma} LK}{D_{s\beta}} \quad (1)$$

A Biot number exceeding 10 indicates that internal diffusion within the solid is the controlling step of the extraction process. In the present study, values of $Bi > 10^4$ were determined for all factor combinations, confirming that the internal diffusion within the solid was indeed the rate limiting step of the extraction process. Such high Biot numbers are due to the constant mixing and relatively high liquid velocity, whereas in a traditional red wine fermentation scenario this is unlikely to be the case. Mixing operations during fermentation are typically performed intermittently throughout the extraction process, and for the majority of the time, any mixing in the liquid phase would be the result of evolved CO_2 displacing the liquid. Because of this, the internal mass transfer rates solved for each set of conditions in this study represent the maximum extraction rates possible for a real red wine fermentation and provide insight into the minimum time required to achieve the maximum potential M3G concentration.

Nonetheless, understanding the Biot number and how it can be manipulated under different conditions could be used in the targeted development of mixing technology to optimise the mass transfer coefficient in the liquid phase. This could be accomplished by controlling the fluid velocity in a way that does not compromise the quality of the wine through increased oxidation nor interfere with downstream processing through the potentially increased destruction of grape solids (primarily skins) resulting from vigorous extraction procedures and mixing operations. Schmidt and Velten [15] found the average velocity of the liquid phase at the most active stages of wine fermentation to be approximately 0.21–0.60 m s^{-1}. At the lower end of these velocities and where the effects of mixing due to fermentation are minimal, extraction could be such that internal diffusion is no longer the rate-determining step in the extraction of M3G (and other phenolic compounds). As such, an interesting area for further study would be to examine the effects of free convective conditions at various stages of red wine fermentation in order to calculate external mass transfer coefficients and gain further insight into the importance of mixing operations, their induced liquid velocities, the timing of mixing, and the length of time required to adequately facilitate the extraction process. Such insight would be of additional value due to the compressible nature of grape solids, whereby the upward force of evolving carbon dioxide during fermentative maceration results in a separation of the solids with the bulk of the liquid. This could be considered to be causing an additional liquid phase mass transfer step, as the solute at the solid-liquid interface must first diffuse into the interstitial liquid within the skin cap before making its way into the liquid bulk via liquid phase diffusion through the cap or by forced convection caused by mixing operations.

In agreement with other studies that model the extraction of anthocyanins from various biological materials [7,9,13], the internal diffusion and mass transfer coefficients were found to be higher at higher temperatures, and the inclusion of ethanol in the liquid phase at wine-relevant concentrations was also found to promote the rate of internal diffusion. For each set of solvent conditions, the distribution constant K at high temperature is found to be approximately double that found at the respective

low temperature (shown in Table 1). Because the distribution constant is a linear function of the solid-liquid ratio (as shown in Equation (8)), the values found at each condition could be used to either help maximise the concentration of M3G or optimise it towards a specific desired concentration in red wine ferments that will maximise the perceived quality of the finished product. Notably, the lower distribution constant values found in this study at low ethanol concentrations (Table 1) provide evidence that maceration techniques prior to fermentation (particularly when conducted at colder temperatures) may have little impact on the final concentration of anthocyanins after the skins are removed from the wine, and that extended maceration upon the completion of fermentation, where a higher concentration of ethanol is in the liquid phase, is more likely to increase the final anthocyanin concentration. This finding also helps to explain experimental results from other studies such as that by Koyama et al. [16], who found that undertaking a cold soaking operation prior to the fermentation of red wine resulted in a slower initial extraction rate of anthocyanins and proanthocyanidins but has no significant effect on the maximum concentrations of these phenolic compounds at the end of a 10-day maceration period.

2.2. Response Surface Analysis

From the design of the experiment and the applied statistical analysis, expressions were generated that allowed for the estimation of the internal diffusion coefficient ($D_{s\beta}$) and distribution constant (K) within the range of experimental conditions using statistically significant variables:

$$D_{s\beta} = 2.75 \times 10^{-13} + 2.11 \times 10^{-13}T + 1.09 \times 10^{-16}C_{EtOH} + 8.52 \times 10^{-14}TC_{EtOH} \quad (2)$$

$$\begin{aligned} K = 9.97 \times 10^{-2} &+3.33 \times 10^{-2}T + 1.04 \times 10^{-2}C_g + 3.74 \times 10^{-2}C_{EtOH} \\ &+1.23 \times 10^{-2}TC_g - 9.64 \times 10^{-3}TC_{EtOH} + 7.91 \times 10^{-3}C_gC_{EtOH} \\ &+9.86 \times 10^{-3}TC_gC_{EtOH} \end{aligned} \quad (3)$$

where T is the temperature (°C), C_g is the concentration of sugar in the liquid phase (g L^{-1}) and C_{EtOH} is the concentration of ethanol in the liquid phase (% v/v) scaled in terms of the coded variables used in the ANOVA (-1 for low, 0 for the midpoint and 1 for the high values, respectively). Graphical representations of the resulting response surfaces are presented in Figure 3, where the effect of ethanol and glucose concentrations at the low and high temperature conditions used for the factorial design are shown. From Figure 3, a clear increase in $D_{s\beta}$ with increasing ethanol concentration can be seen, as well as an order of magnitude increase in $D_{s\beta}$ from low to high temperature. From the analysis of variance in Table 2, it can be seen that the factor effect of glucose on internal diffusion is negative, however the overall significance across the range of the factorial experiment is negligible ($p > 0.05$).

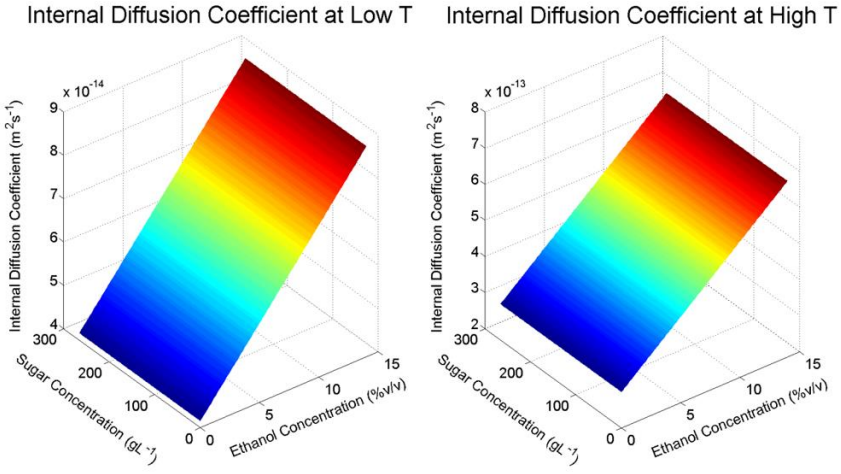

Figure 3. *Cont.*

Molecules **2018**, *23*, 2159

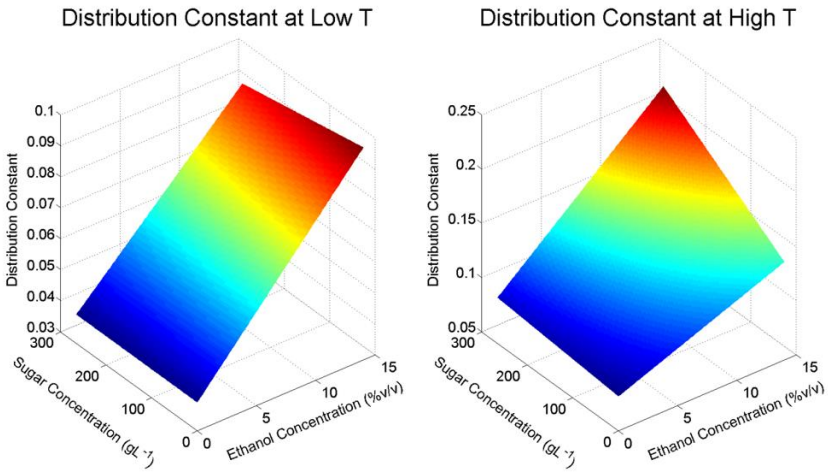

Figure 3. Surface response of malvidin-3-glucoside internal diffusion coefficient, $k_{c\beta}$ (**upper**) and distribution constant, K (**lower**) at changing solvent conditions for low temperature (**left**) and high temperature (**right**) in the factorial design.

2.3. Application

In recent years, several studies have highlighted a lack of knowledge regarding the kinetics and mechanisms of phenolic extraction during red wine fermentation [1,17]. Due to this absence of understanding and despite the crucial role of phenolics to wine quality, a distinct difficulty exists with the informed manipulation of the phenolic content during the fermentative maceration phase. The method developed in this study to model the extraction of M3G from fresh grape solids under simulated red wine processing conditions allows for the separation of the mass transfer properties in the solid and liquid phases respectively—An important distinction from studies that have previously modelled extraction during fermentation. The current method gives greater insight into the extractive behaviour of M3G under different process conditions simulating those found during real winemaking scenarios. In doing this, the mass transfer properties determined in this study could be used to simulate the extraction of M3G under different conditions and various fermentation scenarios where the liquid phase is a medium with continuously changing ethanol and sugar concentrations. In this way, simulations using the presented mass transfer coefficients and distribution constants could be used to inform winemakers of optimal temperature conditions, the extent and time of fermentative mixing operations, and the time of pressing from skins to achieve a desired extraction rate or final anthocyanin concentration, prior to commencing a real-time fermentation. Additionally, the ability to predict and simulate extraction scenarios could be used to inform the targeted development of mixing technologies that include the optimisation of velocity in a way that maximises the external mass transfer and extraction potential without compromising the quality of the finished product or the ability to manage the grape solids in downstream processes.

3. Materials and Methods

3.1. Experimental

3.1.1. Experimental Design

A 2^3 full factorial design run in duplicate with centre point run in quadruplicate was used to investigate the effect of temperature, ethanol concentration, sugar (glucose) concentration, and their interactions, on the rate and extent of M3G extraction. Ethanol and glucose were added to water at low and high level concentrations chosen to emulate conditions that would be found in unfermented juice (0% v/v ethanol and 266 g L^{-1} sugar) and in the equivalent finished red wine (14% v/v ethanol and 0 g L^{-1} sugar). Other chemical compounds typically found in wine were not included in order to

understand the direct impact of the two largest components of red grade juice and wine responsible for the physical properties of the liquid, thus limiting confounding variables. As such, pH values were not adjusted but were determined to be 3.7 and 3.9 after one hour of extraction. Low and high extraction temperatures nominally set at 0 °C and 20 °C were chosen to investigate the impact on extraction rate during fermentation as well as to allow for conclusions to be drawn regarding extraction during low temperature processes common in commercial winemaking such as pre-fermentative cold soaking. Real-time data logging of the winery cold rooms used for this investigation showed ambient air temperatures of 4.4 °C and 23.1 °C, respectively, with a mid-point temperature of 12.2 °C. As such, these temperatures were used for the purposes of mathematical modelling and subsequent generation of results as they represent realistic industry conditions.

3.1.2. Sample Preparation

Fresh Merlot grapes were hand harvested (total soluble solids of 14.3° Baumé, pH 3.6, titratable acidity (to pH 8.2) of 3.9 g L^{-1}) on 24 February 2016 and kept for 7 days in a 0 °C cool room until crushing. Berries were destemmed by hand and the total weight prior to crushing was recorded. A total of 9.05 kg of randomly sampled berries were then crushed by hand using a hand plunger until all berries were visibly crushed and no whole berries remained intact. The must was then pressed using a 4.4 L, hand operated, stainless steel basket press to separate the solids (skins and seeds) and liquid juice. The total mass of pressed solids was 4.00 kg and the volume of juice was 4.55 L. giving a solid to liquid ratio of 0.88 kg L^{-1}.

3.1.3. Extraction Procedure

Portions of the pressed solids (150 g of skins and seeds) were placed into 2 L containers and 1.5 L of extraction solvent (as described in Section 3.1.1) were then added to begin the extraction process. A lower solid/liquid ratio than found in a typical red wine fermentation was chosen for the extraction procedure in order to limit the reaction rate between anthocyanins and other extracted compounds that could impact the perceived extraction rate. These solvents were prepared 48 h prior to the commencement of extraction and placed into the respective 0, 10 and 20 °C cool rooms to equilibrate to the ambient air temperature. Upon the addition of the liquid phase, lids were placed on the vessels with each having an approximately 1 cm diameter hole to allow insertion of the shaft of an overhead mechanical stirrer. The vessel contents were continually stirred at a speed of approximately 300 rpm to ensure the system was well-mixed and to allow for the calculation of mass transfer variables within the liquid phase. Samples (10 mL) were taken throughout the extraction process until an equilibrium was reached, with samples taken more frequently within the first 12 h of the extraction so that appropriate concentration curves could be generated. Samples were immediately centrifuged at 3220 rcf for 10 min and the supernatant decanted and kept at −20 °C until their analysis by HPLC. Solid phase M3G concentrations were calculated via mass balance based on the initial concentration in the solids.

3.1.4. Quantification of Malvidin-3-Glucoside

Prior to HPLC analysis, samples were defrosted at ambient conditions and 2 mL of sample were then centrifuged at 9300 rcf to remove any suspended solids. 1.5 mL of supernatant was then transferred to amber HPLC vials for analysis. HPLC analyses were performed using an Agilent 1100 Instrument (Agilent, Forest Hill, VIC, Australia) equipped with a quaternary pump and diode array detector (DAD), using gradient elution based on the method described by Cozzolino et al. [18] with a slight modification as detailed by Mercurio et al. [19]. Data acquisition and processing were performed using Agilent ChemStation software (version B.01.03). A 20 µL injection volume was used for each sample, and chromatograms were recorded at 280, 320, 370 and 520 nm. M3G was quantified at 520 nm by comparison of its retention time and absorbance using malvidin-3-*O*-glucoside chloride (≥95% by HPLC) purchased from Extrasynthese (Genay, France) and prepared volumetrically in 0.2% aqueous acetic acid as an external standard.

3.1.5. Measurement of Total Malvidin-3-Glucoside Concentration in Solids

Triplicate samples of 250 g of the freshly pressed grape solids were homogenised using a Grindomix GM200 homogeniser (Retsch, Haan, Germany) at a speed of 8000 rpm for 20 seconds. The homogenate was then well mixed and approximately 1 g was transferred to a 10 mL centrifuge tube, 10 mL of 50% v/v aqueous ethanol was added and the mixture was inverted every 10 min by hand throughout a one hour extraction period. The mixture was then centrifuged at 3220 rcf for 10 min and the supernatant transferred to a new centrifuged tube and frozen at -20 °C until HPLC analysis as described above (method adapted from Mercurio et al. [19]). Prior to injection, these samples were diluted to 12.5% v/v aqueous ethanol in water.

3.1.6. Measurement of Physical Parameters

A Viscoball Höppler viscometer (Fungilab, Barcelona, Spain) was used to measure the viscosity of the extraction solutions at the extraction temperatures used during this experiment. Cameras (model KYT-U130-01MBWCS, Kayeton Technology Company Ltd, Shenzhen, China) at a frame rate of 30 frames per second were used to monitor the start and end points of the viscometer in order to increase the precision of time measurements.

3.2. Model Development

During the maceration stage of winemaking, anthocyanins compounds from the grape skins are extracted by two main mechanisms. The first of these is a fast leakage that occurs at the edges of broken skin cells as a result of crushing, followed by diffusion across the solid layers in a direction perpendicular to the surface of the skin towards the interior of the berry for the remainder of the solid-liquid contact period [1,20,21]. In general, the solid-liquid extraction of phenolic compounds from porous solid particles is a concentration-driven process that involves three steps which encapsulate internal diffusion. These are:

(1) Solvent diffusion into the porous solid
(2) Solute dissolution into the solvent
(3) Dissolved solute diffusion to the particle surface

From here, a final mass transfer step takes place whereby the dissolved solute must then travel from the particle surface to the surrounding solvent, either through free convective diffusion or through forced convective mixing [1,13,14]. Because grape skins have an outer waxy layer that impedes liquid penetration (and thus extraction of anthocyanins and other phenolics) it was assumed that after crushing, diffusion within the solid occurred primarily along the perpendicular axis to the main face of the skin in a single direction across the whole thickness of the skin (L), which can be considered a plane surface. As such, Fick's second law can be applied to describe diffusion within the solid phase:

$$\frac{\partial c_\beta}{\partial t} = D_{s\beta} \frac{\partial^2 c_\beta}{\partial x^2} \tag{4}$$

where x is the distance co-ordinate in the direction of diffusion. Diffusion takes place only in a single direction (as opposed to a leaf for instance where diffusion would take place in both directions perpendicular to the face of the leaf) so the distance coordinate extends from $x = 0$ to $x = L$.

For particles of a fixed geometry, previous studies [20,21] have demonstrated that the mass transfer by averaged effective diffusion within both phases can be represented as a macroscopic mass transfer system of ordinary differential equations—A typical simplification used in mass transfer operations [22] which has previously been used to model solid-liquid phenolic extraction in vanilla pods [10] and coffee beans [11]:

$$\varepsilon \frac{dc_\gamma}{dt} = k_{c\gamma} a \left(c_{\gamma i} - c_\gamma\right) \tag{5}$$

$$(1-\varepsilon) \frac{dc_\beta}{dt} = k_{c\beta} a \left(c_{\beta i} - c_\beta\right) \tag{6}$$

$$k_{c\gamma} \left(c_{\gamma i} - c_\gamma\right) = -k_{c\beta} a \left(c_{\beta i} - c_\beta\right) \tag{7}$$

$$c_{\gamma i} = K c_{\beta i} \tag{8}$$

where Equation (8) presents a distribution constant allowing for the description of the equilibrium between phases.

In order to relate the microscopic and macroscopic mass transfer properties, an analytical solution of Fick's second law is required. The solution to Equation (4) is an infinite Fourier series analogous to conductive heat transfer in 1-dimension:

$$\begin{aligned} \frac{c_\beta - c_{\beta i}}{c_{\beta 0} - c_{\beta i}} = \frac{4}{\pi} \Big[\frac{1}{1} exp\Big(-\frac{1^2 \pi^2 X}{4}\Big) sin \frac{1\pi x}{2L} + \frac{1}{3} exp\Big(-\frac{3^2 \pi^2 X}{4}\Big) sin \frac{3\pi x}{2L} \\ + \frac{1}{5} exp\Big(-\frac{5^2 \pi^2 X}{4}\Big) sin \frac{5\pi x}{2L} + \ldots \Big] \end{aligned} \tag{9}$$

where:

$$X = \frac{D_{s\beta} t}{L^2} \tag{10}$$

Using an approximation described by Stapley [23] and employed by others [10,11], the faster decaying terms of the summation can be neglected due to the fact that for sufficiently high values of t, these terms decay to a negligible amount (second and third terms decay 9 and 25 times faster than the first with a third and fifth of the amplitude, respectively), and the first term can be used to approximate the solution. Therefore, at the boundary layer where $x = L$:

$$\frac{c_\beta - c_{\beta i}}{c_{\beta 0} - c_{\beta i}} = \frac{4}{\pi} exp\left(-\frac{\pi^2 D_{s\beta} t}{4L^2}\right) \tag{11}$$

Rearranging Equation (11) and taking the derivative of c_β with respect to t gives:

$$\frac{dc_\beta}{dt} = \frac{\pi^2 D_{s\beta}}{4L^2} \left(c_{\beta i} - c_\beta\right) \tag{12}$$

The simplified microscopic model, Equation (12), can now be compared with the macroscopic model, Equation (6), to yield the following equation relating internal diffusion and internal mass transfer:

$$D_{s\beta} = \frac{k_{c\beta} 4L}{(1-\varepsilon)\pi^2} \tag{13}$$

3.3. Parameter Estimation and Statistical Analysis

An analytical solution to the macroscopic model described by Equations (5) and (6) obtained by Laplace transformation was proposed by Espinoza-Pérez, Vargas, Robles-Olvera, Rodrıíguez-Jimenes and Garcıía-Alvarado [11] and yielded the following set of simultaneous equations describing the average concentration within both phases:

$$c_\beta = c_{\beta 0} \left(C_1 e^{r_1 t} + C_2 e^{r_2 t}\right) \tag{14}$$

$$c_\gamma = c_{\beta 0} \left(C_3 e^{r_1 t} + C_4 e^{r_2 t}\right) \tag{15}$$

where:

$$r_{1,2} = -\frac{b_1+b_2}{2} \pm \frac{\sqrt{(b_1+b_2)^2-4(b_1b_2-b_3b_4)}}{2}$$

$$C_1 = \frac{r_1+b_1}{r_1-r_2}, C_2 = \frac{r_2+b_1}{r_2-r_1}, C_3 = \frac{b_3}{r_1-r_2}, C_4 = \frac{b_3}{r_2-r_1}$$

$$b_1 = \frac{k_{c\gamma}a(1-\psi_1)}{\varepsilon}, b_2 = \frac{k_{c\beta}a\left(1-\frac{\psi_2}{K}\right)}{(1-\varepsilon)}, b_3 = \frac{k_{c\gamma}a\psi_2}{\varepsilon}, b_4 = \frac{k_{c\beta}a\frac{\psi_1}{K}}{(1-\varepsilon)}$$

$$\psi_1 = \frac{1}{1+\frac{k_{c\beta}}{Kk_{c\gamma}}}, \ \psi_2 = \frac{k_{c\beta}/k_{c\gamma}}{1+\frac{k_{c\beta}}{Kk_{c\gamma}}}$$

In order to calculate the external mass transfer coefficient, the following system of dimensionless equations that describe the forced convective mass transfer around spheres was used [22]:

$$Sh = 2 + 0.95Re^{\frac{1}{2}}Sc^{\frac{1}{3}} \tag{16}$$

where the Reynolds number (Re) was estimated as a function of the mixer diameter (D) and revolutionary speed (N) in revolutions per second:

$$Re = \frac{ND^2\rho_\gamma}{\mu_\gamma}, \ \ Sh = \frac{k_{c\gamma}L}{D_{s\gamma}}, \ \ Sc = \frac{\mu_\gamma}{\rho_\gamma D_{s\gamma}} \tag{17}$$

In order to obtain the external diffusion coefficient ($D_{s\gamma}$) required to calculate the Schmidt and Sherwood numbers and thus solve the dimensionless system, the Wilke-Chang correlation was used:

$$D_{s\gamma} = \frac{1.173 \times 10^{-16}(\varphi M_\gamma)^{1/2}T}{\mu_\gamma V_A^{0.6}} \tag{18}$$

The molar volume of the solute (V_A) was estimated using an additive method described by Geankoplis [22] based on the chemical structure of M3G, and the average molecular mass and association factor of the liquid phases were estimated based on the mole fractions of ethanol, water and glucose in each trial:

$$M_\gamma = x_{EtOH}M_{EtOH} + x_{water}M_{water} + x_{Glucose}M_{Glucose} \tag{19}$$

$$\varphi = x_{EtOH}\varphi_{EtOH} + x_{water}\varphi_{water} + x_{Glucose}\varphi_{Glucose} \tag{20}$$

Finally, the internal mass transfer coefficient of M3G ($k_{c\beta}$) was obtained through a non-linear regression of Equations (14) and (15) using MATLAB software (version R2013a), whereby the residuals of the model solution were set to be minimised. A summary of the physical parameters, system variables and their method for determination is presented in Table 3.

Table 3. Summary of shape variables and physical properties of the system.

Property or Shape Variable	Value	Source
a (m^2 m^{-3})	5747	Mathematically derived
ε	0.9173	Experimentally determined
$c_{\beta 0}$ (kg m^{-3})	6.987×10^{-1}	Experimentally determined
L (m)	1.74×10^{-4}	Jin et al. [24]
V_A (L mol^{-1})	0.5259	Geankoplis [22]
μ_γ (cP)	Varied	Experimentally determined
ρ_γ (kg m^{-3})	Varied	HYSYS (Hysys, Operations Guide., 2005)
M_γ (g mol^{-1})	Varied	Equation (19)
φ	Varied	Equation (20)

Molecules **2018**, *23*, 2159

In order to determine the efficacy of the proposed model's fit with respect to experimental data, two parameters, the coefficient of determination (R^2) and the root mean square error ($RMSE$), were analysed for each set of experimental conditions. The coefficient of determination and root mean square error were determined by:

$$R^2 = 1 - \frac{\sum_{i=1}^{N}\left(c_{\gamma,pred,i} - c_{\gamma,exp,i}\right)^2}{\sum_{i=1}^{N}\left(c_{\gamma,pred,i} - \overline{c}_{\gamma,exp}\right)^2} \tag{21}$$

$$RMSE = \sqrt{\frac{1}{N}\sum_{i=1}^{N}\left(c_{\gamma,pred,i} - c_{\gamma,exp,i}\right)^2} \tag{22}$$

where $c_{\gamma,exp,i}$ is the experimentally determined concentration in the liquid phase, $c_{\gamma,pred,i}$ is the concentration in the liquid phase predicted by the model, $\overline{c}_{\gamma,exp}$ is the mean value of the experimentally-determined concentrations in the liquid phase and N is the number of data points for each experimental condition. The influence of changing experimental conditions was assessed for the internal diffusion coefficient ($D_{s\beta}$), external mass transfer coefficient ($k_{c\gamma}$) and distribution constant (K) by the analysis of variance (ANOVA). The significance of each parameter was determined by the corresponding p values, where values of $p < 0.05$ were deemed significant.

The inclusion of a centre point in the experimental design allowed for the development of a response surface (R) to be generated, where values of the internal diffusion coefficient and distribution constant were solved at each set of conditions were used to minimise the sum of squared residuals:

$$R = b_0 + b_1T + b_2C_g + b_3C_{EtOH} + b_4TC_g + b_5TC_{EtOH} + b_6C_gC_{EtOH} + b_7TC_gC_{EtOH} \tag{23}$$

where b_0 is the value of the function at the centre point conditions b_1, b_2, b_3 represent the effects of individual parameters associated to their respective variable, and b_4, b_5, b_6 and b_7 represent the crossed effects between variables. A clear distinction should be noted between the response surface equation and that which would be generated from the main effects in the ANOVA analysis, as the response equation is calculated by minimising the mean square error and includes a centre point to improve the model fit and thus the predictive capacity of response variables at points within the range of the experimental design. Furthermore, the inclusion of a centre point in the experimental design allowed for the calculation of standard error and standard deviation for this set of experimental conditions, which gave insight into the repeatability of the extractions across the experimental design.

4. Conclusions

Extraction curves showing M3G extraction from fresh Merlot grape solids under simulated red wine processing conditions have been reported and analysed. Rigorous mass transfer equations based on first principles and empirical correlations that describe this process were used to develop a complete mathematical model capable of accounting for both diffusion within the solid phase and the effect of mixing. The R^2 values of the proposed model indicated that it can be reliably used to predict M3G extraction through the calculation of internal and external mass transfer coefficients. In this study, the limiting factor for M3G extraction was found to be internal mass transfer while changes to the temperature and liquid phase composition directly impacted the distribution constant (and thus the maximum extractability). The design of the experiment allowed for a response surface equation to be developed that is capable of predicting the internal diffusion coefficient and distribution constant at conditions not experimentally evaluated. The development of these equations will allow for future computer simulation case studies to be conducted in order to predict the extraction of M3G (or other phenolics) during an active red wine fermentation scenario with continuously changing liquid phase conditions.

Supplementary Materials: Supplementary Materials are available online.

Author Contributions: P.C.S., R.A.M., D.W.J. and P.R.G. conceived and designed experiments; P.C.S. performed the experiments and conducted laboratory analysis of samples; P.C.S., R.A.M., D.W.J. and P.R.G. interpreted the data; P.C.S. and R.A.M. conducted the mathematical modelling; P.C.S. drafted the original manuscript; R.A.M., D.W.J. and P.R.G. provided critical feedback and editing. All authors have read and approved the final manuscript.

Funding: P.C.S. is supported through a UA School of Agriculture, Food and Wine Scholarship [1606990] and was also a recipient of a Wine Australia supplementary scholarship [AGW Ph1505]. The authors acknowledge the financial support from the School of Agriculture, Food and Wine, UA, and Australian grapegrowers and winemakers through their investment body, Wine Australia, with matching funds from the Australian Government.

Conflicts of Interest: The authors declare no conflicts of interest.

Appendix A

a	Specific surface area for mass transfer (m^2 m^{-3})
$b_1, \ldots, b_4$	Constants required to solve Equations (14) and (15)
c	Phenolic compound concentration (g m^{-3})
$C_1, \ldots, C_4$	Constants required to solve Equations (14) and (15)
C_{EtOH}	Ethanol concentration (% v/v)
C_g	Glucose concentration (g L^{-1})
D	Mechanical stirrer diameter (m)
D_s	Solute (s) mass diffusivity (m^2 s^{-1})
k_c	Mass transfer coefficient (m s^{-1})
K	Distribution constant
L	Characteristic length for diffusive mass transfer (m)
M	Molar mass (g mol^{-1})
N	Stirrer speed (rpm)
$r_{1,2}$	Constants required to solve Equations (14) and (15)
R^2	Coefficient of determination
$RMSE$	Root mean square error
t	Time (s)
T	Temperature (°C)
V_A	Solute molar volume (L mol^{-1})

Appendix B

Bi	Biot number
Re	Reynolds number
Sc	Schmidt number
Sh	Sherwood number

Appendix C

ε	Solvent volume fraction
φ	Association parameter
μ	Dynamic viscosity (kg m^{-1} s^{-1})
ρ	Density (kg m^{-3})
$\psi_{1,2}$	Constants required to solve Equations (14) and (15)

Appendix D

0	At the initial or reference point
e	At the equilibrium stage
exp	Experimentally obtained
i	At the solid-liquid interface
$pred$	Predicted by model
β	Solid phase
γ	Liquid phase

References

1. Setford, P.C.; Jeffery, D.W.; Grbin, P.R.; Muhlack, R.A. Factors affecting extraction and evolution of phenolic compounds during red wine maceration and the role of process modelling. *Trends Food Sci. Technol.* **2017**, *69*, 106–117. [CrossRef]
2. Fischer, U.; Strasser, M.; Gutzler, K. Impact of fermentation technology on the phenolic and volatile composition of german red wines. *Int. J. Food Sci. Technol.* **2000**, *35*, 81–94. [CrossRef]
3. Leone, A.; La Notte, E.; Antonacci, D. Some Characteristics of Polyphenolic Substances in Red Wines Obtained by Different Processes of Maceration. In *Progress in Food Engineering*; Peri, C., Cantarelli, C., Eds.; Forster-Verlag: Kusnacht, Switzerland, 1983; pp. 267–277.
4. Amendola, D.; De Faveri, D.M.; Spigno, G. Grape marc phenolics: Extraction kinetics, quality and stability of extracts. *J. Food Eng.* **2010**, *97*, 384–392. [CrossRef]
5. Zanoni, B.; Siliani, S.; Canuti, V.; Rosi, I.; Bertuccioli, M. A kinetic study on extraction and transformation phenomena of phenolic compounds during red wine fermentation. *Int. J. Food Sci. Technol.* **2010**, *45*, 2080–2088. [CrossRef]
6. Bucić-Kojić, A.; Planinić, M.; Tomas, S.; Bilić, M.; Velić, D. Study of solid–liquid extraction kinetics of total polyphenols from grape seeds. *J. Food Eng.* **2007**, *81*, 236–242. [CrossRef]
7. Mantell, C.; Rodríguez, M.; Martínez de la Ossa, E. Semi-batch extraction of anthocyanins from red grape pomace in packed beds: Experimental results and process modelling. *Chem. Eng. Sci.* **2002**, *57*, 3831–3838. [CrossRef]
8. Guerrero, M.S.; Torres, J.S.; Nunez, M.J. Extraction of polyphenols from white distilled grape pomace: Optimization and modelling. *Bioresour. Technol.* **2008**, *99*, 1311–1318. [CrossRef] [PubMed]
9. Cacace, J.E.; Mazza, G. Mass transfer process during extraction of phenolic compounds from milled berries. *J. Food Eng.* **2003**, *59*, 379–389. [CrossRef]
10. Rodríguez-Jimenes, G.C.; Vargas-Garcia, A.; Espinoza-Pérez, D.J.; Salgado-Cervantes, M.A.; Robles-Olvera, V.J.; García-Alvarado, M.A. Mass transfer during vanilla pods solid liquid extraction: Effect of extraction method. *Food Bioprocess Technol.* **2013**, *6*, 2640–2650. [CrossRef]
11. Espinoza-Pérez, J.; Vargas, A.; Robles-Olvera, V.; Rodríguez-Jimenes, G.; García-Alvarado, M. Mathematical modeling of caffeine kinetic during solid–liquid extraction of coffee beans. *J. Food Eng.* **2007**, *81*, 72–78. [CrossRef]
12. Bonfigli, M.; Godoy, E.; Reinheimer, M.; Scenna, N. Comparison between conventional and ultrasound-assisted techniques for extraction of anthocyanins from grape pomace. Experimental results and mathematical modeling. *J. Food Eng.* **2017**, *207*, 56–72. [CrossRef]
13. Cissé, M.; Bohuon, P.; Sambe, F.; Kane, C.; Sakho, M.; Dornier, M. Aqueous extraction of anthocyanins from hibiscus sabdariffa: Experimental kinetics and modeling. *J. Food Eng.* **2012**, *109*, 16–21. [CrossRef]
14. Gertenbach, D. Solid–Liquid Extraction Technologies for Manufacturing Nutraceuticals from Botanicals. In *Functional Foods Biochemical and Processing Aspects*; Shi, J., Mazza, G., Le Maguer, M., Eds.; Taylor and Francis Group: Boca Raton, Florida, USA, 2001; Volume 2, pp. 331–366.
15. Schmidt, D.; Velten, K. Modeling and simulation of the bubble-induced flow in wine fermentation vessels. In *BIO Web of Conferences*; EDP Sciences: Mainz, Germany, 2015; p. 02015.
16. Koyama, K.; Goto-Yamamoto, N.; Hashizume, K. Influence of maceration temperature in red wine vinification on extraction of phenolics from berry skins and seeds of grape (*Vitis vinifera*). *Biosci. Biotechnol. Biochem.* **2007**, *71*, 958–965. [CrossRef] [PubMed]

17. Lerno, L.; Reichwage, M.; Panprivech, S.; Ponangi, R.; Hearne, L.; Oberholster, A.; Block, D.E. Chemical gradients in pilot-scale cabernet sauvignon fermentations and their effect on phenolic extraction. *Am. J. Enol. Viticult.* **2017**, *68*, 401–411. [CrossRef]
18. Cozzolino, D.; Kwiatkowski, M.; Parker, M.; Cynkar, W.; Dambergs, R.; Gishen, M.; Herderich, M. Prediction of phenolic compounds in red wine fermentations by visible and near infrared spectroscopy. *Anal. Chim. Acta* **2004**, *513*, 73–80. [CrossRef]
19. Mercurio, M.D.; Dambergs, R.G.; Herderich, M.J.; Smith, P.A. High throughput analysis of red wine and grape phenolics adaptation and validation of methyl cellulose precipitable tannin assay and modified somers color assay to a rapid 96 well plate format. *J. Agric. Food. Chem.* **2007**, *55*, 4651–4657. [CrossRef] [PubMed]
20. Sparrow, A.M.; Smart, R.E.; Dambergs, R.G.; Close, D.C. Skin particle size affects the phenolic attributes of pinot noir wine: Proof of concept. *Am. J. Enol. Viticult.* **2015**, *67*, 29–37. [CrossRef]
21. Cerpa-Calderón, F.K.; Kennedy, J.A. Berry integrity and extraction of skin and seed proanthocyanidins during red wine fermentation. *J. Agric. Food. Chem.* **2008**, *56*, 9006–9014. [CrossRef] [PubMed]
22. Geankoplis, C.J. *Transport Processes and Separation Process Principles*, 4th ed.; Prentice Hall Professional Technical Reference: Upper Saddle River, NJ, USA, 2003.
23. Stapley, A.G.F. Modelling the kinetics of tea and coffee infusion. *J. Sci. Food Agric.* **2002**, *82*, 1661–1671. [CrossRef]
24. Jin, X.; Wu, X.; Liu, X.; Liao, M. Varietal heterogeneity of textural characteristics and their relationship with phenolic ripeness of wine grapes. *Sci. Hort.* **2017**, *216*, 205–214. [CrossRef]

Sample Availability: Not available.

Supporting Information for

Modelling the Mass Transfer Process of Malvidin-3-Glucoside during Simulated Extraction from Fresh Grape Solids under Wine-Like Conditions

Patrick C. Setford[1], David W. Jeffery[1,2], Paul R. Grbin[1,2] and Richard A. Muhlack[1,2,*]

[1]Department of Wine and Food Science, School of Agriculture, Food and Wine, The University of Adelaide (UA), PMB 1, Glen Osmond SA 5064, Australia

[2]The Australian Research Council Training Centre for Innovative Wine Production, The University of Adelaide, PMB 1, Glen Osmond SA 5064, Australia

Table of Contents

Page

Table S1. Full ANOVA for M3G internal diffusion coefficient S-2

Table S2. Full ANOVA for M3G external mass transfer coefficient S-3

Table S3. Full ANOVA for M3G distribution constant S-4

Table S1. Full ANOVA for M3G internal diffusion coefficient

						n (ie # of replicates)	2						
Trial Conditions			Diffusion/Mass transfer property										
A	B	C	run 1	run 2	sum								
T	Glucose	Ethanol	$D_{s\beta}$	$D_{s\beta}$	$D_{s\beta}$	A	B	C	AB	AC	BC	ABC	
Low	Low	Low	5.97E-14	6.11E-14	1.21E-13	-1	-1	-1	1	1	1	-1	
Low	High	Low	5.77E-14	5.56E-14	1.13E-13	-1	1	-1	-1	1	-1	1	
Low	Low	High	1.26E-13	1.31E-13	2.57E-13	-1	-1	1	1	-1	-1	1	
Low	High	High	8.95E-14	7.59E-14	1.65E-13	-1	1	1	-1	-1	1	-1	
High	Low	Low	4.24E-13	3.03E-13	7.27E-13	1	-1	-1	-1	-1	1	1	
High	High	Low	2.81E-13	2.62E-13	5.43E-13	1	1	-1	1	-1	-1	-1	
High	Low	High	5.86E-13	9.43E-13	1.53E-12	1	-1	1	-1	1	-1	-1	
High	High	High	6.62E-13	6.24E-13	1.29E-12	1	1	1	1	1	1	1	
					main effect	4.29E-13	-6.58E-14	2.17E-13	-4.09E-14	1.70E-13	-1.77E-14	3.35E-15	
					sum of squares	7.35E-25	1.73E-26	1.88E-25	6.70E-27	1.15E-25	1.26E-27	4.50E-29	
						sum of squares	degrees of freedom	mean square	F0	p			
				T	A	7.35E-25	1	7.35E-25	8.15E+01	1.81E-05			
				Glucose	B	1.73E-26	1	1.73E-26	1.92E+00	2.03E-01			
				Ethanol	C	1.88E-25	1	1.88E-25	2.08E+01	1.84E-03			
					AB	6.70E-27	1	6.70E-27	7.43E-01	4.14E-01			
					AC	1.15E-25	1	1.15E-25	1.28E+01	7.28E-03			
					BC	1.26E-27	1	1.26E-27	1.40E-01	7.18E-01			
					ABC	4.50E-29	1	4.50E-29	4.99E-03	9.45E-01			
					Error	7.21E-26	8	9.02E-27					
					Total	1.13E-24	15						

S2

Table S2. Full ANOVA for M3G external mass transfer coefficient

						n (ie # of replicates)						
Trial Conditions			Diffusion/Mass transfer property			2						
A	B	C	run 1	run 2	sum							
T	Glucose	Ethanol	$k_{c\beta}$	$k_{c\beta}$	$k_{c\beta}$	A	B	C	AB	AC	BC	ABC
Low	Low	Low	7.01E-11	7.17E-11	1.42E-10	-1	-1	-1	1	1	1	-1
Low	High	Low	6.77E-11	6.52E-11	1.33E-10	-1	1	-1	-1	1	-1	1
Low	Low	High	1.48E-10	1.54E-10	3.02E-10	-1	-1	1	1	-1	-1	1
Low	High	High	1.05E-10	8.90E-11	1.94E-10	-1	1	1	-1	-1	1	-1
High	Low	Low	4.97E-10	3.56E-10	8.53E-10	1	-1	-1	-1	-1	1	1
High	High	Low	3.29E-10	3.07E-10	6.36E-10	1	1	-1	1	-1	-1	-1
High	Low	High	6.87E-10	1.11E-09	1.79E-09	1	-1	1	-1	1	-1	-1
High	High	High	7.77E-10	7.32E-10	1.51E-09	1	1	1	1	1	1	1
					main effect	5.03E-10	-7.71E-11	2.54E-10	-4.80E-11	1.99E-10	-2.08E-11	3.94E-12
					sum of squares	1.01E-18	2.38E-20	2.58E-19	9.21E-21	1.58E-19	1.73E-21	6.20E-23

		sum of squares	degrees of freedom	mean square	F0	p
T	A	1.01E-18	1	1.01E-18	8.15E+01	1.81E-05
Glucose	B	2.38E-20	1	2.38E-20	1.92E+00	2.03E-01
Ethanol	C	2.58E-19	1	2.58E-19	2.08E+01	1.84E-03
	AB	9.21E-21	1	9.21E-21	7.43E-01	4.14E-01
	AC	1.58E-19	1	1.58E-19	1.28E+01	7.28E-03
	BC	1.73E-21	1	1.73E-21	1.40E-01	7.18E-01
	ABC	6.20E-23	1	6.20E-23	5.00E-03	9.45E-01
	Error	9.92E-20	8	1.24E-20		
	Total	1.56E-18	15			

S3

Table S3. Full ANOVA for M3G distribution constant

						n (ie # of replicates)		2					
Trial Conditions			Diffusion/Mass transfer property										
A	B	C	run 1	run 2	sum								
T	Glucose	Ethanol	K	K	K	A		B		C	AB	AC	BC	ABC
Low	Low	Low	3.92E-02	4.10E-02	8.02E-02	-1		-1		-1	1	1	1	-1
Low	High	Low	4.09E-02	3.93E-02	8.02E-02	-1		1		-1	-1	1	-1	1
Low	Low	High	9.86E-02	1.00E-01	1.99E-01	-1		-1		1	1	-1	-1	1
Low	High	High	9.18E-02	9.17E-02	1.83E-01	-1		1		1	-1	-1	1	-1
High	Low	Low	7.34E-02	9.26E-02	1.66E-01	1		-1		-1	-1	-1	1	1
High	High	Low	9.88E-02	8.63E-02	1.85E-01	1		1		-1	1	-1	-1	-1
High	Low	High	1.26E-01	1.57E-01	2.83E-01	1		-1		1	-1	1	-1	-1
High	High	High	2.37E-01	2.08E-01	4.45E-01	1		1		1	1	1	1	1
					main effect	6.70E-02		2.06E-02		7.49E-02	2.45E-02	1.93E-02	1.58E-02	1.98E-02
					sum of squares	1.80E-02		1.70E-03		2.24E-02	2.41E-03	1.49E-03	1.00E-03	1.56E-03
						sum of squares		degrees of freedom		mean square	F0	p		
				T	A	1.80E-02		1		1.80E-02	1.26E+02	3.56E-06		
				Glucose	B	1.70E-03		1		1.70E-03	1.19E+01	8.64E-03		
				Ethanol	C	2.24E-02		1		2.24E-02	1.57E+02	1.53E-06		
					AB	2.41E-03		1		2.41E-03	1.69E+01	3.39E-03		
					AC	1.49E-03		1		1.49E-03	1.05E+01	1.19E-02		
					BC	1.00E-03		1		1.00E-03	7.05E+00	2.91E-02		
					ABC	1.56E-03		1		1.56E-03	1.09E+01	1.07E-02		
					Error	1.14E-03		8		1.43E-04				
					Total	4.97E-02		15						

CHAPTER 3

Mass Transfer of Anthocyanins during Extraction from Pre-Fermentative Grape Solids under Simulated Fermentation Conditions: Effect of Convective Conditions

Patrick C. Setford[1], David W. Jeffery[1], Paul R. Grbin[1], Richard A. Muhlack[1,*]

[1] Department of Wine and Food Science, School of Agriculture, Food and Wine, The University of Adelaide (UA), PMB 1 Glen Osmond SA 5064, Australia

Molecules - **2019**, 24, 73

Statement of Authorship

Title of Paper	Mass Transfer of Anthocyanins during Extraction from Pre-Fermentative Grape Solids under Simulated Fermentation Conditions: Effect of Convective Conditions
Publication Status	☑ Published ☐ Accepted for Publication ☐ Submitted for Publication ☐ Unpublished and Unsubmitted work written in manuscript style
Publication Details	Setford, P., Jeffery, D., Grbin, P., & Muhlack, R. (2019). Mass Transfer of Anthocyanins during Extraction from Pre-Fermentative Grape Solids under Simulated Fermentation Conditions: Effect of Convective Conditions. Molecules, vol. 24, no. 1, p. 73.

Principal Author

Name of Principal Author (Candidate)	Patrick C. Setford		
Contribution to the Paper	Designed experiments, performed experimental work, performed laboratory analysis of samples (HPLC, viscometer), analysed and interpreted data, performed mathematical modelling, prepared entire first draft of the manuscript and helped address reviewer comments.		
Overall percentage (%)	70%		
Certification:	This paper reports on original research I conducted during the period of my Higher Degree by Research candidature and is not subject to any obligations or contractual agreements with a third party that would constrain its inclusion in this thesis. I am the primary author of this paper.		
Signature		Date	7/5/19

Co-Author Contributions

By signing the Statement of Authorship, each author certifies that:

i. the candidate's stated contribution to the publication is accurate (as detailed above);

ii. permission is granted for the candidate in include the publication in the thesis; and

iii. the sum of all co-author contributions is equal to 100% less the candidate's stated contribution.

Name of Co-Author	David W. Jeffery		
Contribution to the Paper	Contributed to the research idea and experimental design, assisted with laboratory analysis, assisted with interpretation of data, critically reviewed and edited the manuscript and helped address reviewer comments.		
Signature		Date	7/5/19

Name of Co-Author	Paul R. Grbin		
Contribution to the Paper	Contributed to the research idea and experimental design, assisted with interpretation of data, critically reviewed and edited the manuscript and helped address reviewer comments.		
Signature		Date	13/5/19

Name of Co-Author	Richard A. Muhlack		
Contribution to the Paper	Contributed to the conception of the article and experimental design, assisted with mathematical modelling, assisted with experimental setup and supervised the work. Helped prepare, edit and critically review the manuscript and helped address reviewer comments. Acted as the corresponding author.		
Signature		Date	7.5.2019

Please cut and paste additional co-author panels here as required.

molecules

MDPI

Article

Mass Transfer of Anthocyanins during Extraction from Pre-Fermentative Grape Solids under Simulated Fermentation Conditions: Effect of Convective Conditions

Patrick C. Setford, David W. Jeffery, Paul R. Grbin and Richard A. Muhlack *

Department of Wine and Food Science, School of Agriculture, Food and Wine, The University of Adelaide, PMB 1 Glen Osmond SA 5064, Australia; patrick.setford@adelaide.edu.au (P.C.S.); david.jeffery@adelaide.edu.au (D.W.J.); paul.grbin@adelaide.edu.au (P.R.G.)

* Correspondence: richard.muhlack@adelaide.edu.au; Tel.: +61-8-8313-6771

Received: 14 December 2018; Accepted: 24 December 2018; Published: 26 December 2018

Abstract: The colour of red wine is largely determined by the concentration of anthocyanins that are extracted from grape skins during fermentation. Because colour is a key parameter in determining the overall quality of the finished product, understanding the effect of processing variables on anthocyanin extraction is critical for producing a red wine with the desired sensorial characteristics. In this study, the effect of convective conditions (natural and forced) on the mass transfer properties of malvidin-3-glucoside (M3G) from pre-fermentative grape solids was explored at various liquid phase conditions representing stages of fermentation. A mathematical model that separates solid and liquid phase mass transfer parameters was applied to experimental extraction curves, and in all cases, provided a coefficient of determination exceeding 0.97. Calculated mass transfer coefficients indicated that under forced convective conditions, the extraction process was controlled by internal diffusion whereas under natural convection, both internal diffusion and liquid-phase mass transfer were relevant in determining the overall extraction rate. Predictive simulations of M3G extraction during active fermentation were accomplished by incorporating the current results with a previously developed fermentation model, providing insight into the effect of a dynamic liquid phase on anthocyanin extraction.

Keywords: phenolic extraction; diffusion; anthocyanin; process modelling; wine colour; mass transfer

1. Introduction

Monomeric anthocyanins existing in pH-dependent equilibrium forms are among the largest class of phenolic compounds present in young red wines. In their cationic flavylium form, these compounds are directly responsible for the red colour in young red wines and over time interact with other (typically colourless) organic compounds, leading to long term stability of colour in older wines. As such, anthocyanins are regarded as one of the most important phenolic compounds responsible for the overall quality of red wine. During the red winemaking process, anthocyanins are extracted from the skins into the fermenting liquid through a multi-stage solid-liquid mass transfer process. This process first involves the diffusion of dissolved anthocyanins from within the grape skins to the solid-liquid boundary layer, followed by a liquid phase mass transfer step to the bulk of the fermenting liquid [1–3].

Following extraction, monomeric anthocyanins undergo a series of chemical and physical reactions, which include, but are not limited to, oxidation, copigmentation, self-association, adsorption to yeast lees, and re-adsorption to grape solids [3]. Due to the vast array of reactions and interactions, a distinct

Molecules **2019**, *24*, 73

difficulty exists in accurately describing the extraction kinetics of anthocyanins and calculating kinetic coefficients during fermentative maceration. In previous years, phenolic extraction kinetics during red wine fermentation have been described using simple first- and second-order rate models, where a single term is used to describe the extractive phase and a second term is used to describe the subsequent reaction or degradation stage [4,5]. Due to the continuous evolution of ethanol during fermentative maceration, describing the extraction step of this process using a single term is a clear oversimplification that, although providing certain insights, is limited in providing quantitative predictions of future fermentative maceration scenarios. In addition, these models do not account for variability in the type, frequency, and duration of mixing operations employed during fermentative maceration—all of which would be expected to influence the overall rate of phenolic extraction [3,6].

During mixing operations, the rate of anthocyanin mass transfer from the solid-liquid boundary layer to the liquid bulk is a forced convective mass transfer process and can be well described with empirical correlations commonly employed in chemical engineering [7–9]. For the majority of red-wine maceration, however, the system is under natural convective conditions. To the authors' knowledge, natural convective mass transfer of phenolic compounds—a critical step for furthering the understanding the extractive process of anthocyanins during winemaking—is as yet undescribed and external mass transfer parameters have not been quantified.

Previously, internal diffusion rates of malvidin-3-*O*-β-D-glucoside (M3G), the predominant anthocyanin found in the skin of red wine grapes, have been quantified under various liquid-phase and industry-relevant temperature conditions [8]. The present study sought to extend upon this by evaluating the natural convective rates of external mass transfer of M3G in solutions emulating various stages of red wine fermentation, to simulate anthocyanin extraction under active fermentation scenarios.

2. Results and Discussion

2.1. Forced Convective Mass Transfer

To calculate the rate of natural convective mass transfer in the liquid phase, it was essential to first calculate the rate of internal mass transfer within the solid phase (grape skins). This was achieved using freshly pressed grape solids in solutions with varying concentrations of ethanol and sugar that were continuously stirred to achieve a well-mixed system. The rate of solute movement in the liquid phase could thereby be quantified using dimensionless numbers (described in Section 3.2). As such, the rate of external mass transfer could be separated from the overall extraction rate, allowing for solid phase mass transfer parameters at the varying liquid-phase conditions to be quantified (further details provided in Sections 3.2 and 3.3). Three liquid-phase conditions representing the start (266 g L^{-1} sugar), middle (133 g L^{-1} sugar, 7% ethanol), and end point (14% ethanol) of a red-wine fermentation were chosen to determine the changes in mass transfer parameters over the course of a simulated fermentation.

Figure 1 presents the experimental extraction curves of M3G from the grape solids (Figure 1a) and accumulation of M3G in the liquid phase (Figure 1b) at these varying conditions as well as the fit of Equations (14) and (15) of the forced convection model developed in Section 3.2 to the curves. Small error bars can be observed for each set of liquid phase conditions in Figure 1 (% RSD < 5.32, after the first hour of extraction), showing the high level of reproducibility among replicates. The root mean square error (RMSE) and R^2 values were also calculated for each set of liquid phase conditions and in all cases, small RMSE (<1.58) and R^2 values > 0.97 were observed (Table 1), indicating good agreement between experimental and mathematically-derived M3G concentrations. From Figure 1, it can be clearly observed that both the overall extraction rate (which in this case, can be approximated by the internal mass transfer rate) and maximum extractability of M3G are improved under conditions that emulate the later stages of fermentation (i.e., when more ethanol is produced). This is in agreement with other studies seeking to understand the influence of ethanol on phenolic extraction [8,10,11] and can be explained by the solvent properties of ethanol improving the solutions' relative permittivity

Molecules **2019**, *24*, 73

(the dielectric constant) [3], which may improve the rate of internal diffusion and extractability by aiding in the dissolution of M3G and in overcoming the liquids' ability to penetrate the solid phase.

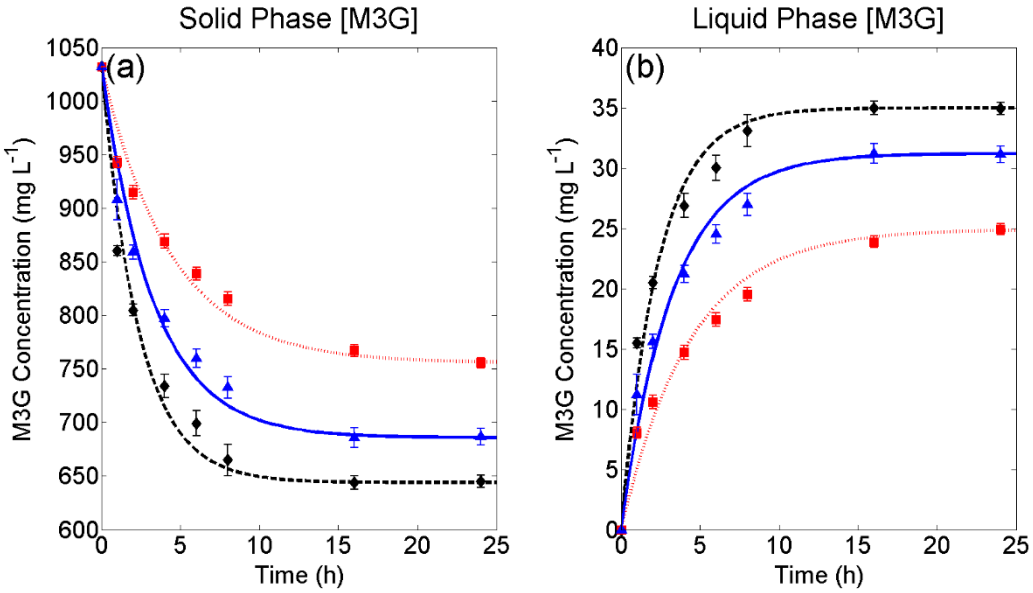

Figure 1. Experimental and fitted models under forced convection conditions for (**a**) solid phase depletion and (**b**) liquid phase accumulation of malvidin-3-glucoside. 266 g L^{-1} sugar; ▲, 133 g L^{-1} sugar, and 7% *v*/*v* ethanol; ◆, 14% *v*/*v* ethanol. Error bars represent the standard deviation across three replicates.

Table 1. Summary of liquid phase conditions, mass transfer properties ($D_{s\gamma}$, $k_{c\gamma}$, $D_{s\beta}$, $k_{c\beta}$, and K), Biot number (Bi), and statistical parameters ($RMSE$ and R^2) for malvidin-3-glucoside solved using the method outlined in Section 3.2 for forced convective extraction.

	Liquid Phase Conditions		
Property or Mass Transfer Variable	**Juice**	**Mid-Ferment**	**Wine**
Sugar (g L^{-1})	266	133	0
Ethanol (% *v*/*v*)	0	7	14
$D_{s\gamma}$ (m^2 s^{-1})	4.22×10^{-12}	5.01×10^{-12}	5.66×10^{-12}
$k_{c\gamma}$ (m s^{-1})	1.70×10^{-4}	1.94×10^{-4}	2.16×10^{-4}
$D_{s\beta}$ (m^2 s^{-1})	2.09×10^{-13}	3.49×10^{-13}	5.47×10^{-13}
$k_{c\beta}$ (m s^{-1})	2.45×10^{-10}	4.10×10^{-10}	6.41×10^{-10}
K	3.30×10^{-2}	4.55×10^{-2}	5.43×10^{-2}
Bi	4.71×10^{3}	4.43×10^{3}	3.76×10^{3}
$RMSE$	1.33	1.44	1.58
R^2	0.972	0.972	0.980

Table 1 presents a summary of mass transfer parameters for each set of forced convective experimental conditions, calculated according to the method outlined in Section 3.2. Here, the external diffusion coefficient ($D_{s\gamma}$) was calculated from the Wilke-Chang correlation (Equation (11)) and subsequently used to calculate the rate of external mass transfer ($k_{c\gamma}$) using a system of dimensionless values that describe fluid flow around particles (Equation (10)). From here, the rate of internal diffusion could be derived by fitting experimental data to Equations (14) and (15), and Equation (8) could then be used to calculate the internal diffusion coefficient. In each case, high rates of external mass transfer ($k_{c\gamma}$) were observed, indicating that the solid-liquid systems studied were indeed well-mixed. This is confirmed by the relatively high Biot numbers (>3.76×10^3) calculated for each set of experimental

Molecules **2019**, *24*, 73

conditions, where a value exceeding 10 would typically indicate that the overall extraction rate is controlled by internal diffusion [12]:

$$Bi = \frac{k_{c\gamma} LK}{D_{s\beta}} \quad (1)$$

Although not the primary focus of this study, the use of grape berries for extraction experiments, which had been previously frozen, allowed for additional observation and comparison to be drawn regarding the effects of freezing on phenolic extraction. This is made possible as this study follows on directly from previous work [8] seeking to understand the relationship between liquid phase conditions and temperature on internal mass transfer parameters of M3G from fresh grape solids. For the same set of experimental conditions (266 g L^{-1} sugar and 14% *v*/*v* ethanol) and using the same parcel of berries as the previous study, we found distribution constant (K) values approximately three times larger with fresh berries [8] than those calculated in the present study using previously frozen berries at similar extraction temperature conditions. This result can be rationalised given that freezing causes the skin cells to burst, thus improving the fast leakage stage of extraction prior to solid-liquid diffusion [6]. A higher concentration of M3G in the juice would therefore occur due to leaking from broken cells upon crushing, lowering the available solid-phase M3G concentration at the onset of liquid contact, and thus decreasing the observed distribution constant. Similar results (in terms of rapid anthocyanin extraction into juice) have also been observed during flash release processing [13–15] and accentuated cut edge (ACE) maceration [16]. As such, the impact of pre-fermentative techniques, including must-freezing, flash détente, ultrasound, and skin size modification, on the initial leakage and overall distribution constant are important areas for future research, which, together with an understanding of mass transfer parameters developed in the present study, offer the potential to optimize extraction of M3G and other phenolic compounds relevant to wine quality. However, with the primary aim of this study being to explore the effect of convective conditions during extraction of anthocyanins, the use of previously frozen berries is not expected to impact on the conclusions drawn as the evaluation of external mass transfer parameters in the liquid phase are independent of internal mass transfer variables that may change as a result of grape freezing.

2.2. Natural Convective Mass Transfer

Natural convective mass transfer rates of M3G were evaluated in liquid solutions that were representative of different stages of red wine fermentation to better understand the extraction kinetics that would occur during the majority of a red wine fermentation (i.e., mixing is only conducted intermittently throughout the maceration period). This was accomplished by fitting Equations (14) and (15) to experimental data using the respective internal mass transfer coefficients ($k_{c\beta}$) that were evaluated during forced convective extractions (described in Section 2.1) and instead solving for the external mass transfer coefficients for each set of liquid phase conditions.

Figure 2 presents the experimental extraction curves of M3G from the grape solids (Figure 2a) and accumulation of M3G in the liquid phase (Figure 2b) under natural convection as well as the fit of Equations (14) and (15) of the forced convection model developed in Section 3.2 to these curves for each set of liquid phase conditions. As before, small error bars can be observed (% RSD < 8.94), and in all cases, shows good experimental reproducibility between replicated extractions. Small RMSE values together with R^2 values >0.97 in all cases indicates a good agreement between experimental and mathematically-derived M3G concentrations (Table 2) and that the model can be adequately used to describe M3G extraction under static liquid phase conditions. When compared to Figure 1, the overall rate of M3G extraction under natural convective conditions, as shown in Figure 2, is much slower than under forced convective conditions. This result can be explained, as the internal mass transfer rate of M3G is limited by the concentration at the solid-liquid interface and mixing minimises the concentration gradient between the solid-liquid boundary layer to the bulk of the liquid phase, creating a homogenous solution. As with forced convection, a higher overall extraction rate and maximum

Molecules **2019**, *24*, 73

extractability can be seen with an increase in the extent of simulated fermentation (i.e., higher ethanol concentration, Figure 2).

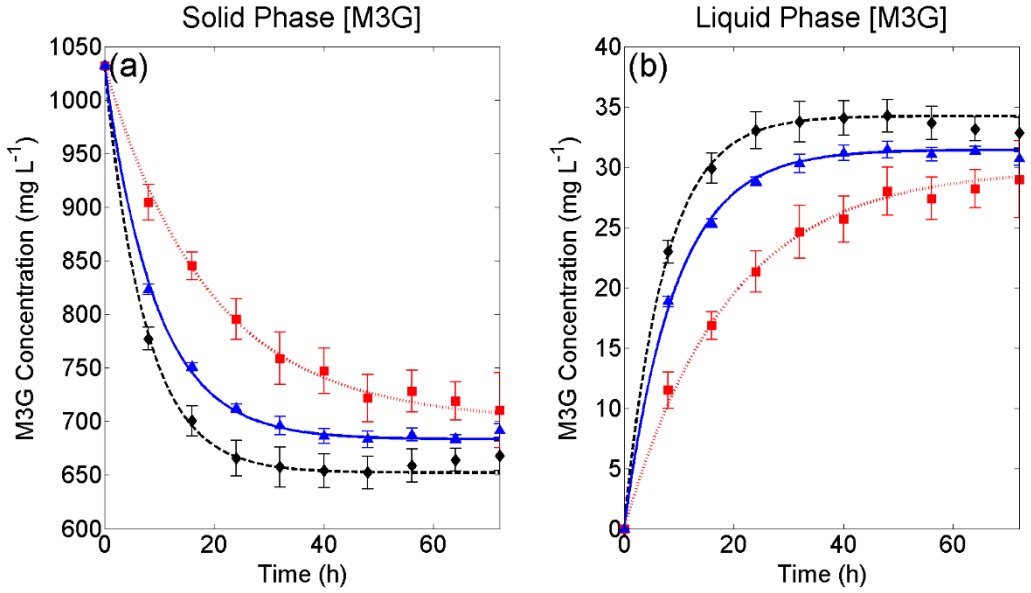

Figure 2. Experimental and fitted models under natural convection conditions for (**a**) solid phase depletion and (**b**) liquid phase accumulation of malvidin-3-glucoside. 266 g L^{-1} sugar; ▲, 133 g L^{-1} sugar and 7% *v*/*v* ethanol; ◆, 14% *v*/*v* ethanol. Error bars represent the standard deviation across three replicates.

Table 2. Summary of liquid phase conditions, mass transfer properties ($D_{s\gamma}$, $k_{c\gamma}$, $D_{s\beta}$, $k_{c\beta}$, and K), Biot number (Bi), and statistical parameters ($RMSE$ and R^2) for malvidin-3-glucoside solved using the method outlined in Section 3.2 for natural convective extraction.

	Liquid Phase Conditions		
Mass Transfer Variable	**Juice**	**Mid-Ferment**	**Wine**
Sugar (g L^{-1})	266	133	0
Ethanol (% *v*/*v*)	0	7	14
K	4.26×10^{-2}	4.60×10^{-2}	5.25×10^{-2}
$k_{c\beta}$ (m s^{-1})	2.45×10^{-10}	4.10×10^{-10}	6.41×10^{-10}
$k_{c\gamma}$ (m s^{-1})	2.20×10^{-9}	4.93×10^{-9}	5.53×10^{-9}
Bi	7.83×10^{-2}	1.13×10^{-1}	9.23×1^{-2}
$RMSE$	0.58	0.59	1.61
R^2	0.996	0.995	0.970

Table 2 presents the mathematically derived mass transfer parameters for natural convective extraction of M3G at the liquid phase conditions investigated. Values for the internal mass transfer coefficient (solved in Section 2.1) are presented for comparison with the derived external mass transfer coefficients at natural convective conditions. For the liquid compositions representing mid-fermentation and the end of fermentation, similar values for the distribution constant were calculated for natural and forced convective conditions. This is rationalised due to the effect of forced convection, which should only affect the rate at which M3G is transferred from the solid-liquid interface to the bulk of the liquid and should not impact the maximum extractability. Calculated external mass transfer rates ($k_{c\gamma}$) under natural convective conditions were found to be lower in juice-like solutions than in wine-like solutions (Table 2). Because diffusivity is inversely proportional to the viscosity of the liquid [17], a likely explanation for this is the effect of sugar on the rheological properties of the liquid, whereby a higher viscosity caused by dissolved sugar would be expected to hinder mass transfer. Under natural

Molecules **2019**, *24*, 73

convective conditions, the Biot numbers for M3G at various simulated fermentation stages were found to be between 7.83×10^{-2} and 1.13×10^{-1}, indicating that mass transfer in the liquid phase has a strong influence on the overall rate of extraction. This result demonstrates the importance of both internal and external mass transfer to the overall rate of anthocyanin extraction in winemaking. Additionally, although previous mathematical models based on first- and second-order kinetics [4,5] may be adequately used to fit experimental extraction data during fermentation, the present work shows a more complex relationship, whereby knowledge of both solid and liquid phase mass transfer parameters is critical to informing extraction models with predictive capabilities.

2.3. Application in Simulated Wine Fermentations

Previous studies have highlighted a lack of understanding of the extraction mechanisms of phenolic compounds during fermentation, leading to a distinct difficulty in manipulating the phenolic content of finished wines [3,18]. Ultimately, the goal of modelling mass transfer under different conditions is the ability to predict phenolic extraction under various winemaking scenarios and thus close the previously highlighted gap. To further this knowledge, simulations of extraction scenarios for M3G under dynamic (continuously changing) liquid phase conditions were undertaken. This was accomplished by incorporating a previously developed wine fermentation model from Coleman et al. [19] (described in Section 3.4) with surface response models from Setford, Jeffery, Grbin, and Muhlack [8] for M3G that describe the distribution constant (Equation (2)) and the internal diffusion coefficient (Equation (3)), and calculating the rate of internal mass transfer (Equation (8)) as functions of the liquid phase conditions:

$$\begin{aligned} K = 9.97 \times 10^{-2} + 3.33 \times 10^{-2}T + 1.04 \times 10^{-2}C_g + 3.74 \times 10^{-2}C_{EtOH} \\ + 1.23 \times 10^{-2}TC_g - 9.64 \times 10^{-3}TC_{EtOH} \\ + 7.91 \times 10^{-3}C_gC_{EtOH} + 9.86 \times 10^{-3}TC_gC_{EtOH} \end{aligned} \quad (2)$$

$$D_{s\beta} = 2.75 \times 10^{-13} + 2.11 \times 10^{-13}T + 1.09 \times 10^{-16}C_{EtOH} + 8.52 \times 10^{-14}TC_{EtOH} \quad (3)$$

Further extending these predictive models, a second-degree polynomial was fitted to the experimentally determined values of external mass transfer coefficients for natural convective mass transfer presented in Table 2, allowing the prediction of $k_{c\gamma}$ as a function of the relative extent of fermentation:

$$k_{c\gamma} = -4.94 \times 10^{-9}Ex^2 + 8.27 \times 10^{-9}Ex + 2.20 \times 10^{-9} \quad (4)$$

where Ex represents the extent of liquid phase fermentation (i.e., 266 g L^{-1} sugar, 0% *v*/*v* ethanol = 0, 0 g L^{-1} sugar, 14% *v*/*v* ethanol = 1). The values for K, $k_{c\beta}$, and $k_{c\gamma}$ calculated using this method were then used to solve Equations (14) and (15) and generate extraction curves with continuously changing mass transfer variables resulting from changes in liquid phase concentrations of sugar and ethanol.

Figure 3a presents a typical red wine fermentation curve at 20 °C (black curve), solved using the fourth order Runge-Kutta method in MATLAB according to the method outlined in Section 3.4 and using the following set of initial conditions: T = 20 °C μ_0 = 0.05 h^{-1}, $k_{d,0}$ = 0.0001 h^{-1}, B_0 = 0.05 g_{EtOH} $g_{biomass}$ h^{-1}, $X_0 = X_{A,0}$ = 0.05 g L^{-1}, N_0 = 0.08 g L^{-1}, E_0 = 0 g L^{-1}, S_0 = 266 g L^{-1}. Evidently, M3G extraction is initially limited by the fermentation lag-phase, where the liquid phase contains a high concentration of sugar and no ethanol. Although experimental extractions of M3G under fixed liquid phase and natural convective conditions reached a maximum liquid phase concentration within 72 h (Figure 2b), the simulated extraction curve presented in Figure 3b supported literature observations of extraction during active fermentation, where the time taken to reach a maximum anthocyanin concentration was seen to be considerably longer (up to a week) than extraction under fixed solvent conditions [4,5,20]. Figure 3b highlights the importance of ethanol in maximising extracted anthocyanins and implies that pre-fermentative maceration techniques, such as cold-soaking,

Molecules **2019**, *24*, 73

in the absence of ethanol would not be expected to improve the concentration of M3G at the end of fermentation.

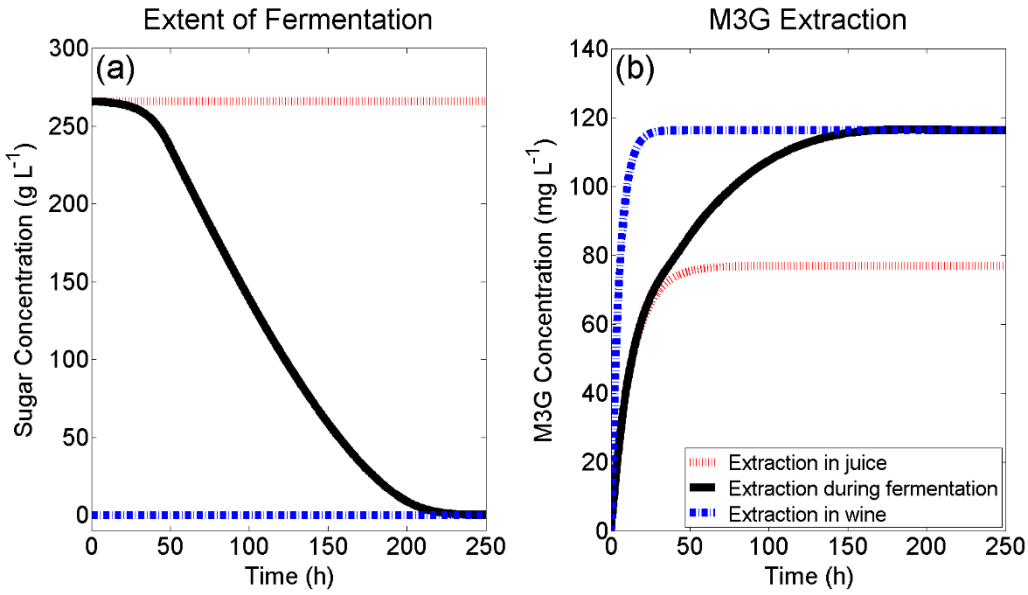

Figure 3. (**a**) Simulated red wine fermentation kinetics and (**b**) the resulting simulated extraction kinetics of M3G. Red and blue lines indicate the rate and extent of M3G extraction that would occur under constant liquid phase conditions for juice and wine, respectively.

Figure 4a shows overlapping fermentation curves for the three simulated M3G extractions in Figure 4b. This is because the same initial conditions were used to solve for the fermentation model (described in Section 3.4), which does not consider liquid phase mass transfer as a fermentation parameter. In Figure 4b, 'Forced Convection' was modelled using an external mass transfer coefficient of 1×10^{-4} (Biot number > 1000), 'Natural Convection' was modelled using a varying external mass transfer coefficient according to Equation (4), and 'Hindered Convection' was modelled using a fixed system Biot number of 0.01 to show the effect of further limiting the rate of external mass transfer.

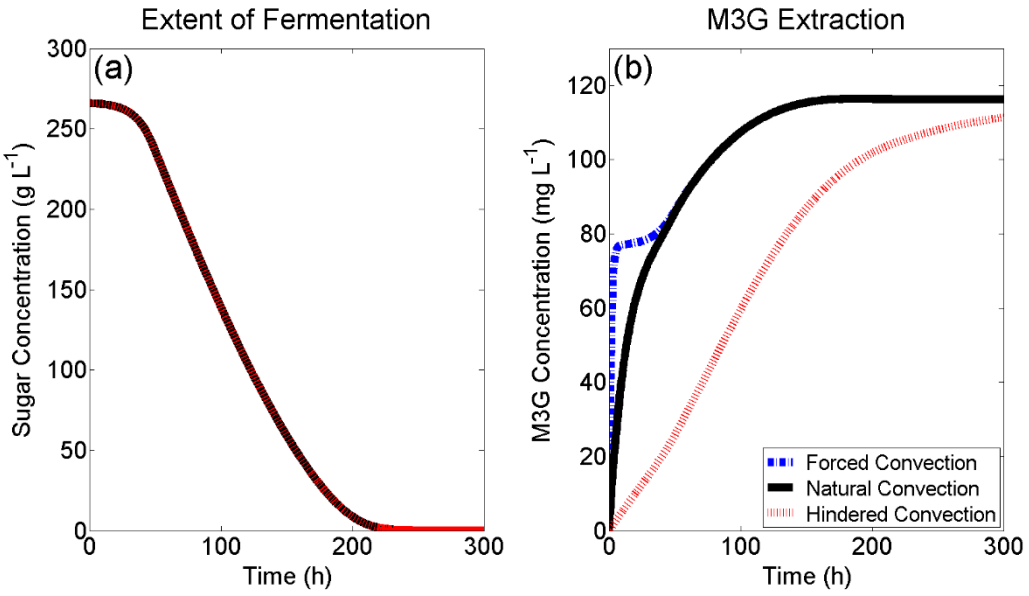

Figure 4. (**a**) Simulated red wine fermentation kinetics and (**b**) the resulting simulated extraction kinetics of M3G under different modes of liquid phase convection.

Under forced convective conditions, where internal mass transfer is the rate-controlling step for extraction, a fast initial extraction within the first few hours of fermentation can be observed followed by a lag in the extraction (Figure 4b) that follows the fermentation lag period (Figure 4a) due to a lack of ethanol in the liquid phase. Following this, M3G extraction is limited by the concentration of ethanol in the system, which increases the distribution constant. Under natural convective conditions, M3G extraction appears to follow a simple first-order rate curve—a commonly used model for anthocyanin extraction during fermentation [4,5].

The initial extractive phase for M3G is slower than with forced convection due to the lower rate of external mass transfer, which in turn means the overall extraction rate is dependent on both internal and external mass transfer properties. Despite this, a similar observation to forced convective conditions can be seen (Figure 4b), whereby after the initial fermentation lag phase (Figure 4a), the rate of M3G extraction is limited by the concentration of ethanol in the system. This implies that in an evenly distributed natural convective system, the same maximum M3G concentration can be achieved as in a well-mixed system, due to the requirement of ethanol in the liquid phase to increase the distribution constant (K) and maximise the M3G concentration. A simulation of 'Hindered Convection' was selected to show the case where normal natural convective extraction may be slowed, such as within the "cap" (grape skins, seeds, stems) of an active red wine fermentation. In this case, a solute particle (such as M3G) within the centre of the cap would need to diffuse through the tortuous path around the solids to the boundary layer separating the cap and the bulk of the liquid phase. Under these conditions, an initial lag in liquid phase M3G concentration would be expected, as a lower external mass transfer coefficient decreases the rate at which M3G is moved from the solid-liquid boundary layer to the liquid bulk, which in-turn lowers the M3G concentration gradient within the grape skin. From Figure 4b, it can also be observed that under hindered convective conditions (Bi = 0.01), ethanol production is no longer the rate limiting step for M3G extraction, as was the case for both forced and natural convection (after the initial fermentation lag phase), and that the rate of liquid phase mass transfer is limiting.

3. Materials and Methods

3.1. Experimental

3.1.1. Experimental Design

For each of the forced and natural convective conditions, three different liquid solutions differing in concentrations of sugar (glucose), ethanol, and water were chosen to emulate extractive conditions representative of the start, middle, and end of a red wine fermentation process for a wine finishing at 14% *v*/*v* of ethanol. Extractions were undertaken in a temperature controlled room nominally set at an ambient temperature of 20 °C. These experimental conditions are presented in Tables 1 and 2. Liquid solutions were prepared and allowed to equilibrate to the ambient air temperature 48 h prior to the commencement of extraction. The local temperature around the extractions was monitored by way of a temperature data logger (model XC0424, Jaycar Electronics, Adelaide, Australia) and was observed to average at 20.2 °C throughout the extraction period. The pH values of liquid phases after one hour of extraction were found to be between 3.81 and 4.16 and finished between 3.64 and 4.03. This variation in pH is not expected to have had an impact on the extraction results as previous work [21] on polyphenol extraction from grape wastes found comparable anthocyanin extraction yields within the pH range of 2 to 8.66 in hydro-alcoholic solutions of 0% and 25% ethanol.

3.1.2. Sample Preparation

Merlot grapes from the University of Adelaide's Coombe vineyard were hand harvested (total soluble solids of 14.3 °Bé, pH 3.6, titratable acidity of 3.9 g L^{-1}) on 24 February 2016 and were frozen at −20 °C until processing. Prior to crushing, berries were thawed overnight at an ambient

temperature of 10 °C and destemmed by hand while still cool. In total, 11.02 kg of randomly sampled berries were then crushed by hand using a stainless steel plunger until all berries were visibly crushed. The must was pressed using a 4.4 L hand operated stainless steel basket press to separate the solids (skins and seeds) from liquid juice. The total mass of pressed solids was 4.58 kg and the collected juice volume was 5.70 L.

3.1.3. Extraction Procedure

For each extraction, 150 g of pressed solids were added to 2 L extraction vessels prior to the addition of 1.5 L of liquid solution to begin the extraction process. Following liquid addition, lids containing a 1 cm diameter hole to allow the insertion of an overhead mechanical stirrer were fitted to the extraction vessels. For the extractions conducted under forced convective conditions, the contents of the vessels were continually stirred throughout the extraction period at a rotational speed of approximately 300 rpm to allow for the calculation of mass transfer parameters within the solid phase. For the extractions conducted under natural convective conditions, the overhead stirrers remained off throughout the extraction with mixing only occurring for 5 s immediately prior to sample collection to ensure a homogenous liquid phase representative of the entire mixture. All extractions were conducted in triplicate. For each set of conditions, 10 mL samples were collected throughout the extraction process until an equilibrium was reached. For the trials under forced convective conditions, samples were collected more frequently within the first 8 h of the extraction to produce appropriate concentration curves. After collection, samples were immediately centrifuged and kept at −20 °C until analysis by HPLC.

3.1.4. Quantification of Malvidin-3-glucoside in Extracts

Samples taken throughout the extraction period were thawed at ambient temperature and sonicated using a benchtop sonicator (model FXP10M, Unisonics, Sydney, Australia) at 50 Hz for 10 min to dissolve precipitated solids. These samples were then centrifuged at 10,000 rcf and 1.5 mL of supernatant transferred to amber HPLC vials for analysis by HPLC using the method described by Setford, Jeffery, Grbin, and Muhlack [1].

3.1.5. Quantification of Malvidin-3-glucoside in Solids

Freshly pressed grape solids (250 g) used in the extraction trials were homogenised using a Grindomix GM200 homogeniser (Retsch, Haan, Germany) for 20 s at a speed of 8000 rpm. The homogenate was then well mixed by hand and 1 g samples of the mixture were transferred to 10 mL centrifuge tubes, in triplicate. To each tube, 10 mL of 50% *v*/*v* aqueous ethanol was added and the mixture inverted by hand at 10 min intervals for a one hour extraction period. The mixtures were then centrifuged at 3220 rcf for 10 min and the supernatant decanted to a new centrifuge tube. These extracts were kept at −20 °C until analysis by HPLC as described in Section 3.1.4. Thawed samples were diluted to 12.5% *v*/*v* aqueous ethanol with water prior to injection. These initial M3G concentrations were used to calculate all other solid-phase M3G concentrations though a mass balance of the extraction system based on the respective liquid-phase samples collected throughout the experiment.

3.1.6. Determination of Physical Parameters

A Viscoball Höppler viscometer (Fungilab, Barcelona, Spain) was used to measure the dynamic viscosity of the extraction solutions, at the same temperature of 20 °C as used during the extraction experiment. Temperature was maintained by circulating cooling water through the outer shell of the viscometer, with cooling water maintained at 20 °C via an external water bath (model TBC-3-22, Thermoline L + M, Smithfield, NSW, Australia) with active temperature control (controller model TBC-TU4, Thermoline L + M, Smithfield, NSW, Australia). Cameras (model KYT-U130-01MBWCS, Kayeton Technology Company Ltd., Shenzhen, China) at a frame rate of 30 frames per second were used to monitor the start and end points of the viscometer to increase the precision of time measurements.

Aspen HYSYS software (Aspen Technology Inc, Bedford, MA, USA) was used to calculate the density at each set of liquid phase conditions based on the liquid phase composition. The solvent molecular mass and association parameter were calculated by the sum of individual ethanol, sugar, and water concentrations in the liquid phase (Equations (12) and (13), respectively).

3.2. Forced Convection Model

The extraction of anthocyanins during fermentative maceration is a solid-liquid mass transfer process controlled by diffusion after the initial leakage around broken skin cells [16,22]. This process consists of three steps commonly grouped together and known as internal diffusion, where the liquid first penetrates the solid to the location of the solute, dissolves the solute, and finally diffuses from within the solid to the solid-liquid boundary layer. At this point, the dissolved solute is then transferred into the bulk of the liquid either by liquid-phase diffusion in the case of natural convection (where no external force is applied to the liquid phase), or by forced convective mass transfer as would be observed during mixing operations. Due to the waxy outer layer of grape skins, diffusion is considered only to take place radially inwards, perpendicular to the surface of the grape skin. A mechanistic model for this process taking into account solute diffusion within the solid, solute mass transfer from the interface to the liquid bulk, and an equilibrium relationship between solid and liquid concentrations can be summarised as follows [8,23,24]:

$$(1-\varepsilon)\frac{dc_\beta}{dt} = k_{c\beta}a\left(c_{\beta i} - c_\beta\right) \tag{5}$$

$$\varepsilon\frac{dc_\gamma}{dt} = k_{c\gamma}a\left(c_{\gamma i} - c_\gamma\right) \tag{6}$$

$$c_{\gamma i} = Kc_{\beta i} \tag{7}$$

Here, the rate of internal diffusion within the solid phase ($D_{s\beta}$) can be determined through a correlation developed in Setford, Jeffery, Grbin, and Muhlack [8] for one-dimensional mass transfer across a plane:

$$D_{s\beta} = \frac{k_{c\beta}4L}{(1-\varepsilon)\pi^2} \tag{8}$$

Under forced convective conditions, the rate of external mass transfer can be determined through a correlation of dimensionless values describing the physical properties of the system:

$$Sh = 2 + 0.95Re^{\frac{1}{2}}Sc^{\frac{1}{3}} \tag{9}$$

where the Reynolds number (Re) can be calculated as a function of the revolutionary speed (N), in revolutions per second, and mixer diameter (D) and:

$$Re = \frac{nD^2\rho_\gamma}{\mu_\gamma}, Sh = \frac{k_{c\gamma}L}{D_{s\gamma}}, Sc = \frac{\eta}{\rho_\gamma D_{s\gamma}} \tag{10}$$

The rate of liquid phase diffusion necessary for calculating the Sherwood (Sh) and Schmidt (Sc) numbers can be determined from the Wilke-Chang correlation:

$$D_{s\gamma} = \frac{1.173\times10^{-16}\left(\varphi M_\gamma\right)^{1/2}T}{\eta V_A^{0.6}} \tag{11}$$

An additive method described by Geankoplis [9] based on the chemical structure of M3G is then used to determine the volume of the solute (V_A), and the average liquid phase association factors and molecular mass can be determined from the mole fractions of the major components of the liquid phase:

$$M_\gamma = x_{EtOH}M_{EtOH} + x_{water}M_{water} + x_{Glucose}M_{Glucose} \quad (12)$$

$$\varphi = x_{EtOH}\varphi_{EtOH} + x_{water}\varphi_{water} + x_{Glucose}\varphi_{Glucose} \quad (13)$$

An analytical solution to Equations (5) to (7) that describes the average solute concentration in both phases (first proposed by Espinoza-Pérez, Vargas, Robles-Olvera, Rodríguez-Jimenes, and García-Alvarado [23]) yielded the following system of equations:

$$c_\beta = c_{\beta 0}\left(C_1 e^{r_1 t} + C_2 e^{r_2 t}\right) \quad (14)$$

$$c_\gamma = c_{\beta 0}\left(C_3 e^{r_1 t} + C_4 e^{r_2 t}\right) \quad (15)$$

where:

$$r_{1,2} = -\frac{b_1 + b_2}{2} \pm \frac{\sqrt{(b_1 + b_2)^2 - 4(b_1 b_2 - b_3 b_4)}}{2}$$

$$C_1 = \frac{r_1 + b_1}{r_1 - r_2}, C_2 = \frac{r_2 + b_1}{r_2 - r_1}, C_3 = \frac{b_3}{r_1 - r_2}, C_4 = \frac{b_3}{r_2 - r_1}$$

$$b_1 = \frac{k_{c\gamma} a(1 - \psi_1)}{\varepsilon}, b_2 = \frac{k_{c\beta} a\left(1 - \frac{\psi_2}{K}\right)}{(1 - \varepsilon)}, b_3 = \frac{k_{c\gamma} a \psi_2}{\varepsilon}, b_4 = \frac{k_{c\beta} a \frac{\psi_1}{K}}{(1 - \varepsilon)}$$

$$\psi_1 = \frac{1}{1 + \frac{k_{c\beta}}{K k_{c\gamma}}}, \ \psi_2 = \frac{k_{c\beta}/k_{c\gamma}}{1 + \frac{k_{c\beta}}{K k_{c\gamma}}}$$

To determine the rate of internal mass transfer, $k_{c\beta}$, MATLAB software (version R2013a) was used to fit non-linear regressions to Equations (14) and (15) using experimentally determined M3G concentrations, whereby the residuals of the model are minimised by adjusting $k_{c\beta}$. Table 3 presents a summary of the physical parameters and system variables used for the model solution.

Table 3. Summary of physical properties and shape variables of the experimental extraction system.

Property or Shape Variable	Value	Source
a (m^2 m^{-3})	5747	Mathematically derived
ε	0.9173	Experimentally determined
$c_{\beta 0}$ (kg m^{-3})	1.032	Experimentally determined
L (m)	1.74×10^{-4}	Jin, et al. [25]
V_A (L mol^{-1})	0.5259	Geankoplis [9]
η (cP)	Varied	Experimentally determined
ρ_γ (kg m^{-3})	Varied	HYSYS (Hysys, Operations Guide., 2005)
M_γ (g mol^{-1})	Varied	Equation (12)
φ	Varied	Equation (13)

3.3. Natural Convection Model

Because the rate of internal diffusion and mass transfer within the solid phase is independent of the mode of convection [23,24], the internal mass transfer coefficients ($k_{c\beta}$) for natural convective trials are taken as those solved under forced convective conditions at the respective temperature and solvent conditions. The external mass transfer coefficient ($k_{c\gamma}$) for natural convective trials was then obtained through a non-linear regression of Equations (14) and (15) whereby the residuals of the model solution were set to be minimised.

3.4. Simulating Extraction during Fermentation

To simulate M3G extraction under active fermentation scenarios, a predictive wine fermentation model originally proposed in Cramer et al. [26] and later modified in Coleman, Fish, and Block [19] was used, which consists of five coupled ordinary differential equations (ODEs):

$$\frac{dX}{dt} = \mu X_A \tag{16}$$

$$\frac{dX_A}{dt} = \mu X_A - k_d X_A \tag{17}$$

$$\frac{dN}{dt} = -\frac{\mu X_A}{Y_{X/N}} \tag{18}$$

$$\frac{dE}{dt} = B X_A \tag{19}$$

$$\frac{dS}{dt} = -\frac{B X_A}{Y_{E/S}} \tag{20}$$

Here, X is the yeast biomass concentration, X_A is the active yeast concentration, N is the nitrogen concentration (which is the yeast-growth limiting nutrient in the model), E is the ethanol concentration, and S is the sugar concentration. The specific yeast cell growth rate and sugar consumption rate are described by Michaelis-Menten kinetics:

$$\mu = \frac{\mu_{max} N}{K_N + N} \tag{21}$$

$$B = \frac{B_{max} S}{K_S + S} \tag{22}$$

where μ_{max} is the maximum yeast growth rate, K_N is the Monod constant for nitrogen consumption, B_{max} is the maximum sugar consumption rate, and K_S is the constant for sugar consumption. The yeast cell death rate is defined as a function of the ethanol concentration:

$$k_d = k'_d E \tag{23}$$

where k'_d denotes the sensitivity of yeast cells to ethanol. To solve this system of ODEs describing fermentation kinetics, a series of temperature-dependent multi-linear models described by Coleman, Fish, and Block [19] were used to estimate the values of parameters within Equations (16) to (23). A summary of the coefficients used for each parameter is provided in Table 4.

Table 4. Coefficients for estimating fermentation model parameters as a function of temperature, where: $Parameter = a_0 + a_1 T + a_2 T^2$.

	Coefficients for Regression Models		
Parameter	a_0	a_1	a_2
$log(\mu_{max})$	−3.92	7.82×10^{-2}	-
$log(K_N)$	−4.73	-	-
$log(k'_d)$	−9.81	-1.08×10^{-3}	4.78×10^{-3}
$log(Y_{X/N})$	3.50	−3.61	-
$log(Y_{E/S})$	-5.98×10^{-1}	-	-
$log(B_{max})$	−2.30	7.71×10^{-2}	-
$log(K_S)$	2.33	-	-

3.5. Statistical Analysis

For each set of experimental conditions, the efficacy of the proposed model's fit was determined based on two parameters: The root mean square error (*RMSE*) and the coefficient of determination (R^2). These values were determined by:

$$RMSE = \sqrt{\frac{1}{N}\sum_{i=1}^{N}\left(c_{\gamma,pred,i} - c_{\gamma,exp,i}\right)^2} \tag{24}$$

$$R^2 = 1 - \frac{\sum_{i=1}^{N}\left(c_{\gamma,pred,i} - c_{\gamma,exp,i}\right)^2}{\sum_{i=1}^{N}\left(c_{\gamma,pred,i} - \bar{c}_{\gamma,exp}\right)^2} \tag{25}$$

Here, $c_{\gamma,exp,i}$ is the experimentally determined M3G liquid phase concentration, $c_{\gamma,pred,i}$ is the concentration predicted by the model, $\bar{c}_{\gamma,exp}$ is the replicate mean of experimentally-determined concentrations in the liquid phase, and N is the number of replicates for each trial.

4. Conclusions

The extraction of M3G from pre-fermentative red grape solids under conditions emulating different stages of fermentation with respect to sugar and ethanol concentrations were explored under natural and forced convective conditions. A previously developed mathematical model based on first principles and a series of empirical correlations were used to describe the solid-liquid extraction process and calculate relevant mass transfer parameters at all experimental conditions. Calculated Biot numbers indicate that under forced convection, the process was controlled by internal diffusion, whereas under natural convection, both internal diffusion and liquid-phase convection controlled the extraction rate. Predictive simulations of extraction under fermentation conditions (continuously evolving liquid phase) showed that under natural convective conditions, the extraction of M3G was also strongly influenced by the rate of ethanol evolution. This observation of a more complex extraction relationship, which includes the influence of ethanol, provides insight into other studies comparing the effectiveness of mixing technologies during fermentation, where conflicting results have previously been observed.

Author Contributions: P.C.S., R.A.M., D.W.J. and P.R.G. conceived and designed experiments; P.C.S. performed the experiments and conducted laboratory analysis of samples; P.C.S., R.A.M., D.W.J. and P.R.G. interpreted the data; P.C.S. and R.A.M. conducted the mathematical modelling; P.C.S. drafted the original manuscript; R.A.M., D.W.J. and P.R.G. provided critical feedback and editing. All authors have read and approved the final manuscript.

Funding: P.C.S. is supported through a UA School of Agriculture, Food and Wine Scholarship [1606990] and was also a recipient of a Wine Australia supplementary scholarship [AGW Ph1505]. The authors acknowledge the financial support from the School of Agriculture, Food and Wine, UA, and Australian grapegrowers and winemakers through their investment body, Wine Australia, with matching funds from the Australian Government.

Conflicts of Interest: The authors have no conflict of interest.

Abbreviations

Nomenclature

a	Specific surface area for mass transfer ($m^2\ m^{-3}$)
$b_1, \ldots, b_4$	Constants required to solve Equations (14) and (15)
B	Rate of sugar consumption per cell ($g_{EtOH}\ g_{biomass}\ h^{-1}$)
B_{max}	Maximum sugar consumption rate ($g_{EtOH}\ g_{biomass}\ h^{-1}$)
c	Phenolic compound concentration ($mg\ L^{-1}$)
$C_1, \ldots, C_4$	Constants required to solve Equations (14) and (15)
C_{EtOH}	Ethanol concentration (% *v/v*)
C_g	Glucose concentration ($g\ L^{-1}$)
D	Mechanical stirrer diameter (m)

Nomenclature

D_s	Solute (s) mass diffusivity ($m^2\ s^{-1}$)
k_c	Mass transfer coefficient ($m\ s^{-1}$)
k_d	Yeast cell death rate (h^{-1})
k'_d	Coefficient describing yeast sensitivity to ethanol
K	Distribution constant
K_N	Constant for nitrogen-limited yeast growth
K_S	Constant for sugar consumption by yeast
L	Characteristic length for diffusive mass transfer (m)
M	Molar mass ($g\ mol^{-1}$)
n	Stirrer speed (rpm)
N	Nitrogen concentration ($g\ L^{-1}$)
$r_{1,2}$	Constants required to solve Equations (14) and (15)
R^2	Coefficient of determination
$RMSE$	Root mean square error
S	Sugar concentration ($g\ L^{-1}$)
t	Time (s)
T	Temperature (°C)
V_A	Solute molar volume ($L\ mol^{-1}$)
X	Yeast biomass concentration ($g\ L^{-1}$)
X_A	Active yeast biomass concentration ($g\ L^{-1}$)
$Y_{E/S}$	Yield coefficient for ethanol production to sugar consumption
$Y_{X/N}$	Yield coefficient for cell growth to nitrogen consumption

Dimensionless groups

Bi	Biot number
Re	Reynolds number
Sc	Schmidt number
Sh	Sherwood number

Greek symbols

ε	Solvent volume fraction
φ	Association parameter
η	Dynamic viscosity (cP)
μ	Specific yeast cell growth rate (s^{-1})
μ_{max}	Maximum specific yeast cell growth rate (s^{-1})
ρ	Density ($kg\ m^{-3}$)
$\psi_{1,2}$	Constants required to solve Equations (14) and (15)

Subscripts

0	At the initial or reference point
exp	Experimentally obtained
i	At the solid-liquid interface
$pred$	Predicted by model
β	Solid phase
γ	Liquid phase

References

1. Gertenbach, D. Solid–liquid extraction technologies for manufacturing nutraceuticals from botanicals. In *Functional Foods Biochemical and Processing Aspects*; Taylor and Francis Group: Boca Raton, FL, USA, 2001; Volume 2, pp. 331–366.
2. Cissé, M.; Bohuon, P.; Sambe, F.; Kane, C.; Sakho, M.; Dornier, M. Aqueous extraction of anthocyanins from *Hibiscus sabdariffa*: Experimental kinetics and modeling. *J. Food Eng.* **2012**, *109*, 16–21. [CrossRef]
3. Setford, P.C.; Jeffery, D.W.; Grbin, P.R.; Muhlack, R.A. Factors affecting extraction and evolution of phenolic compounds during red wine maceration and the role of process modelling. *Trends Food Sci. Technol.* **2017**, *69*, 106–117. [CrossRef]

4. Zanoni, B.; Siliani, S.; Canuti, V.; Rosi, I.; Bertuccioli, M. A kinetic study on extraction and transformation phenomena of phenolic compounds during red wine fermentation. *Int. J. Food Sci. Technol.* **2010**, *45*, 2080–2088. [CrossRef]
5. Boulton, R.; Singleton, V.; Bisson, L.; Kunkee, R. *Principles and Practices of Winemaking*; Chapman and Hall: New York, NY, USA, 1996.
6. Sacchi, K.L.; Bisson, L.F.; Adams, D.O. A review of the effect of winemaking techniques on phenolic extraction in red wines. *Am. J. Enol. Viticult.* **2005**, *56*, 197–206.
7. Mantell, C.; Rodríguez, M.; Martínez de la Ossa, E. Semi-batch extraction of anthocyanins from red grape pomace in packed beds: Experimental results and process modelling. *Chem. Eng. Sci.* **2002**, *57*, 3831–3838. [CrossRef]
8. Setford, P.C.; Jeffery, D.W.; Grbin, P.R.; Muhlack, R.A. Modelling the mass transfer process of malvidin-3-glucoside during simulated extraction from fresh grape solids under wine-like conditions. *Molecules* **2018**, *23*, 2159. [CrossRef] [PubMed]
9. Geankoplis, C.J. *Transport Processes and Separation Process Principles*; Prentice Hall Professional Technical Reference: Upper Saddle River, NJ, USA, 2003.
10. Canals, R.; Llaudy, M.; Valls, J.; Canals, J.; Zamora, F. Influence of ethanol concentration on the extraction of color and phenolic compounds from the skin and seeds of Tempranillo grapes at different stages of ripening. *J. Agric. Food Chem.* **2005**, *53*, 4019–4025. [CrossRef] [PubMed]
11. González-Manzano, S.; Rivas-Gonzalo, J.C.; Santos-Buelga, C. Extraction of flavan-3-ols from grape seed and skin into wine using simulated maceration. *Anal. Chim. Acta* **2004**, *513*, 283–289. [CrossRef]
12. Pérez-Galindo, J.; López-Miranda, J.; Martín-Dominguez, I. Geometric and Reynolds number effects on oregano (*Lippia Berlandieri Schauer*) essential oil extraction. *J. Food Eng.* **2000**, *44*, 127–133. [CrossRef]
13. Doco, T.; Williams, P.; Cheynier, V. Effect of flash release and pectinolytic enzyme treatments on wine polysaccharide composition. *J. Agric. Food Chem.* **2007**, *55*, 6643–6649. [CrossRef]
14. Morel-Salmi, C.; Souquet, J.-M.; Bes, M.; Cheynier, V. Effect of flash release treatment on phenolic extraction and wine composition. *J. Agric. Food Chem.* **2006**, *54*, 4270–4276. [CrossRef] [PubMed]
15. Smith, P.; McRae, J.; Bindon, K. Impact of winemaking practices on the concentration and composition of tannins in red wine. *Aust. J. Grape Wine Res.* **2015**, *21*, 601–614. [CrossRef]
16. Sparrow, A.M.; Smart, R.E.; Dambergs, R.G.; Close, D.C. Skin particle size affects the phenolic attributes of Pinot Noir wine: Proof of concept. *Am. J. Enol. Viticult.* **2015**, *67*, 29–37. [CrossRef]
17. Cacace, J.E.; Mazza, G. Mass transfer process during extraction of phenolic compounds from milled berries. *J. Food Eng.* **2003**, *59*, 379–389. [CrossRef]
18. Lerno, L.; Reichwage, M.; Panprivech, S.; Ponangi, R.; Hearne, L.; Oberholster, A.; Block, D.E. Chemical gradients in pilot-scale cabernet sauvignon fermentations and their effect on phenolic extraction. *Am. J. Enol. Viticult.* **2017**, *68*, 401–411. [CrossRef]
19. Coleman, M.C.; Fish, R.; Block, D.E. Temperature-dependent kinetic model for nitrogen-limited wine fermentations. *Appl. Environ. Microbiol.* **2007**, *73*, 5875–5884. [CrossRef] [PubMed]
20. González-Neves, G.; Gil, G.; Barreiro, L. Influence of grape variety on the extraction of anthocyanins during the fermentation on skins. *Eur. Food Res. Technol.* **2008**, *226*, 1349. [CrossRef]
21. Silva, S.; Costa, E.; Calhau, C.; Morais, R.; Pintado, M. Anthocyanin extraction from plant tissues: A review. *Crit. Rev. Food Sci. Nutr.* **2017**, *57*, 3072–3083. [CrossRef]
22. Cerpa-Calderón, F.K.; Kennedy, J.A. Berry integrity and extraction of skin and seed proanthocyanidins during red wine fermentation. *J. Agric. Food Chem.* **2008**, *56*, 9006–9014. [CrossRef]
23. Espinoza-Pérez, J.; Vargas, A.; Robles-Olvera, V.; Rodríguez-Jimenes, G.; García-Alvarado, M. Mathematical modeling of caffeine kinetic during solid–liquid extraction of coffee beans. *J. Food Eng.* **2007**, *81*, 72–78. [CrossRef]
24. Rodríguez-Jimenes, G.C.; Vargas-Garcia, A.; Espinoza-Pérez, D.J.; Salgado-Cervantes, M.A.; Robles-Olvera, V.J.; García-Alvarado, M.A. Mass transfer during vanilla pods solid liquid extraction: Effect of extraction method. *Food Bioprocess Technol.* **2013**, *6*, 2640–2650. [CrossRef]

25. Jin, X.; Wu, X.; Liu, X.; Liao, M. Varietal heterogeneity of textural characteristics and their relationship with phenolic ripeness of wine grapes. *Sci. Hort.* **2017**, *216*, 205–214. [CrossRef]
26. Cramer, A.C.; Vlassides, S.; Block, D.E. Kinetic model for nitrogen-limited wine fermentations. *Biotechnol. Bioeng.* **2002**, *77*, 49–60. [CrossRef] [PubMed]

Sample Availability: Samples of the compounds are not available from the authors.

CHAPTER 4

Mathematical modelling of anthocyanin mass transfer to predict extraction in simulated red wine fermentation scenarios

Patrick C. Setford[1], David W. Jeffery[1], Paul R. Grbin[1], Richard A. Muhlack[1,*]

[1] Department of Wine and Food Science, School of Agriculture, Food and Wine, The University of Adelaide (UA), PMB 1 Glen Osmond SA 5064, Australia

Food Research International - **2019**, 121, 705-713

Statement of Authorship

Title of Paper	Mathematical modelling of anthocyanin mass transfer to predict extraction in simulated red wine fermentations scenarios
Publication Status	☑ Published ☐ Accepted for Publication ☐ Submitted for Publication ☐ Unpublished and Unsubmitted w ork w ritten in manuscript style
Publication Details	Setford, P. C., Jeffery, D. W., Grbin, P. R., & Muhlack, R. A. (2019). Mathematical modelling of anthocyanin mass transfer to predict extraction in simulated red wine fermentation scenarios. Food Research International, vol. 121, pp. 705-713.

Principal Author

Name of Principal Author (Candidate)	Patrick C. Setford		
Contribution to the Paper	Designed experiments, performed experimental work, performed laboratory analysis of samples (HPLC, viscometer), analysed and interpreted data, performed mathematical modelling, prepared entire first draft of the manuscript and helped address reviewer comments.		
Overall percentage (%)	70%		
Certification:	This paper reports on original research I conducted during the period of my Higher Degree by Research candidature and is not subject to any obligations or contractual agreements with a third party that would constrain its inclusion in this thesis. I am the primary author of this paper.		
Signature		Date	19/05/19

Co-Author Contributions

By signing the Statement of Authorship, each author certifies that:

i. the candidate's stated contribution to the publication is accurate (as detailed above);

ii. permission is granted for the candidate in include the publication in the thesis; and

iii. the sum of all co-author contributions is equal to 100% less the candidate's stated contribution.

Name of Co-Author	David W. Jeffery		
Contribution to the Paper	Contributed to the research idea and experimental design, assisted with laboratory analysis, assisted with interpretation of data, critically reviewed and edited the manuscript and helped address reviewer comments.		
Signature		Date	20/5/19

Name of Co-Author	Paul R. Grbin		
Contribution to the Paper	Contributed to the research idea and experimental design, assisted with interpretation of data, critically reviewed and edited the manuscript and helped address reviewer comments.		
Signature		Date	20/05/2019

Name of Co-Author	Richard A. Muhlack		
Contribution to the Paper	Contributed to the conception of the article and experimental design, assisted with mathematical modelling, assisted with experimental setup and supervised the work. Helped prepare, edit and critically review the manuscript and helped address reviewer comments. Acted as the corresponding author.		
Signature		Date	20.5.2019

Please cut and paste additional co-author panels here as required.

Food Research International 121 (2019) 705–713

Contents lists available at ScienceDirect

Food Research International

journal homepage: www.elsevier.com/locate/foodres

Mathematical modelling of anthocyanin mass transfer to predict extraction in simulated red wine fermentation scenarios

Patrick C. Setford, David W. Jeffery, Paul R. Grbin, Richard A. Muhlack*

Department of Wine and Food Science, School of Agriculture, Food and Wine, The University of Adelaide (UA), PMB 1, Glen Osmond, SA 5064, Australia

ARTICLE INFO

Keywords:
Phenolic extraction
Anthocyanin
Process modelling
Wine colour
Mass transfer
Simulation

ABSTRACT

Anthocyanins are polyphenolic compounds present in grapes that are responsible for the initial colour of red wine and their incorporation into derived pigments leads to long term colour stability. The ability to predict the effect of process variables, either controlled by winemakers or that naturally change throughout fermentation, on the extraction of anthocyanins is vital to producing red wine of high quality. A 2^3 factorial experiment with additional points located at central factor conditions was used to determine the impact of temperature, sugar and ethanol concentrations on the mass transfer properties of anthocyanins from fresh Pinot noir grape solids. Factor conditions were chosen to replicate ethanol and sugar concentrations that would be found in a 14% red wine and its respective unfermented juice. A previously described mathematical model was applied to anthocyanin extraction curves to determine mass transfer coefficients and distribution constants for the generation of response surface models able to predict these mass transfer variables for dynamic fermentation scenarios. The coefficient of determination for the model solution exceeded 0.94 in all cases, demonstrating a good agreement between experimental and mathematically-derived anthocyanin concentrations. Following this, simulations of anthocyanin extraction under fermentation conditions were conducted using a previously developed wine fermentation model allowing for the prediction of extraction rates and anthocyanin concentrations under various winemaking scenarios. The extraction simulations predicted a previously observed but so far undescribed anthocyanin extraction pattern during fermentation.

1. Introduction

From 2010 to 2016, global wine production has averaged an approximate annual rate of 27 billion litres, highlighting its importance as a commodity in the food industry (Anderson, Nelgen, & Pinilla, 2018). In the case of red wine, although water and alcohol are the two main components in terms of weight, phenolic compounds extracted from the skins and seeds during fermentative maceration are the main drivers of colour, taste and overall quality of the finished product (Sparrow, Holt, Pearson, Dambergs, & Close, 2016). As such, understanding the mechanisms of extraction and developing process models capable of accurately describing and predicting the extraction process is of utmost importance to controlling wine quality and improving the efficiency of winery operations (Lerno et al., 2017; Setford, Jeffery, Grbin, & Muhlack, 2017).

During the red winemaking process, grape solids (skins and seeds) typically remain in contact with the pre-fermentative juice from the onset of crushing until the end of alcoholic fermentation or until the must contains the desired colour and flavor. Throughout this time, phenolic compounds including anthocyanins and tannins are extracted in a multi-step process. For anthocyanins, this process involves a fast initial leakage step around the broken skin edges caused by crushing, followed by a slower concentration-driven step controlled by solid-liquid diffusion perpendicular to the face of the grape skin (Cerpa-Calderón & Kennedy, 2008; Sparrow, Smart, Dambergs, & Close, 2015). This diffusion step is comprised of three distinct steps whereby the liquid must first penetrate the solid, dissolve the anthocyanins into the liquid, and finally diffuse back to the surface of the solid (Gertenbach, 2001). Once the solute has reached the solid-liquid boundary layer, it must then find its way from the surface into the bulk of the liquid either by diffusion through the liquid (free convection) or during mixing operations (forced convection).

Existing kinetic models describing the extraction of phenolic compounds during red wine maceration (such as simple first and second order kinetic rate models) can be used to effectively fit experimental extraction curves and give insight into the effect of changing process conditions (Boulton, Singleton, Bisson, & Kunkee, 1996; Zanoni, Siliani, Canuti, Rosi, & Bertuccioli, 2010). Despite this, they have limited

* Corresponding author.
E-mail address: richard.muhlack@adelaide.edu.au (R.A. Muhlack).

https://doi.org/10.1016/j.foodres.2018.12.044
Received 22 October 2018; Received in revised form 6 December 2018; Accepted 22 December 2018
Available online 24 December 2018
0963-9969/

Nomenclature

a	Specific surface area for mass transfer ($m^2\,m^{-3}$)
a_0, …, a_7	Response surface coefficients
b_1, …, b_4	Constants required to solve Eqs. (7) and (8)
B	Rate of sugar consumption per cell
B_{max}	Maximum sugar consumption rate
c	Phenolic compound concentration ($g\,m^{-3}$)
C_1, …, C_4	Constants required to solve Eqs. (7) and (8)
C_{EtOH}	Ethanol concentration (% *v/v*)
C_S	Sugar concentration ($g\,L^{-1}$)
D	Mechanical stirrer diameter (m)
D_s	Solute (*s*) mass diffusivity ($m^2\,s^{-1}$)
E	Ethanol concentration ($g\,L^{-1}$)
k_c	Mass transfer coefficient ($m\,s^{-1}$)
k_d	Yeast cell death rate
k_d'	Coefficient describing yeast sensitivity to ethanol
K	Distribution constant
K_N	Constant for nitrogen-limited yeast growth
K_S	Constant for sugar consumption by yeast
L	Characteristic length for internal diffusion (m)
M	Molar mass ($g\,mol^{-1}$)
n	Stirrer speed (rpm)
N	Nitrogen concentration ($g\,L^{-1}$)
$r_{1,\,2}$	Constants required to solve Eqs. (11) and (12)
R^2	Coefficient of determination
RMSE	Root mean square error
S	Sugar concentration ($g\,L^{-1}$)
t	Time (*s*)
T	Temperature (°C)
V_A	Solute molar volume ($L\,mol^{-1}$)
X	Yeast biomass concentration ($g\,L^{-1}$)
X_A	Active yeast biomass concentration ($g\,L^{-1}$)
$Y_{E/S}$	Yield coefficient for ethanol production to sugar consumption
$Y_{X/N}$	Yield coefficient for cell growth to nitrogen consumption

Dimensionless groups

Bi	Biot number
Re	Reynolds number
Sc	Schmidt number
Sh	Sherwood number

Greek symbols

ε	Solvent volume fraction
φ	Association parameter
η	Dynamic viscosity ($kg\,m^{-1}\,s^{-1}$)
μ	Specific yeast cell growth rate (s^{-1})
μ_{max}	Maximum specific yeast cell growth rate (s^{-1})
ρ	Density ($kg\,m^{-3}$)
$\psi_{1,\,2}$	Constants required to solve Eqs. (7) and (8)

Subscripts

0	At the initial or reference point
i	At the solid-liquid interface
pred	Predicted by model
β	Solid phase
γ	Liquid phase

ability to accurately predict the effect of process variables that change throughout a real world fermentation (such as temperature and ethanol concentration), as well as those variables that can be actively manipulated by a winemaker (Setford et al., 2017).

The present work follows from a previous study on developing process models for the extraction of anthocyanins (Setford, Jeffery, Grbin, & Muhlack, 2018) by using a different grape varietal (Pinot noir) that is notorious in terms of its low pigment stability and difficulty in extracting colour (Busse-Valverde et al., 2010). A previously developed model based on numerical solutions to Fick's second law of diffusion was used to evaluate relevant mass transfer parameters of anthocyanins from pre-fermentative Pinot noir grape solids in solid-liquid extraction systems emulating various stages of the red wine making process. The parameters were then used to generate surface response models capable of predicting the internal mass transfer coefficients and distribution constants at different liquid phase concentrations of sugar and ethanol as well as at varying extraction temperatures. Finally, these surface response models were incorporated with a predictive wine fermentation model developed by Coleman, Fish, and Block (2007) to simulate the extraction of anthocyanins in active fermentation scenarios, demonstrating how process variables can be manipulated to achieve faster extraction rates and higher (or lower) final concentrations of anthocyanins for the purposes of reducing processing times and improving the overall efficiency of commercial wine production.

2. Materials and methods

2.1. Experimental

2.1.1. Experimental design

For the construction of surface response models of specific anthocyanin mass transfer parameters at different concentrations of ethanol and sugar (specifically glucose, the predominant wine-grape sugar) and at different temperatures, a 2^3 full factorial experiment run in duplicate was used. Concentrations of sugar and ethanol were chosen to replicate those that would be found in a finished dry red wine (14% *v/v* ethanol, 0 $g\,L^{-1}$ sugar) and its equivalent in unfermented must (0% *v/v* ethanol, 266 $g\,L^{-1}$ sugar). The simplification of the liquid phase into the principal components of wine and fermenting juice (water, ethanol and water, sugar, respectively) was chosen to limit the potential for confounding variables and to investigate the impact of those components most responsible for the physical properties of the liquid phase. As such, the pH values of extraction solutions were not adjusted and were determined to be between 3.71 and 3.99 after the first hour of extraction. Temperature-controlled rooms, were used with low and high extraction temperatures nominally set at 0 °C and 20 °C, respectively, which were chosen to replicate extraction conditions found at various stages of red wine production (from cold soaking through to fermentation). Real time data logging of the rooms showed average temperatures of 4.9 °C and 20.6 °C, respectively, and these temperatures were used for all mathematical modelling as they are representative of industry conditions. Additional data points were included at a mid-point temperature condition (nominally set at 10 °C) within the experimental design to improve the reliability of response surfaces.

2.1.2. Sample preparation

Fresh Pinot noir grapes were harvested by hand (total soluble solids of 12.2° Baumé, pH 3.4, titratable acidity (to pH 8.2) of 7.2 $g\,L^{-1}$) on 27 March 2017 and kept refrigerated until crushing. A total of 14.2 kg of berries were destemmed by hand and manually crushed using a stainless steel hand plunger until all berries were crushed and none remained visibly intact. The berry solids were then separated from the liquid juice using a 4.4 L hand operated stainless steel basket press. The mass of the collected grape solids was 5.32 kg and yielded 7.98 L of grape juice.

2.1.3. Solid-liquid extractions

Immediately following solid pressing, 150 g of solids were individually weighed into the extraction vessels and 1.5 L of the respective liquid solutions was added to begin the solid-liquid extraction process giving a solid/liquid ratio of 1:10. Liquid solutions were prepared approximately 48 h prior to grape solids processing and allowed to equilibrate to ambient extraction conditions in the respective temperature-controlled rooms. To limit liquid phase reactions between extracted phenolic compounds and yield more accurate values for diffusion and mass transfer coefficients, this lower solid/liquid ratio compared to a typical red wine fermentation was used. Although this method will affect the final liquid phase concentration, simulations using solid/liquid ratios typical for red wine fermentations can be achieved using experimentally-determined values for the distribution constant, K (Eq. (4)). Upon liquid addition, lids containing a 1 cm diameter hole were added to the extraction vessels allowing the insertion of a 6 cm diameter overhead mechanical stirrer. Stirrers were purpose built in-house for this experiment using a Powertech MP3209 12 V Motor Speed Controller connected directly to a Powertech YM2718 12 V 6500 rpm DC Motor (Jaycar Electronics, Adelaide, Australia) which was coupled to a 6 cm diameter stainless steel four-armed tilted-anchor-type stirrer. All vessels were stirred continuously at a speed of approximately 300 rpm to achieve a well-mixed system and allow for the calculation of external mass transfer parameters. Throughout the extraction, 10 mL samples were taken at increasing time intervals within the first 24 h to generate appropriate concentration curves. Upon collection, samples were immediately centrifuged for 10 min at 3220 rcf and the supernatant decanted and kept at −20 °C until HPLC analysis.

2.1.4. Anthocyanin quantification

An Agilent 1100 HPLC (Agilent, Forest Hill, VIC, Australia) equipped with a quaternary pump and diode array detector (DAD) was used to perform sample analyses. Gradient elution was used based on the method described by (Cozzolino et al., 2004) with a slight modification as detailed by (Mercurio, Dambergs, Herderich, & Smith, 2007). Agilent ChemStation software (version B.01.03) was used for data acquisition and processing. A 20 µL injection volume was used for each sample and anthocyanins were quantified at 520 nm by comparison of retention time and absorbance using an external standard of malvidin-3-*O*-glucoside chloride (≥95% by HPLC) purchased from Extrasynthese (Genay, France).

2.1.5. Solid-phase anthocyanin quantification

Triplicate samples of 250 g of the freshly pressed grape solids were homogenised using a Retsch Grindomix GM200 homogeniser (Retsch, Haan, Germany) at a speed of 8000 rpm for 20 s. The homogenate was then well mixed and approximately 1 g was transferred to a 10 mL centrifuge tube, 10 mL of 50% *v/v* aqueous ethanol was added, and the mixture was shaken by hand to redistribute the solids every 10 min throughout a one hour extraction period. The mixture was then centrifuged at 3220 rcf for 10 min and the supernatant transferred to a new centrifuged tube and frozen at −20 °C until HPLC analysis using a method adapted from Mercurio et al. (2007). Samples were diluted to 12.5% *v/v* aqueous ethanol in water prior to injection.

2.1.6. Measurement of viscosity

A Viscoball Höppler viscometer (Fungilab, Barcelona Spain) was used to measure the viscosity of the extraction solutions at the extraction temperatures used during this experiment. Cameras (model KYT-U130-01MBWCS, Kayeton Technology Company Ltd., Shenzhen, China) at a framerate of 30 frames per second were used to monitor the start and end points of the viscometer to increase the precision of time measurements.

2.2. Mass transfer model

The derivation of the mathematical model applied for anthocyanin extraction from grape skins is described in full in Setford et al. (2018). Similar models have been previously used to describe the mass transfer of phenolic compounds from vanilla pods (Rodríguez-Jimenes et al., 2013) and coffee beans (Espinoza-Pérez, Vargas, Robles-Olvera, Rodríguez-Jimenes, & García-Alvarado, 2007). Briefly, this method involves the simplification of Fick's second law of diffusion into a series of ordinary differential equations (ODEs) describing the macroscopic mass transfer:

$$\varepsilon \frac{dc_\gamma}{dt} = k_{c\gamma} a (c_{\gamma i} - c_\gamma) \tag{1}$$

$$(1-\varepsilon)\frac{dc_\beta}{dt} = k_{c\beta} a (c_{\beta i} - c_\beta) \tag{2}$$

$$k_{c\gamma}(c_{\gamma i} - c_\gamma) = -k_{c\beta} a (c_{\beta i} - c_\beta) \tag{3}$$

$$c_{\gamma i} = K c_{\beta i} \tag{4}$$

Eq. (2) is then related to a simplified analytical solution of Fick's second law describing the system at the microscopic level for 1-dimensional diffusion across a plane sheet (Setford et al., 2018):

$$\frac{dc_\beta}{dt} = \frac{\pi^2 D_{s\beta}}{4L^2}(c_{\beta i} - c_\beta) \tag{5}$$

to yield Eq. (6) which relates diffusion and mass transfer within the solid phase:

$$D_{s\beta} = \frac{k_{c\beta} 4L}{(1-\varepsilon)\pi^2} \tag{6}$$

2.3. Mass transfer parameter estimation

An analytical solution of Eqs. (1) and (2), first proposed by Espinoza-Pérez et al. (2007) yielded the following set of simultaneous equations describing the change in concentration of phenolic compounds in both the solid and liquid phases:

$$c_\beta = c_{\beta 0}(C_1 e^{r_1 t} + C_2 e^{r_2 t}) \tag{7}$$

$$c_\gamma = c_{\beta 0}(C_3 e^{r_1 t} + C_4 e^{r_2 t}) \tag{8}$$

Where:

$$r_{1,2} = -\frac{b_1 + b_2}{2} \pm \frac{\sqrt{(b_1+b_2)^2 - 4(b_1 b_2 - b_3 b_4)}}{2} \tag{9}$$

$$C_1 = \frac{r_1 + b_1}{r_1 - r_2}, \quad C_2 = \frac{r_2 + b_1}{r_2 - r_1}, \quad C_3 = \frac{b_3}{r_1 - r_2}, \quad C_4 = \frac{b_3}{r_2 - r_1} \tag{10}$$

$$b_1 = \frac{k_{c\gamma} a (1-\psi_1)}{\varepsilon}, \quad b_2 = \frac{k_{c\beta} a \left(1 - \frac{\psi_2}{K}\right)}{(1-\varepsilon)}, \quad b_3 = \frac{k_{c\gamma} a \psi_2}{\varepsilon}, \quad b_4 = \frac{k_{c\beta} a \frac{\psi_1}{K}}{(1-\varepsilon)} \tag{11}$$

$$\psi_1 = \frac{1}{1 + \frac{k_{c\beta}}{K k_{c\gamma}}}, \psi_2 = \frac{k_{c\beta}/k_{c\gamma}}{1 + \frac{k_{c\beta}}{K k_{c\gamma}}} \tag{12}$$

Here, K was calculated by the concentration of solute in the solid and liquid phases at equilibrium (Eq. (4)) and the external mass transfer coefficient ($k_{c\gamma}$) was calculated using the following empirical correlation describing forced convective mass transfer (Geankoplis, 2003):

$$Sh = 2 + 0.95 Re^{1/2} Sc^{1/3} \tag{13}$$

Where:

$$Re = \frac{nD^2\rho_\gamma}{\eta}, \quad Sh = \frac{k_{c\gamma}L}{D_{s\gamma}}, \quad Sc = \frac{\eta}{\rho_\gamma D_{s\gamma}} \tag{14}$$

The external diffusion coefficient ($D_{s\gamma}$) used to solve the above dimensionless system was calculated using the Wilke-Chang correlation (Wilke & Chang, 1955):

$$D_{s\gamma} = \frac{1.173 \times 10^{-16}(\varphi M_\gamma)^{1/2}T}{\eta V_A^{0.6}} \tag{15}$$

The molar volume of the solute (V_A) was estimated based on the chemical structure of malvidin-3-glucoside (the predominant monomeric anthocyanin in red wine-grape varieties) using an additive method described by Geankoplis (2003). The average molecular mass and association factor for the liquid phase in each set of experimental conditions were estimated based on the mole fractions of water, sugar (glucose) and ethanol, where:

$$M_\gamma = x_{EtOH}M_{EtOH} + x_{water}M_{water} + x_g M_g \tag{16}$$

$$\varphi = x_{EtOH}\varphi_{EtOH} + x_{water}\varphi_{water} + x_g\varphi_g \tag{17}$$

Using MATLAB software (version R2013a), the internal mass transfer coefficient of the solute ($k_{c\beta}$) was obtained through a non-linear regression of Eqs. (7) and (8), whereby the residuals of the model solution were set to be minimised. Table 1 presents a summary of the system variables and physical parameters as well as their method of determination.

2.4. Statistical analysis

The efficacy of the proposed model's fit respective to the experimental data for each set of experimental conditions was analysed by way of the coefficient of determination (R^2) and the root mean square error (*RMSE*). The influence of changing experimental conditions was assessed for the internal and external diffusion coefficient and the distribution constant by the analysis of variance (ANOVA). The significance of each parameter was determined by the corresponding p values, where significance was determined at $p < 0.05$.

2.5. Response surface analysis

In addition to the extractions conducted within the 2^3 factorial design, additional conditions representing the liquid phase mid-fermentation as well as at additional temperature conditions (nominally set at 10 °C) were also studied. This allowed for the development of surface response (R) models for important mass transfer parameters with increased sensitivity at values within the design of the experiment that were not directly measured, and allowed for curvature within the models. Response surfaces were generated for the internal mass transfer coefficient and distribution constant whereby values at each set of conditions were used to minimise the sum of squared residuals of the following function:

$$R = a_0 + a_1T + a_2C_S + a_3C_{EtOH} + a_4TC_S + a_5TC_{EtOH} + a_6C_SC_{EtOH} + a_7TC_SC_{EtOH} \tag{18}$$

Here, a_0 is the value of the function at the centre point conditions, a_1, a_2, a_3 represent the effects of individual parameters associated to their respective variable, and a_4, a_5, a_6 and a_7 represent the crossed effects between variables. For each of the response models, only those terms deemed significant by the ANOVA were used.

2.6. Extraction simulations

A wine fermentation model first proposed by Cramer, Vlassides, and Block (2002) and modified by Coleman et al. (2007), which treats nitrogen concentration as the limiting factor for yeast biomass growth and consists of a system of five ODEs, was used as a basis for simulating anthocyanin extraction during active fermentation scenarios:

$$\frac{dX}{dt} = \mu X_A \tag{19}$$

$$\frac{dX_A}{dt} = \mu X_A - k_d X_A \tag{20}$$

$$\frac{dN}{dt} = -\frac{\mu X_A}{Y_{X/N}} \tag{21}$$

$$\frac{dE}{dt} = BX_A \tag{22}$$

$$\frac{dS}{dt} = -\frac{BX_A}{Y_{E/S}} \tag{23}$$

where X is the total biomass concentration, X_A is the active biomass concentration, N is the nitrogen concentration, E is the ethanol concentration, and S is the sugar concentration. The specific biomass growth rate (μ), cell inactivation rate (k_d) and sugar utilisation per cell (B) are given as follows, and are functions of the nitrogen, ethanol and sugar concentrations, respectively:

$$\mu = \frac{\mu_{max}N}{K_N + N} \tag{24}$$

$$k_d = k_d'E \tag{25}$$

$$B = \frac{B_{max}S}{K_S + S} \tag{26}$$

Here, μ_{max} is the maximum yeast biomass growth rate, K_N is the Monod constant, k_d' describes the ethanol sensitivity of yeast, B_{max} is the maximum sugar utilisation rate, and K_S is the Michaelis-Menten-type constant for sugar consumption. The values for each of the model parameters can be well predicted as functions of the fermentation temperature (Coleman et al., 2007), where:

$$log(\mu_{max}) = -3.92 + 7.82 \times 10^{-2}T \tag{27}$$

$$log(K_N) = -4.73 \tag{28}$$

$$log(k_d') = -9.81 - 1.08 \times 10^{-3}T + 4.78 \times 10^{-3}T^2 \tag{29}$$

$$log(Y_{X/N}) = 3.50 - 3.61T \tag{30}$$

$$log(Y_{E/S}) = -5.98 \times 10^{-1} \tag{31}$$

$$log(B_{max}) = -2.30 + 7.71 \times 10^{-2}T \tag{32}$$

$$log(K_S) = 2.33 \tag{33}$$

By adjusting the temperature (T), initial yeast biomass concentration (B_0) and nitrogen concentration (N_0), the extent of the

Table 1
Summary of shape variables and system properties used for process modelling and their source.

System property or shape variable	Value	Source
Specific surface area (a)	4831 $m^2\,m^{-3}$	Mathematically derived
Liquid volume fraction (ε)	0.9173	Experimentally-determined
Initial anthocyanin concentration ($c_{\beta 0}$)	1812 $mg\,L^{-1}$	Experimentally-determined
Internal diffusion path length (L)	2.07×10^{-4} m	Jin, Wu, Liu, and Liao (2017)
Impeller diameter (D)	0.06 m	Experimentally-determined
Solute molar volume (V_A)	0.5259 $L\,mol^{-1}$	Geankoplis (2003)
Dynamic viscosity (η)	Varied	Experimentally-determined
Liquid density (ρ_γ)	Varied	HYSYS (Hysys, Operations Guide, 2005)
Liquid molecular mass (M_γ)	Varied	Eq. (12)
Liquid association factor φ	Varied	Eq. (17)

fermentation lag phase, ethanol production rate and total time until the end of fermentation can be controlled. MATLAB software (version R2013a) was used to incorporate this system of ODEs with the surface response models for internal mass transfer ($k_{c\beta}$) and distribution constant (K) generated in this work to simulate the extractive behavior of anthocyanins in fermentation scenarios, where temperature and starting nutrient concentrations impact the extractive behavior. Simulations were also conducted by adjusting the system Biot number to explore the effect of mixing operations on the rate of extraction and how this can be used to optimise the process by shortening the required solid-liquid contact time.

3. Results and discussion

3.1. Convective extraction model solution

Anthocyanins are important contributors to red wine quality and as such understanding the impact of process variables on the extraction rates and extractability is a crucial step towards modelling for the purpose of improving process efficiency. The mass transfer properties of anthocyanins from fresh Pinot noir grape solids (skins and seeds) were explored under forced convection with temperature conditions that simulated various stages of the red winemaking process. Pinot noir was selected for this study due to its high value in terms of $/tonne (Wine Australia, 2018) and the relative importance of colour to the quality of the finished wine. Solutions were continuously agitated throughout the extraction period to calculate external mass transfer parameters in the liquid phase and solve for the rate of internal mass transfer within the grape solids under different solute and temperature conditions. As in Setford et al. (2018), this work is focused solely on the extractive behavior of anthocyanins and as such experimental data up to and including the maximum liquid phase anthocyanin concentrations are presented and used for the purposes of mathematical modelling. Fig. 1 presents solid phase depletion (Fig. 1a, 1c) solved by mass balance of monomeric anthocyanins for each set of liquid phases (water, sugar, ethanol) and liquid phase accumulation (Fig. 1b, 1d) at low (4.9 °C, upper) and high (20.6 °C, lower) temperatures, as well as the mathematical model solutions solved by linear regression of Eqs. (7) and (8) as described in Materials and Methods. In agreement with Setford et al. (2018), ethanol and temperature positively influenced both the extraction rate and the maximum anthocyanin concentrations from the solids. Furthermore, the inclusion of sugar in the liquid phase in the present study appears to have lowered the anthocyanin extraction rate irrespective of temperature (Fig. 1). A summary of all relevant mass transfer parameters (internal and external mass transfer and diffusion coefficients and distribution constants) for each set of conditions is presented in Table 2.

3.2. Statistical analysis

For each set of experimental conditions, R^2 and *RMSE* were calculated to confirm the proposed models' validity, with R^2 values > 0.94 and small *RMSE* values observed in all cases. A centre point replicated four times was included in the experimental design at the nominal temperature of 10 °C (actual 12.2 °C) allowing for an estimate of standard error (which ranges from 0.45 to 3.29) and repeatability (coefficient of variation, which ranges from 0.12 to 0.19). Fig. 2 presents the experimental results at the centre point, along with additional points for sugar and ethanol solutions at the mid-point temperature condition. At the mid-point condition in Fig. 2, it can be clearly observed that the regression is consistent with the standard error range, verifying that the model presented in Sections 2.2–2.3 can be used to successfully describe solid-liquid mass transfer of anthocyanins from fresh Pinot noir grape solids.

The significance of experimental variables (ethanol concentration, sugar concentration, and temperature) on experimentally-determined

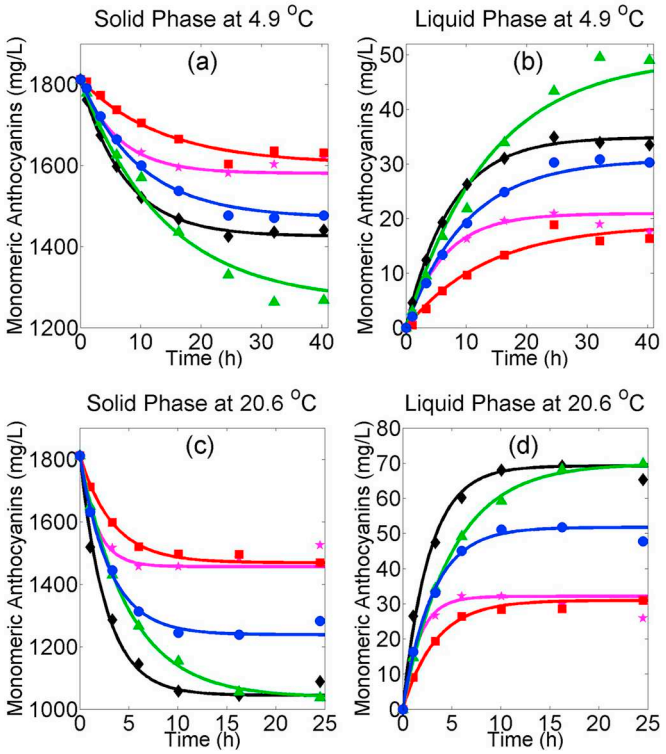

Fig. 1. Experimental and fitted models for monomeric anthocyanin solid phase depletion (a, c) and liquid phase accumulation (b, d) at the low temperature, 4.9 °C, (a, b), and high temperature, 20.6 °C, (c, d) conditions studied. ★, water; ■, 266 g L^{-1} sugar; ●, 133 g L^{-1} sugar, 7% ethanol; ◆, 14% *v/v* ethanol; ▲, 266 g L^{-1} sugar and 14% *v/v* ethanol.

mass transfer parameters ($k_{c\beta}$ and K) was tested using a full factorial analysis of variance (ANOVA). The factor effects and associated statistical significance for each experimental parameter (and their interactions) are presented in Table 3. Complete ANOVA tables for $k_{c\beta}$ and K can be found in Tables S1 and S2 respectively. From the factorial analysis, all individual experimental variables as well as the combined interaction of temperature with ethanol and temperature with sugar had a significant impact on rate of internal mass transfer. The positive effect of ethanol and temperature on the extraction rate and extractability of phenolic compounds from biological solids has previously been well established (Cacace & Mazza, 2003; Canals, Llaudy, Valls, Canals, & Zamora, 2005; González-Manzano, Rivas-Gonzalo, & Santos-Buelga, 2004; Mantell, Rodríguez, & Martínez de la Ossa, 2002) due to their influence on the liquid phase dielectric constant and the permeability of cell membranes (Cacace & Mazza, 2003; Koyama, Goto-Yamamoto, & Hashizume, 2007), however the negative impact of sugar on the rate of extraction of anthocyanins is to the authors' knowledge unreported. A possible explanation relates to the effect of sugar on certain physical properties such as density and dynamic viscosity, which will hinder free diffusion in the liquid phase and would therefore be expected to inhibit penetration and diffusion through porous solids. Although affecting the internal mass transfer rate, sugar appeared to have no significant impact on the maximum extractability of anthocyanins (represented by K), implying that sugar at the concentrations studied did not inhibit the maximum solubility of anthocyanins in the liquid phase.

3.3. Response surface analysis

Surface response expressions for $k_{c\beta}$ and K were generated based on the factors and factor interactions deemed statistically significant from the analysis of variance. To improve the accuracy of the surface

Table 2
Summary of internal ($D_{s\beta}$, $k_{c\beta}$) and external ($D_{s\gamma}$, $k_{c\gamma}$) diffusion and mass transfer coefficients, distribution constants (K) and statistical parameters ($RMSE$ and R^2) for anthocyanins at the specified extraction conditions.

Trial conditions			Mass transfer parameters					Statistical parameters	
Temp. (°C)	Sugar (g L^{-1})	Ethanol (% *v/v*)	$D_{s\gamma}$ (m^2 s^{-1})	$k_{c\gamma}$ (m s^{-1})	$D_{s\beta}$ (m^2 s^{-1})	$k_{c\beta}$ (m s^{-1})	K	$RMSE$	R^2
4.9	0	0	4.69×10^{-12}	1.59×10^{-4}	9.72×10^{-14}	9.58×10^{-11}	1.32×10^{-2}	1.314	0.966
4.9	266	0	2.15×10^{-12}	8.23×10^{-5}	4.16×10^{-14}	4.11×10^{-11}	1.18×10^{-2}	1.282	0.963
4.9	0	14	2.77×10^{-12}	1.01×10^{-4}	1.40×10^{-13}	1.38×10^{-10}	2.45×10^{-2}	0.630	0.998
4.9	266	14	1.17×10^{-12}	4.92×10^{-5}	1.07×10^{-13}	1.05×10^{-10}	3.92×10^{-2}	2.372	0.983
4.9	133	7	2.65×10^{-12}	9.12×10^{-5}	9.12×10^{-14}	8.99×10^{-11}	2.10×10^{-2}	0.947	0.993
12.2	266	0	2.87×10^{-12}	1.04×10^{-4}	8.36×10^{-14}	8.24×10^{-11}	1.13×10^{-2}	0.603	0.992
12.2	0	14	3.74×10^{-12}	1.30×10^{-4}	3.29×10^{-13}	3.25×10^{-10}	4.03×10^{-2}	0.996	0.997
12.2	133	7	3.58×10^{-12}	1.24×10^{-4}	1.96×10^{-13}	1.93×10^{-10}	2.73×10^{-2}	0.318	0.999
20.6	0	0	8.22×10^{-12}	2.51×10^{-4}	5.58×10^{-13}	5.50×10^{-10}	2.20×10^{-2}	2.573	0.943
20.6	266	0	4.23×10^{-12}	1.43×10^{-4}	2.72×10^{-13}	2.69×10^{-10}	2.11×10^{-2}	0.959	0.992
20.6	0	14	5.67×10^{-12}	1.82×10^{-4}	7.60×10^{-13}	7.49×10^{-10}	6.63×10^{-2}	2.191	0.992
20.6	266	14	2.75×10^{-12}	9.87×10^{-5}	4.18×10^{-13}	4.12×10^{-10}	6.73×10^{-2}	0.800	0.999
20.6	133	7	5.90×10^{-12}	1.75×10^{-4}	5.03×10^{-13}	4.96×10^{-10}	4.18×10^{-2}	1.702	0.991

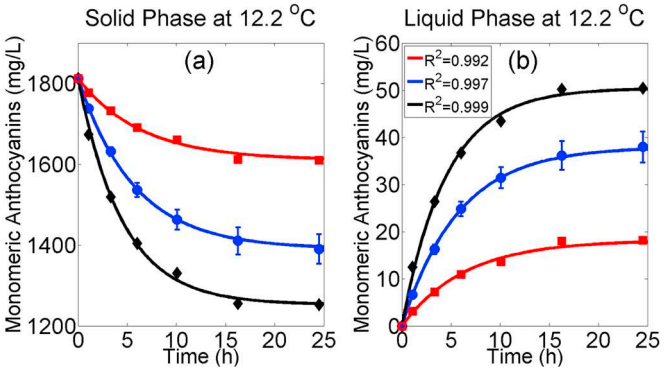

Fig. 2. Experimental and fitted models for monomeric anthocyanin solid phase depletion (a) and liquid phase accumulation (b) at the mid-point temperature conditions studied. ■, 266 g L^{-1} sugar; ●, 133 g L^{-1} sugar, 7% *v/v* ethanol; ◆, 14% *v/v* ethanol.

response equations, all values for $k_{c\beta}$ and K (Table 2) were used to fit response equations even though the ANOVA required the use of only 8 of the experimental trials conducted:

$$k_{c\beta} = -7.61 \times 10^{-11} + 3.03 \times 10^{-11}T + 1.49 \times 10^{-13}C_S + 3.23 \times 10^{-13}C_{EtOH} - 6.28 \times 10^{-14}TC_S + 5.60 \times 10^{-13}TC_{EtOH} \quad (34)$$

$$K = 8.27 \times 10^{-3} + 5.72 \times 10^{-4}T + 7.69 \times 10^{-4}C_{EtOH} + 1.18 \times 10^{-3}TC_{EtOH} \quad (35)$$

where T, C_S and C_{EtOH} are the temperature (°C), concentration of sugar (g L^{-1}) and concentration of ethanol (% *v/v*) respectively. Fig. 3 presents a graphical representation of Eqs. (34) and (35), showing how the rate of extraction and maximum extractability of anthocyanins can change at different stages of fermentation and during different wine-making operations (such as cold soaking, which is a typically employed strategy aimed at enhancing colour extraction). Fig. 3 clearly shows that the extraction kinetics of anthocyanins would not be expected to

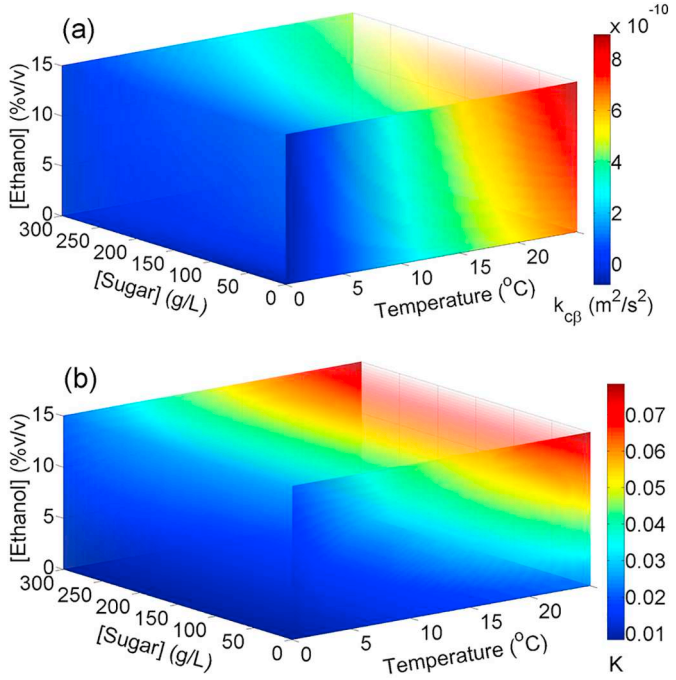

Fig. 3. Response surfaces of monomeric anthocyanins at changing liquid phase and temperature conditions for (a) the internal mass transfer coefficient, $k_{c\beta}$ and (b) distribution constant, K.

Table 3
Factor effects and statistical significance of experimentally-determined model parameters for internal mass transfer coefficient ($k_{c\beta}$), and distribution constant (K).

	$k_{c\beta}$		K	
Coefficient	Factor effect	p value	Factor effect	p value
Temperature (A)	4.00×10^{-10}	6.76×10^{-8} ***	2.14×10^{-2}	2.89×10^{-5} ***
Sugar concentration (B)	-1.76×10^{-10}	3.50×10^{-5} ***	3.46×10^{-3}	2.07×10^{-1}
Ethanol concentration (C)	1.12×10^{-10}	7.76×10^{-4} **	3.29×10^{-2}	1.13×10^{-6} ***
AB	-1.32×10^{-10}	2.61×10^{-4} **	-3.57×10^{-3}	1.95×10^{-1}
AC	5.99×10^{-11}	2.30×10^{-2} *	1.24×10^{-2}	1.19×10^{-3} **
BC	-8.15×10^{-12}	7.13×10^{-1}	4.64×10^{-3}	1.03×10^{-1}
ABC	-1.98×10^{-11}	3.81×10^{-1}	-3.70×10^{-3}	1.81×10^{-1}

*, ** and *** represent factors that are statistically significant at the 5%, 1% and 0.1% levels, respectively.

remain as a static value throughout fermentation, as both the internal rate of mass transfer and distribution constant are several times lower at liquid phase conditions consistent with unfermented juice (266 g L^{-1} sugar) than at conditions more closely resembling a fermented wine (14% *v/v* ethanol).

3.4. Extraction under simulated fermentation conditions

An ultimate goal of extraction modelling is the ability to predict winemaking outcomes based on grape phenolic composition together with other key inputs that affect the resulting wine. Working towards this, simulations using the surface response models developed in Section 3.3 were incorporated with a previously developed model of wine fermentation kinetics (Section 2.6.) to study the evolution of the liquid phase during an active red wine fermentation. The initial conditions used to solve the fermentation model's system of ODEs (Eqs. (19) to (23)) were chosen to show the effect of changing process variables that can be controlled by a winemaker (temperature, nitrogen concentration and rate of liquid phase convection) on the extraction rate and final concentration of anthocyanins. Eqs. (34) and (35) respectively were used to determine the internal mass transfer coefficient ($k_{c\beta}$) and distribution constant (K) at changing liquid phase conditions together with Eq. (6) for the internal diffusion coefficient ($D_{s\beta}$) and Eq. (36) for the external mass transfer coefficient ($k_{c\gamma}$). These were then used to solve Eqs. (7) and (8) at continuously changing concentrations of ethanol and sugar, generating the respective anthocyanin extraction curves. Because the distribution constant (K) is a constant variable, the solid/liquid was adjusted to the original ratio based on the collected volume of juice at grape pressing (as described in Section 2.1.) to provide a more accurate representation of actual red wine fermentation conditions. Table 4 provides a summary of the initial conditions used for the simulations represented in Figs. 4, 5 and 6. For each of Figs. 4, 5 and 6, a single variable – initial nitrogen concentration, fermentation temperature and the systems Biot number respectively were adjusted keeping the other two variables constant. The Biot number is a dimensionless value that can be used to characterise the extent of control that internal and external resistances have in a solid-liquid extraction and gives an indication of the rate controlling step for mass transfer:

$$Bi = \frac{k_{c\gamma} LK}{D_{s\beta}} \tag{36}$$

Typically, a Biot number > 10 implies that the rate controlling step for mass transfer is diffusion within the solid phase ($D_{s\beta}$) (Pérez-Galindo, López-Miranda, & Martín-Dominguez, 2000). For the simulations in Figs. 4 and 5, Biot numbers of 1000 were chosen to limit the extent of control of external resistance on the overall extraction rate and show directly how nutrient (nitrogen) and temperature will impact the rate of internal mass transfer in a well-mixed system.

Fig. 4 presents a series of simulations showing both the kinetics of fermentation (Fig. 4a) as well as the respective simulated extractive behaviour of anthocyanins (Fig. 4b) at changing concentrations of nitrogen, being the limiting nutrient for biomass growth in the fermentation model described in Section 2.6. The model developed in sections 2.2–2.3 and employed here specifically describe only the extraction phase of anthocyanin development during red wine fermentation and as such do not include losses due to liquid phase reactions or binding with yeast lees. As would be expected from the surface response analysis (Fig. 2), the maximum extractability is not reached until the end of fermentation where the ethanol concentration is maximised (Fig. 4). This results in significant differences in the time required to reach the maximum anthocyanin concentration (more than double) when comparing a starting nitrogen concentration of 0.6 g L^{-1} to a starting concentration of 1.2 g L^{-1}. This indicates that the extent of fermentation is a limiting step for anthocyanin extractability and implies that pre-fermentative maceration techniques may be of little value for improving red wine colour. Similarly, an inflection point in the anthocyanin concentration can be observed between approximately 0 and 30 h (Fig. 4b). This appears to coincide with the lag phase of ethanol production (Fig. 4a), indicating that although anthocyanins are readily extracted in sugary solutions, ethanol is required for the system to reach the maximum possible concentration. This can be explained by the combined effect of a decreased rate of internal mass transfer as well as a lower maximum extractability of anthocyanins at low ethanol conditions (as observed in Fig. 2).

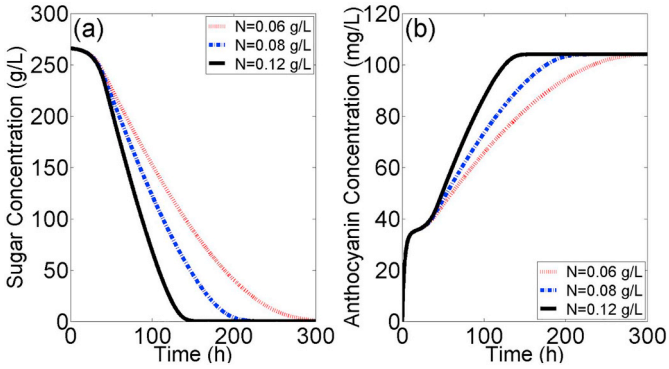

Fig. 4. (a) Simulated kinetics of red wine fermentation with a fixed temperature of 20 °C and varying nitrogen concentration and (b) the resulting simulated extraction of anthocyanins.

Fig. 5 presents a series of simulations showing both the kinetics of fermentation (Fig. 5a) as well as the respective simulated extractive behaviour of anthocyanins (Fig. 5b) at varying temperature conditions, which winemakers could readily control. In this instance, the response

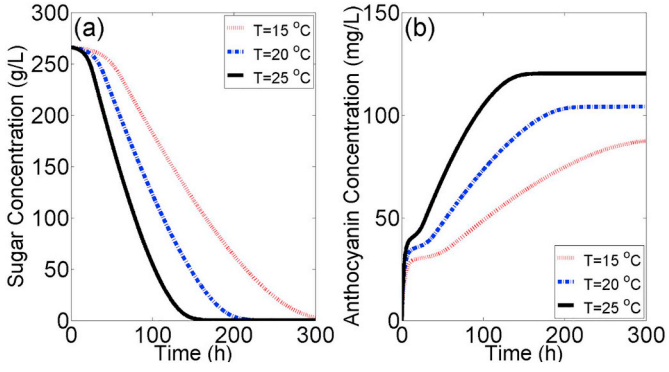

Fig. 5. (a) Simulated kinetics of red wine fermentation with a fixed nitrogen concentration of 0.08 g L^{-1} and varying temperatures and (b) the resulting simulated extraction of anthocyanins.

Table 4
Summary of initial liquid phase composition and temperature conditions used for fermentation simulations presented in Figs. 4, 5 and 6.

	Active Biomass (g L^{-1})	Ethanol (g L^{-1})	Sugar (g L^{-1})	Nitrogen (g L^{-1})	Temperature (°C)	Biot Number
Fig. 4	0.1	0	266	0.08	15	1000
	0.1	0	266	0.08	20	1000
	0.1	0	266	0.08	25	1000
Fig. 5	0.1	0	266	0.06	20	1000
	0.1	0	266	0.08	20	1000
	0.1	0	266	0.12	20	1000
Fig. 6	0.1	0	266	0.08	20	0.01
	0.1	0	266	0.08	20	0.1
	0.1	0	266	0.08	20	1

surface models for the internal and mass transfer coefficients and distribution constant are extrapolated from experimental data to 25 °C. As would be expected from the results presented in Figs. 1 and 2, temperature has a marked effect on both the maximum extractability and extraction rate of anthocyanins, and as such could be exploited by winemakers seeking to improve the total concentration (and thus colour of the wine). As well as directly affecting the extractability of anthocyanins, temperature plays an important role in fermentation kinetics and thus the rate of ethanol production. Because of this, fermentation temperature can be seen to have an additional indirect influence on the extraction rate through its impact on ethanol concentration at a particular time point, which in turn will also affect the rate of anthocyanin extraction. As seen in Fig. 4, Fig. 5 shows a similar pattern around the fermentation lag phase, with the extraction rate and maximum extractability limited by the extent of fermentation and lack of ethanol in the liquid phase.

As with the experimental extractions discussed in section 3.1, Figs. 4 and 5 present extraction simulations under forced convective conditions, whereby internal diffusion is the rate limiting step for anthocyanin extraction. In doing this, the direct impact of fermentation variables (nitrogen concentration and temperature) on the internal mass transfer rate and extractability can be clearly observed. In a typical red wine fermentation, liquid movement is usually the result of evolving CO_2 displacing the liquid phase or through mixing operations typically conducted for a relatively short period several times a day. To study how anthocyanin extraction patterns may change under these lower convective conditions, simulations were conducted at varying rates of external mass transfer, controlled by adjusting the Biot number of the system (Fig. 6).

In Fig. 6 it can be observed that changing the rate of external mass transfer (achieved by adjusting the Biot number of the system) does not impact the fermentation kinetics in the same way that adjusting nutrient (nitrogen) or fermentation temperature would be expected to. Fig. 6b clearly shows the effect that external resistance can have on the shape of anthocyanin extraction curves, and in particular its ability to limit the overall extraction rate, thus increasing the time required for the maximum liquid-phase anthocyanin concentration. This effect negates the inflection point observed when the Biot number is equal to or greater than one and shows that the initial anthocyanin extraction phase can be drastically hindered by low rates of liquid phase convection. This effect is expected, as diffusion within the solid phase is limited by the concentration at the solid-liquid boundary layer, which is directly impacted by rate of external mass transfer. The reliance on both internal and external mass transfer at low convective conditions (as would be expected for the majority of a red wine fermentations) presented in Fig. 6 highlights the importance of the two mass transfer parameters to the overall extraction rate, demonstrating that both should be considered when seeking to model phenolic extraction during red wine fermentation. Additional knowledge on external mass transfer rates under free or low convective conditions (no mixing) would be a valuable addition to the literature, allowing for simulations with different mixing regimes to be conducted and for process optimisation in terms of the associated costs and energy.

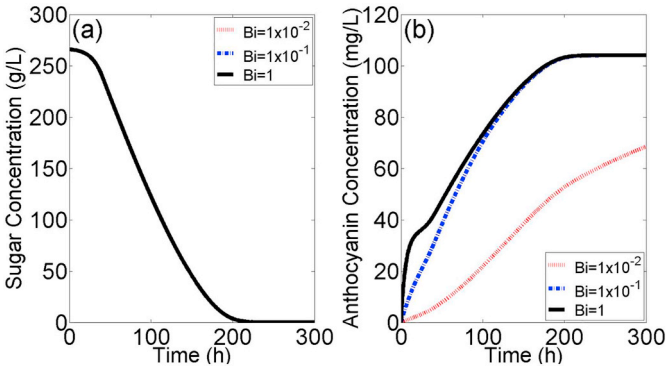

Fig. 6. (a) Simulated kinetics of red wine fermentation with fixed nutrient concentrations and temperature, but with varying external mass transfer coefficients controlled by adjusting the Biot number and (b) the resulting simulated extraction of anthocyanins.

In the past, the extractive phase of anthocyanins during red wine fermentation (Boulton et al., 1996; Zanoni et al., 2010) as well as other phenolic compounds extracted in different biological systems (Amendola, De Faveri, & Spigno, 2010; Bucić-Kojić, Planinić, Tomas, Bilić, & Velić, 2007; Cacace & Mazza, 2003; Simeonov, Tsibranska, & Minchev, 1999) have typically been described by simple first order rate models, followed by a first or zero order degradation step accounting for reactions that take place in the liquid phase. The simulated extraction patterns presented in this study (Figs. 4, 5 and 6) differ in that that they show a fast initial release within the first few hours of fermentation followed by a slower extraction throughout the remainder of the fermentation lag phase, and finally following a more typical first order extraction model. The aforementioned observations help to rationalise results from previous studies. For instance, in the data for anthocyanin extraction presented by Zanoni et al. (2010) (Figs. 2, 3 and 4 of that publication), the experimental anthocyanin concentrations in the liquid phase at approximately 25 h of fermentation were below the curve described by a first order kinetic rate model in all cases and irrespective of the fermentation size (laboratory or commercial scale). Although the fermentation kinetics were not a focus in the work of Zanoni et al. (2010) and were therefore not presented, a typical red wine fermentation will have a lag phase lasting up to 48 h, where yeast consume nutrients (especially assimilable nitrogen) prior to utilising sugar and producing ethanol in large quantities. As such, it is plausible that the experimental data described in Figs. 2, 3 and 4 of Zanoni et al. (2010) could be explained by a lack of ethanol in the liquid phase, which may be inhibiting both the rate of internal mass transfer and maximum extractability of anthocyanins. Such a possibility is supported by the simulations depicted in Figs. 4 and 5 of the present study.

Notably, a similar extraction pattern can be observed in the results from González-Neves, Gil, and Barreiro (2008) for different grape varietals. The rate of individual anthocyanin extraction for Cabernet Sauvignon, Tannat and Merlot (Figs. 1, 2 and 3 of that study) was slower within the first one to two days of fermentation before showing a much greater extraction rate prior to reaching maximum anthocyanin concentrations in the liquid phase at approximately four days into the fermentation (González-Neves et al., 2008). As with the case of Zanoni et al. (2010), the fermentation kinetics were not presented by González-Neves et al. (2008) but fermentations were carried out at 27–30 °C, which would likely result in the maximum ethanol concentrations being reached relatively quickly (i.e., within one week), such that they may coincide with the maximum concentration of anthocyanins.

Based on these observations, future studies could apply the model for anthocyanin extraction presented in this paper to controlled fermentations where both the rate of fermentation (sugar/ethanol concentrations) and liquid phase anthocyanin concentrations are known, to see if similar extraction patterns exist to those observed in Figs. 4, 5 and 6. However, the experimental extractions (and subsequent predictive simulations) were conducted under forced convective conditions, whereby the liquid phase was well mixed and internal mass transfer was the rate-limiting step of the process. An important step for future simulations would therefore be to model the external mass transfer of anthocyanins (and other phenolic compounds) under free convective and low convective conditions. This would allow for predictions on the effectiveness of mixing regimes for the purposes of maximising the phenolic extraction rate and extraction potential while minimising production costs, or controlling extraction to a targeted value for consistency of phenolic composition from vintage-to-vintage.

4. Conclusion

Anthocyanin extraction from fresh Pinot noir grape solids under conditions simulating various stages of the maceration and fermentation stages of the winemaking process were described using a mechanistic model that separates the effect of mass transfer in both solid and liquid phases. Surface response models for predicting the distribution and internal mass transfer coefficients were produced to allow for the generation of anthocyanin extraction curves under simulated wine fermentation conditions, whereby the liquid phase has continuously changing concentrations of ethanol and sugar. These models were extended to include nutrient (nitrogen) and changing Biot number in order to show the effect of manipulating process variables available to a winemaker on the rate and extent of anthocyanin extraction during active fermentation scenarios. Surface response analysis showed that ethanol and higher temperatures are required to improve the maximum concentration of extracted anthocyanins into the liquid phase. In terms of maximising the extraction of anthocyanins during a real red wine fermentation scenario, the results indicated that cold-soaking operations prior to fermentation (a practice designed to assist with colour extraction) are likely to have little impact on the highest achievable concentration of anthocyanins in the liquid phase. Additionally, mixing operations undertaken during the early stages of fermentation may have little impact on the final concentration of anthocyanins provided that the system is well-mixed during the final stages of fermentation when ethanol is at its highest concentration.

Supplementary data to this article can be found online at https://doi.org/10.1016/j.foodres.2018.12.044.

Funding

P.S. is supported through a The University of Adelaide - School of Agriculture, Food and Wine, AUSTRALIA, Scholarship [1606990] and was also a recipient of a Wine Australia, AUSTRALIA, supplementary scholarship AGW [Ph1505]. The authors acknowledge the financial support from the School of Agriculture, Food and Wine, UA, and Australian grapegrowers and winemakers through their investment body, Wine Australia, with matching funds from the Australian Government.

Conflicts of interest

The authors declare no conflict of interest.

References

Amendola, D., De Faveri, D. M., & Spigno, G. (2010). Grape marc phenolics: Extraction kinetics, quality and stability of extracts. *Journal of Food Engineering, 97*, 384–392. https://doi.org/10.1016/j.jfoodeng.2009.10.033.

Anderson, K., Nelgen, S., & Pinilla, V. (2018). *Global wine markets, 1860 to 2016: a statistical compendium.* University of Adelaide Press.

Boulton, R., Singleton, V., Bisson, L., & Kunkee, R. (1996). *Principles and Practices of Winemaking.* New York: Chapman and Hall.

Bucić-Kojić, A., Planinić, M., Tomas, S., Bilić, M., & Velić, D. (2007). Study of solid–liquid extraction kinetics of total polyphenols from grape seeds. *Journal of Food Engineering, 81*, 236–242. https://doi.org/10.1016/j.jfoodeng.2006.10.027.

Busse-Valverde, N., Gómez-Plaza, E., López-Roca, J. M., Gil-Muñoz, R., Fernández-Fernández, J. I., & Bautista-Ortín, A. B. (2010). Effect of different enological practices on skin and seed proanthocyanidins in three varietal wines. *Journal of agricultural and food chemistry, 58*(11), 333–11,339.

Cacace, J. E., & Mazza, G. (2003). Mass transfer process during extraction of phenolic compounds from milled berries. *Journal of Food Engineering, 59*, 379–389. https://doi.org/10.1016/S0260-8774(02)00497-1.

Canals, R., Llaudy, M., Valls, J., Canals, J., & Zamora, F. (2005). Influence of ethanol concentration on the extraction of colour and phenolic compounds from the skin and seeds of Tempranillo grapes at different stages of ripening. *Journal of Agricultural and Food Chemistry, 53*, 4019–4025. https://doi.org/10.1021/jf047872v.

Cerpa-Calderón, F. K., & Kennedy, J. A. (2008). Berry integrity and extraction of skin and seed proanthocyanidins during red wine fermentation. *Journal of Agricultural and Food Chemistry, 56*, 9006–9014. https://doi.org/10.1021/jf801384v.

Coleman, M. C., Fish, R., & Block, D. E. (2007). Temperature-dependent kinetic model for nitrogen-limited wine fermentations. *Applied and Environmental Microbiology, 73*, 5875–5884. https://doi.org/10.1128/AEM.00670-07.

Cozzolino, D., Kwiatkowski, M., Parker, M., Cynkar, W., Dambergs, R., Gishen, M., & Herderich, M. (2004). Prediction of phenolic compounds in red wine fermentations by visible and near infrared spectroscopy. *Analytica Chimica Acta, 513*, 73–80. https://doi.org/10.1016/j.aca.2003.08.066.

Cramer, A. C., Vlassides, S., & Block, D. E. (2002). Kinetic model for nitrogen-limited wine fermentations. *Biotechnology and Bioengineering, 77*, 49–60. https://doi.org/10.1002/bit.10133.

Espinoza-Pérez, J., Vargas, A., Robles-Olvera, V., Rodríguez-Jimenes, G., & García-Alvarado, M. (2007). Mathematical modelling of caffeine kinetic during solid–liquid extraction of coffee beans. *Journal of Food Engineering, 81*, 72–78. https://doi.org/10.1016/j.jfoodeng.2006.10.011.

Geankoplis, C. J. (2003). *Transport processes and separation process principles* (4th ed.). New Jersey: Prentice Hall Professional Technical Reference.

Gertenbach, D. (2001). Solid–liquid extraction technologies for manufacturing nutraceuticals from botanicals. In J. Shi, G. Mazza, & M. Le Maguer (Vol. Eds.), *Functional Foods Biochemical and Processing Aspects. Vol. 2. Functional Foods Biochemical and Processing Aspects* (pp. 331–366). Boca Raton: Taylor and Francis Group.

González-Manzano, S., Rivas-Gonzalo, J. C., & Santos-Buelga, C. (2004). Extraction of flavan-3-ols from grape seed and skin into wine using simulated maceration. *Analytica Chimica Acta, 513*, 283–289. https://doi.org/10.1016/j.aca.2003.10.019.

González-Neves, G., Gil, G., & Barreiro, L. (2008). Influence of grape variety on the extraction of anthocyanins during the fermentation on skins. *European Food Research and Technology, 226*, 1349. https://doi.org/10.1007/s00217-007-0664-2.

Jin, X., Wu, X., Liu, X., & Liao, M. (2017). Varietal heterogeneity of textural characteristics and their relationship with phenolic ripeness of wine grapes. *Scientia Horticulturae, 216*, 205–214. https://doi.org/10.1016/j.scienta.2017.01.010.

Koyama, K., Goto-Yamamoto, N., & Hashizume, K. (2007). Influence of maceration temperature in red wine vinification on extraction of phenolics from berry skins and seeds of grape (Vitis vinifera). *Bioscience, Biotechnology, and Biochemistry, 71*, 958–965. https://doi.org/10.1271/bbb.60628.

Lerno, L., Reichwage, M., Panprivech, S., Ponangi, R., Hearne, L., Oberholster, A., & Block, D. E. (2017). Chemical gradients in pilot-scale cabernet sauvignon fermentations and their effect on phenolic extraction. *American Journal of Enology and Viticulture, 68*, 401–411. https://doi.org/10.5344/ajev.2017.16104.

Mantell, C., Rodríguez, M., & Martínez de la Ossa, E. (2002). Semi-batch extraction of anthocyanins from red grape pomace in packed beds: experimental results and process modelling. *Chemical Engineering Science, 57*, 3831–3838. https://doi.org/10.1016/S0009-2509(02)00320-2.

Mercurio, M. D., Dambergs, R. G., Herderich, M. J., & Smith, P. A. (2007). High throughput analysis of red wine and grape phenolics adaptation and validation of methyl cellulose precipitable tannin assay and modified somers colour assay to a rapid 96 well plate format. *Journal of Agricultural and Food Chemistry, 55*, 4651–4657. https://doi.org/10.1021/jf063674n.

Pérez-Galindo, J., López-Miranda, J., & Martín-Dominguez, I. (2000). Geometric and Reynolds number effects on oregano (*Lippia Berlandieri Schauer*) essential oil extraction. *Journal of Food Engineering, 44*, 127–133. https://doi.org/10.1016/S0260-8774(99)00154-5.

Rodríguez-Jimenes, G. C., Vargas-Garcia, A., Espinoza-Pérez, D. J., Salgado-Cervantes, M. A., Robles-Olvera, V. J., & García-Alvarado, M. A. (2013). Mass transfer during vanilla pods solid liquid extraction: Effect of extraction method. *Food and Bioprocess Technology, 6*, 2640–2650. https://doi.org/10.1007/s11947-012-0975-6.

Setford, P. C., Jeffery, D. W., Grbin, P. R., & Muhlack, R. A. (2017). Factors affecting extraction and evolution of phenolic compounds during red wine maceration and the role of process modelling. *Trends in Food Science & Technology, 69*(*Part A*), 106–117. https://doi.org/10.1016/j.tifs.2017.09.005.

Setford, P. C., Jeffery, D. W., Grbin, P. R., & Muhlack, R. A. (2018). Modelling the mass transfer process of malvidin-3-glucoside during simulated extraction from fresh grape solids under wine-like conditions. *Molecules, 23*, 2159. https://doi.org/10.3390/molecules23092159.

Simeonov, E., Tsibranska, I., & Minchev, A. (1999). Solid–liquid extraction from plants—experimental kinetics and modelling. *Chemical Engineering Journal, 73*, 255–259.

Sparrow, A. M., Holt, H. E., Pearson, W., Dambergs, R. G., & Close, D. C. (2016). Accentuated Cut Edges (ACE): Effects of skin fragmentation on the composition and sensory attributes of Pinot Noir wines. *American Journal of Enology and Viticulture, 67*, 169–178. https://doi.org/10.5344/ajev.2015.15094.

Sparrow, A. M., Smart, R. E., Dambergs, R. G., & Close, D. C. (2015). Skin particle size affects the phenolic attributes of Pinot Noir wine: Proof of concept. *American Journal of Enology and Viticulture, 67*, 29–37. https://doi.org/10.5344/ajev.2015.15055.

Wilke, C., & Chang, P. (1955). Correlation of diffusion coefficients in dilute solutions. *AIChE Journal, 1*, 264–270. https://doi.org/10.1002/aic.690010222.

Wine Australia (2018). National Vintage Report 2018. Retrieved from https://www.wineaustralia.com/getmedia/fce5bf18-468b-4e1b-a478-d6ca231d40f6/VintageReport2018_full.pdf.

Zanoni, B., Siliani, S., Canuti, V., Rosi, I., & Bertuccioli, M. (2010). A kinetic study on extraction and transformation phenomena of phenolic compounds during red wine fermentation. *International Journal of Food Science & Technology, 45*, 2080–2088. https://doi.org/10.1111/j.1365-2621.2010.02374.x.

Supporting Information for

Mathematical modelling of anthocyanin mass transfer to predict extraction in simulated red wine fermentation scenarios

Patrick C. Setford[1], David W. Jeffery[1], Paul R. Grbin[1] and Richard A. Muhlack[1,*]

[1]Department of Wine and Food Science, School of Agriculture, Food and Wine, The University of Adelaide (UA), PMB 1, Glen Osmond SA 5064, Australia

Table of Contents

Page

Table S1. Full ANOVA for anthocyanin internal mass transfer coefficient S-2

Table S2. Full ANOVA for anthocyanin distribution constant S-3

Table S1. Full ANOVA for anthocyanin internal mass transfer coefficient

						n (ie # of replicates)	2						
Trial Conditions			Diffusion/Mass transfer property										
A	B	C	run 1	run 2	sum								
T	Glucose	Ethanol	$k_{c\beta}$	$k_{c\beta}$	$k_{c\beta}$	A	B	C	AB	AC	BC	ABC	
Low	Low	Low	9.54E-11	9.69E-11	1.92E-10	-1	-1	-1	1	1	1	-1	
Low	High	Low	4.21E-11	3.91E-11	8.13E-11	-1	1	-1	-1	1	-1	1	
Low	Low	High	1.76E-10	9.69E-11	2.73E-10	-1	-1	1	1	-1	-1	1	
Low	High	High	1.29E-10	7.95E-11	2.09E-10	-1	1	1	-1	-1	1	-1	
High	Low	Low	6.14E-10	4.84E-10	1.10E-09	1	-1	-1	-1	-1	1	1	
High	High	Low	2.72E-10	2.66E-10	5.37E-10	1	1	-1	1	-1	-1	-1	
High	Low	High	7.74E-10	7.24E-10	1.50E-09	1	-1	1	-1	1	-1	-1	
High	High	High	4.27E-10	3.98E-10	8.25E-10	1	1	1	1	1	1	1	
					main effect	4.00E-10	-1.76E-10	1.12E-10	-1.32E-10	5.99E-11	-8.15E-12	-1.98E-11	
					sum of squares	6.42E-19	1.24E-19	5.02E-20	7.00E-20	1.43E-20	2.66E-22	1.57E-21	

		sum of squares	degrees of freedom	mean square	F0	p
T	A	6.42E-19	1	6.42E-19	3.52E+02	6.76E-08
Glucose	B	1.24E-19	1	1.24E-19	6.80E+01	3.50E-05
Ethanol	C	5.02E-20	1	5.02E-20	2.75E+01	7.76E-04
	AB	7.00E-20	1	7.00E-20	3.84E+01	2.61E-04
	AC	1.43E-20	1	1.43E-20	7.86E+00	2.30E-02
	BC	2.66E-22	1	2.66E-22	1.46E-01	7.13E-01
	ABC	1.57E-21	1	1.57E-21	8.60E-01	3.81E-01
	Error	1.46E-20	8	1.82E-21		
	Total	9.17E-19	15			

Table S2. Full ANOVA for anthocyanin distribution constant

						n (ie # of replicates)						
Trial Conditions			Diffusion/Mass transfer property			2						
A	B	C	run 1	run 2	sum							
T	Glucose	Ethanol	K	K	K	A	B	C	AB	AC	BC	ABC
Low	Low	Low	1.20E-02	1.45E-02	2.65E-02	-1	-1	-1	1	1	1	-1
Low	High	Low	1.44E-02	9.46E-03	2.39E-02	-1	1	-1	-1	1	-1	1
Low	Low	High	2.84E-02	2.25E-02	5.10E-02	-1	-1	1	1	-1	-1	1
Low	High	High	4.79E-02	3.38E-02	8.17E-02	-1	1	1	-1	-1	1	-1
High	Low	Low	2.37E-02	2.06E-02	4.42E-02	1	-1	-1	-1	-1	1	1
High	High	Low	2.11E-02	2.11E-02	4.21E-02	1	1	-1	1	-1	-1	-1
High	Low	High	7.21E-02	6.09E-02	1.33E-01	1	-1	1	-1	1	-1	-1
High	High	High	6.62E-02	6.85E-02	1.35E-01	1	1	1	1	1	1	1
					main effect	2.14E-02	3.46E-03	3.29E-02	-3.57E-03	1.24E-02	4.64E-03	-3.70E-03
					sum of squares	1.83E-03	4.80E-05	4.34E-03	5.09E-05	6.12E-04	8.61E-05	5.46E-05

		sum of squares	degrees of freedom	mean square	F0	p
T	A	1.83E-03	1	1.83E-03	7.17E+01	2.89E-05
Glucose	B	4.80E-05	1	4.80E-05	1.88E+00	2.07E-01
Ethanol	C	4.34E-03	1	4.34E-03	1.70E+02	1.13E-06
	AB	5.09E-05	1	5.09E-05	2.00E+00	1.95E-01
	AC	6.12E-04	1	6.12E-04	2.40E+01	1.19E-03
	BC	8.61E-05	1	8.61E-05	3.38E+00	1.03E-01
	ABC	5.46E-05	1	5.46E-05	2.14E+00	1.81E-01
	Error	2.04E-04	8	2.55E-05		
	Total	7.23E-03	15			

CHAPTER 5

A new method for predicting the extraction of anthocyanins during red wine fermentation

Patrick C. Setford[1], David W. Jeffery[1], Paul R. Grbin[1], Richard A. Muhlack[1,*]

[1] Department of Wine and Food Science, School of Agriculture, Food and Wine, The University of Adelaide (UA), PMB 1 Glen Osmond SA 5064, Australia

Submitted for publication to *Food and Bioprocess Technology*

Statement of Authorship

Title of Paper	A new method for predicting the extraction of anthocyanins during red wine fermentation
Publication Status	☐ Published ☐ Accepted for Publication ☑ Submitted for Publication ☐ Unpublished and Unsubmitted work written in manuscript style
Publication Details	Submitted to Food and Bioprocess technology

Principal Author

Name of Principal Author (Candidate)	Patrick C. Setford
Contribution to the Paper	Contributed to the research idea, performed laboratory analysis of samples (HPLC), assisted in the design of the mathematical model, performed fermentation simulations, performed statistical analyses, interpreted the data and prepared entire first draft of the manuscript.
Overall percentage (%)	70%
Certification:	This paper reports on original research I conducted during the period of my Higher Degree by Research candidature and is not subject to any obligations or contractual agreements with a third party that would constrain its inclusion in this thesis. I am the primary author of this paper.
Signature	Date 19/05/19

Co-Author Contributions

By signing the Statement of Authorship, each author certifies that:

i. the candidate's stated contribution to the publication is accurate (as detailed above);

ii. permission is granted for the candidate in include the publication in the thesis; and

iii. the sum of all co-author contributions is equal to 100% less the candidate's stated contribution.

Name of Co-Author	David W. Jeffery
Contribution to the Paper	Contributed to the research idea, assisted with laboratory analysis, assisted with interpretation of data, critically reviewed and edited the manuscript.
Signature	Date 20/5/19

Name of Co-Author	Paul R. Grbin
Contribution to the Paper	Contributed to the research idea and experimental design, assisted with interpretation of data, critically reviewed and edited the manuscript.
Signature	Date 20/05/2019

Name of Co-Author	Richard A. Muhlack		
Contribution to the Paper	Contributed to the conception of the article, assisted with mathematical modelling and supervised the work. Helped prepare, edit and critically review the manuscript.		
Signature		Date	20.5.2019

Please cut and paste additional co-author panels here as required.

A new method for predicting the extraction of anthocyanins during red wine fermentation

Patrick C. Setford[1], David W. Jeffery[1], Paul R. Grbin[1] and Richard A. Muhlack[1,*]

[1]Department of Wine and Food Science, School of Agriculture, Food and Wine, The University of Adelaide (UA), PMB 1, Glen Osmond SA 5064, Australia

**Author for correspondence (Telephone: +61 8 8313 6771; Email: richard.muhlack@adelaide.edu.au)*

Key words: Modelling, phenolic extraction, simulation, red wine, anthocyanins, mass transfer

Highlights:

- A new novel method is used to predict M3G extraction during red wine fermentation
- Surface response models are used to predict mass transfer properties
- Simulations showed good agreement with measured M3G concentrations
- Predictive simulations provide potential for process control and automation of winemaking extraction phenomena at large scale

Funding: P.S. is supported through a UA School of Agriculture, Food and Wine Scholarship [1606990] and was also a recipient of a Wine Australia supplementary scholarship [AGW Ph1505]. The authors acknowledge the financial support from the School of Agriculture, Food and Wine, UA, and Australian grapegrowers and winemakers through their investment body, Wine Australia, with matching funds from the Australian Government

Conflicts of Interest: The authors declare no conflict of interest.

Abstract

Red wine quality is largely determined by the concentration of phenolic compounds extracted from the skins and seeds during fermentation. As such, the ability to manage this extraction process is a key consideration for winemakers. Current mathematical models based on regression analysis methods that are used to describe phenolic extraction during fermentation can provide insight into the effect of changing process conditions, however their use as a predictive tool in future fermentation scenarios is limited. In this study, simulations of anthocyanin extraction during commercial fermentations are presented based on a novel first principles mass-transfer model with incorporated response surface equations for calculating relevant mass transfer parameters at conditions present at various stages of fermentation. In each case, simulated concentrations of malvidin-3-glucoside are compared with the respective measured amounts for each ferment in order to study the predictive capabilities of the model and test the robustness. In general, the method employed to simulate this mass transfer process showed similar extraction patterns to that measured and displayed good predictive capabilities for anthocyanin concentrations at the latter stages of fermentation, highlighting its usefulness as a new tool for quality management and process control during winemaking.

38 Nomenclature

a	Specific surface area for mass transfer ($m^2\ m^{-3}$)
$°B$	Degrees Baume
c	Concentration ($mg\ L^{-1}$)
C_{EtOH}	Ethanol concentration (% *v/v*)
C_S	Sugar concentration ($g\ L^{-1}$)
d	Characteristic length
D_s	Solute (s) mass diffusivity ($m^2\ s^{-1}$)
Ex	Extent of fermentation
k_c	Mass transfer coefficient ($m\ s^{-1}$)
K	Distribution constant
L	Internal diffusion path length (m)
OG	Original gravity of liquid
r^2	Coefficient of determination
$RMSE$	Root mean square error
SG	Specific gravity of liquid
t	Time (s)
T	Temperature (°C)

39 Dimensionless Groups

Re	Reynolds number
Sc	Schmidt number
Sh	Sherwood number

40 **Greek Symbols**

ε	Liquid-phase volume fraction
η	Dynamic viscosity (kg m^{-1} s^{-1})
ρ	Density (kg m^{-3})

41 **Subscripts**

0	At initial or reference point
i	At the solid-liquid interface
β	Solid phase
γ	Liquid phase

42

1. Introduction

The extraction of phenolic compounds from the skins and seeds of grapes during fermentation is a critical stage of the red winemaking process. These compounds, which include anthocyanins, tannins, flavan-3-ols, and flavanols, are responsible for the colour, mouthfeel, flavour, ageing ability, and overall quality of the finished wine. Recent studies on anythocyanins (the predominant class of compounds that account for the red pigments and are involved in long term colour stability of red wine) have sought to identify the main factors that influence the extraction process (Setford et al. 2017), and specifically generate response models able to predict important mass transfer parameters at conditions that can be varied by the winemaker (such as the timing and duration of mixing operations) (Setford et al. 2019a) or may naturally vary throughout a fermentative maceration (such as temperature and liquid phase concentrations of sugar and ethanol) (Setford et al. 2019b).

In the past, first and second order rate models have been used to describe the extraction of anthocyanins and other red wine phenolic compounds (Zanoni et al. 2010; Boulton et al. 1996). Although these regressions can be used to fit experimental data with a high degree of accuracy, they typically use a single rate constant to describe the extraction process. In doing so, factors that may vary naturally during fermentation or through the intervention of a winemaker (such as temperature fluctuations or mixing operations) are not explicitly accounted for, thus limiting the predictive capabilities of these models for future fermentation scenarios.

A key objective for modelling phenolic extraction is the ability to predict winemaking outcomes based on initial variables such as grape phenolic composition together with parameters controlled during winemaking such as mixing operations and fermentation temperature. Robust predictive models for basic fermentation parameters such as ethanol formation, nutrient consumption and biomass growth are well established in literature (Boulton

et al. 1996; Coleman et al. 2007), however similar models able to predict the extraction of phenolic compounds are currently lacking.

With the aim of addressing this gap, surface response equations of relevant anthocyanin mass transfer parameters generated in previous studies (Setford et al. 2018; Setford et al. 2019a; Setford et al. 2019b) have been used to simulate the extraction of malvidin-3-glucoside (M3G, the predominant anthocyanin in red wine) in active fermentation scenarios. Process data from commercial large-scale winery fermentations of different grape varieties are used to inform these models under dynamic conditions and the anthocyanin extraction curves from the fermentations are compared to the resulting simulations in order to test the predictive capabilities and robustness of this incorporated extraction model.

2. Materials and Methods

2.1. Sample and winery data collection

Samples from unreplicated commercial red wine fermentations at Pernod Ricard Winemakers (Barossa Valley, South Australia) were collected during the 2018 vintage, with fermentation volumes that ranged from 20 to 125 kL. For each of the tracked fermentations, 50 mL samples were collected daily by winery staff and frozen at −20 °C until further analysis. Daily temperature and Baume readings as well as information regarding the timing of mixing operations were collected by the winery (data presented for individual ferments in Supplementary Tables S1 to S13, where for instance, 30 min/6 hours implies that the fermenter is being pumped over for 30 minutes every 6 hours). Although the temperature of a typical red wine ferment is likely to vary between the liquid and the cap, the measured temperature was assumed to be an average over the whole ferment for the purpose of this study.

2.2. Malvidin-3-glucoside quantification

M3G quantification was performed via gradient elution HPLC following the method described by Cozzolino et al. (2004) with a slight variation in the method described by Mercurio et al. (2007). An Agilent 1100 HPLC (Agilent, Forest Hill, VIC, Australia) with quaternary pump and diode array detector (DAD) was used to perform sample analyses and Agilent ChemStation software (version B.01.03) was used for data acquisition and processing. M3G concentration was quantified at 520 nm by comparison of absorbance using malvidin-3-*O*-glucoside chloride (≥95% by HPLC) purchased from Extrasynthese (Genay, France) as an external standard.

2.3. Mathematical modelling

2.3.1. Mass transfer model

Anthocyanin extraction during fermentative maceration is a multiphase mass transfer process involving diffusion of the dissolved molecule in the solid phase to the solid-liquid boundary layer followed by liquid phase mass transfer from this boundary layer to the bulk of the liquid phase. A mechanistic model for this process, previously described for anthocyanin extraction (Setford et al. 2019a; Setford et al. 2018; Setford et al. 2019b) and used in other biological extraction systems (Rodríguez-Jimenes et al. 2013; Espinoza-Pérez et al. 2007), is as follows:

$$(1-\varepsilon)\frac{dc_\beta}{dt} = k_{c\beta}a\left(c_{\beta i} - c_\beta\right) \quad (1)$$

$$\varepsilon\frac{dc_\gamma}{dt} = k_{c\gamma}a\left(c_{\gamma i} - c_\gamma\right) \quad (2)$$

$$c_{\gamma i} = Kc_{\beta i} \quad (3)$$

Equations 1 and 2 represent the macroscopic mass transfer of M3G in the solid and liquid phases, respectively, and Equation 3 describes the equilibrium relationship at the solid-

liquid interface. A simplified analytical solution of Fick's second law derived in Setford et al. (2018) can be used to describe 1-dimenional diffusion of M3G within the grape solids to the solid-liquid boundary layer.

$$\frac{c_\beta - c_{\beta i}}{c_{\beta 0} - c_{\beta i}} = \frac{4}{\pi} exp\left(-\frac{\pi^2 D_{s\beta} t}{4L^2}\right) \quad (4)$$

The value for L in Equation 4 was taken as a variety-dependent skin thickness based on average values presented in Jin et al. (2017) and is assumed to remain constant throughout fermentation. Equation 4 can be rearranged to calculate the instantaneous solid phase concentration at the solid-liquid interface, as shown in Equation 5.

$$c_{\beta i} = \frac{\frac{4c_{\beta 0}}{\pi} exp\left(-\frac{\pi^2 D_{s\beta} t}{4L^2}\right) - c_\beta}{\frac{4}{\pi} exp\left(-\frac{\pi^2 D_{s\beta} t}{4L^2}\right) - 1} \quad (5)$$

2.3.2. Mass transfer parameter estimation

To determine the solid phase diffusion rate ($D_{s\beta}$) and partition coefficient between the solid and liquid phases (K), response surface equations from Setford et al. (2018) that calculate these parameters as a function of temperature and liquid phase ethanol and sugar concentrations were used:

$$D_{s\beta} = 2.75 \times 10^{-13} + 2.11 \times 10^{-13} T + 1.09 \times 10^{-16} C_{EtOH} + 8.52 \times 10^{-14} T C_{EtOH} \quad (6)$$

$$K = 9.97 \times 10^{-2} + 3.33 \times 10^{-2} T + 1.04 \times 10^{-2} C_g + 3.74 \times 10^{-2} C_{EtOH} + 1.23 \times 10^{-2} T C_g - 9.64 \times 10^{-3} T C_{EtOH} + 7.91 \times 10^{-3} C_g C_{EtOH} + 9.86 \times 10^{-3} T C_g C_{EtOH} \quad (7)$$

It was assumed that these extraction parameters were independent of variety, which is accounted for in other parameters that would change with variety, such as the diffusion path length (L). The parameters T, C_{EtOH} and C_g in Equations 6 and 7 are scaled in terms of the

coded variables used in the ANOVA (−1 for low, 0 for the midpoint and 1 for the high values, respectively). Recalculating these response equations using the uncoded experimental values (in which T, C_{EtOH} and C_g have units °C, % *v/v* and g L^{-1} respectively) yields the following:

$$D_{s\beta} = -1.98 \times 10^{-14} + 1.38 \times 10^{-14}T - 2.44 \times 10^{-15}C_{EtOH} + 1.31 \times 10^{-15}TC_{EtOH} \quad (8)$$

$$K = 2.91 \times 10^{-2} + 2.28 \times 10^{-3}T - 8.76 \times 10^{-6}C_g + 4.26 \times 10^{-3}C_{EtOH} + 1.99 \times 10^{-6}TC_g - 3.44 \times 10^{-6}TC_{EtOH} - 7.08 \times 10^{-6}C_gC_{EtOH} + 1.13 \times 10^{-6}TC_gC_{EtOH} \quad (9)$$

The rate of internal mass transfer can then be determined as a function of the internal diffusion rate ($D_{s\beta}$) and the distance for internal diffusion (L) using a correlation developed in Setford et al. (2018):

$$k_{c\beta} = \frac{D_{s\beta}(1-\varepsilon)\pi^2}{4L} \quad (10)$$

In Equation 10, ε was calculated based on the solid to liquid ratio of pressed must presented in Section 2.1.2 of Setford et al. (2019b). In a follow-up study, the rate of liquid phase mass transfer ($k_{c\gamma}$) under free convective conditions was determined as a function of the extent of fermentation (Setford et al. 2019a):

$$k_{c\gamma} = -4.94 \times 10^{-9}Ex^2 + 8.27 \times 10^{-9}Ex + 2.20 \times 10^{-9} \quad (11)$$

In order to account for the change in liquid phase mass transfer during mixing operations (forced convective conditions), a sufficiently high external mass transfer value (1×10^{-4}) was chosen that allows the system to be considered well-mixed, limiting the impact of external resistances during these time periods and allowing solid phase diffusion to become the rate limiting variable for mass transfer. The assumption of a well-mixed system is commonly adopted in chemical engineering problems that allows for the calculation of

solutions in complex physical processes. This value is of the same order of magnitude calculated in previous studies employing forced convective conditions for anthocyanin extraction from pre-fermentative grape solids (Setford et al. 2019a; Setford et al. 2019b).

2.3.3. Fermentation parameter estimation

Because Equations 8 and 9 require the concentration of sugar in g L^{-1} and the concentration of ethanol in % *v/v*, it was necessary to calculate these values based on winery supplied density readings (recorded in Baume, a common unit of measurement for density used throughout Australia) collected daily for each ferment. To achieve this, specific gravity (at 20 °C) for each day was calculated according to the following equation presented in Boulton et al. (1996):

$$SG = \frac{145}{145 - °B} \quad (12)$$

From this, liquid phase sugar concentrations in g L^{-1} were calculated as follows (Cowey 2016):

$$C_s = (°B \times 1.8) \times SG \times 9.982 \quad (13)$$

Ethanol concentrations at each time interval (in % *v/v*) were calculated based on the extent of fermentation (assuming complete fermentation) and from the potential alcohol based on the following calculation in Boulton et al. (1996):

$$C_{EtOH,potential} = 0.0595 \times (2560 \times (SG - 1) - 22.2) \quad (14)$$

3. Results and Discussion

3.1. Predictive simulations

To simulate the extraction of M3G during fermentative maceration, Equations 1 and 2 were solved in Matlab (version R2013a) using a manually coded fourth order Runge-Kutta

algorithm with a constant step size of 0.005 hours. At each time point, the distribution constant (K) and rate of internal (solid phase) mass transfer ($k_{c\beta}$) were calculated as a function of the temperature and liquid phase conditions according to Equations 8 to 10. During time periods where no external mixing was applied, the rate of external (liquid phase) mass transfer ($k_{c\gamma}$) was calculated using Equation 11 as a function of the extent of fermentation. During time periods where mixing was employed, the rate of external mass transfer was taken as a constant value of 1×10^{-4}, whereby the rate limiting step for the overall mass transfer of M3G was internal diffusion. Baume and temperature data for each fermentation were collected only once daily (Tables S1 to S13). At all other time points, these values were calculated through linear interpolation between daily measurements.

Because the phase distribution constant (K) at equilibrium is a linear function of the solid-liquid ratio (as described by Equation 3), the initial concentration of M3G in the solid phase for each simulation was estimated from the measured concentration of M3G at the end of fermentation in the winery supplied liquid samples and by calculating the distribution constant at equilibrium using Equation 9. For future simulations, an improvement would be to measure the solid phase M3G concentration prior to extraction according to the method described in Section 2.1.5 of Setford et al. (2019b) but the present work was undertaken within the constraints of commercial vintage operations so this data was unavailable.

Figures 1a-m present the results of the M3G simulations together with the measured concentrations from industry supplied samples for fermentations where pump over operations were employed as the predominant mixing technique (see Tables S1 to S13 for mixing regime durations. In each simulation, input values for mixing regime, temperature profile and fermentation rate differed greatly, yielding vastly different extraction curves. A clear observation in these simulations compared with previously described first and second order anthocyanin extraction models (Zanoni et al. 2010; Boulton et al. 1996) is that a stepped rather

than smooth trajectory is apparent in each case. This is due to the particular feature of the model whereby mass transfer rates are adjusted step-wise between periods of natural and forced convective (mixing) conditions. This distinctive feature results in a stepped extraction curve that would be more likely to occur in reality because mixing operations cause the grape solids cap (formed by CO_2 evolution) to break up, redistributing any extracted phenolics caught within the cap's interstitial liquid into the bulk of the fermenting liquid.

Notably, samples for measurement of each ferment were collected from a commercial winery with practical constraints regarding the time required to completely fill (and then safely sample from) a large scale fermentation vessel, therefore there is likely disconnect between the time when grapes were crushed and the initial sample collected (specified as time 0). As such, this is a potential source of error in each simulation – particularly given that a significant proportion of extraction takes place within the first 24 hours of maceration. In some instances (particularly evident in Figures 1b, 1e, 1f and 1g), a drop in M3G concentration can be observed, and this coincides with a decrease in fermentation temperature (see Tables S1 to S13). This occurs as a result of the strong dependence on temperature of the phase distribution constant (K). For example, Figure 1e shows a steep increase in M3G extraction between day one and two, at which point a decrease in liquid phase M3G concentration can be observed that coincides with a reduction in fermentation temperature (controlled by employing a cooling jacket or coil in the fermenter) from 27 to 19 °C (Supplementary Table S5). Although a decline in dynamic M3G concentration caused by a lower temperature is unlikely in practice (a plateau would be more probable, and could be a refinement for future iterations of this model), it is interesting to note a similar M3G concentration curve can be observed from 0 to 6 days in Figure 1g. Here, both the simulated and measured concentrations peak at day 4 (where the highest temperature of 24.6 °C was observed, Supplementary Table 7) followed by a steady decline at around day 6 where the fermentation temperature drops significantly to 13.6 °C.

After the initial lag-phase in yeast activity present during red wine fermentation, the rate of fermentation can generally be observed to peak as seen in Coleman et al. (2007). Because fermentation is an exothermic reaction, this would be expected to result in a peak in fermentation temperatures within the solids cap. At this point, a decrease in anthocyanin concentration can by typically observed (Boulton et al. 1996; Zanoni et al. 2010). A diminished distribution constant resulting from lower temperatures typically observed may in part help to explain the typically observed lower concentration of anthocyanins, as the extraction phase may have slowed to a point where subsequent liquid phase chemical or physical reactions occur at a faster rate.

In most cases, the predicted M3G extraction curves closely resemble the overall shape of the linearly interpolated measured concentration curves (for example, Figures 1a, 1b, 1c, 1f, 1j, 1k, 1l and 1m). In particular, the simulated extraction in Figure 1c very closely resembles the same overall shape of the measured extraction curve. Here, a lag phase can be observed following a fast initial release caused by M3G leakage at crushing (Sparrow et al. 2015) and a subsequent sharper increase in extraction rate concomitant with the increase in temperature caused from vigorous fermentation. Table 1 presents the root mean square error (RMSE) and coefficient of determination (R^2) for each of the simulated M3G extractions calculated using Matlab (version R2013a). Due to the relative infrequency of sampling (resulting from commercial constraints), it was necessary to compare the simulated extractions with interpolated values. In most cases, the simulations showed a good agreement with the commercial fermentations, with relatively low RMSE values and R^2 values > 0.7 observed in 8 out of 13 simulations. Despite some of the R^2 values presented in Table 1 showing a relatively weak agreement (e.g., for Figures 1e and 1g) or indeed a negative correlation in two cases (Figures 1f and 1i), it should be highlighted that these simulations were generated entirely from first principles with extraction parameters based on previously published response models for

mass transfer values (specified in Section 2.3). They are not regressions based on measured concentrations of M3G designed to obtain the best fit with respect to R^2.

Importantly, although the mathematical model presented in Section 2.2 and used to produce the simulations in Figure 1 is a relatively novel concept for red wine extraction systems, it is a relatively simple model that is employed to describe a highly complex extraction process with myriad physical and chemical reactions taking place (Setford et al. 2017). Nonetheless, because the simulations provide a reasonable fit to the commercial extraction data in the majority of cases with respect to R^2 values, it suggests that the model is relatively robust and the methodology sound. However, there are clearly some variability that is not accounted for which is likely related to other external factors that are not considered. This could include factors such as polymeric pigment formation, oxidation and adsorption (Setford et al. 2017). In addition to these naturally occurring phenomena, it is possible (and indeed likely) that the winery, being a commercial facility, may have altered fermentation management or made additions for commercial reasons that were not accounted for in the information provided with the samples. As such, there is further opportunity to expand and optimise the model so that it can better account for these factors.

To the authors' knowledge, the work presented in this study is an entirely new approach used to simulate the extraction of anthocyanins during large scale red wine fermentations. Despite there being limitations to this predictive approach due to the highly complex chemical nature of wine and the uncertainties that come with uncontrollable or ill-defined factors present in a commercial wine setting, the method underpinning the simulations presented in Figure 1 represents a significant step forward for predicting anthocyanin extraction at large scale.

3.2. Future Directions

A method to predict the extractive behaviour of anthocyanins during fermentative maceration has been applied to commercial fermentations. A useful step would be to extend this approach to include other phenolic compounds important to red wine quality. In particular, tannins and tannin constituents that are extracted from both the skins and seeds during fermentation play a significant role in the finished wine quality and also interact with anthocyanins to form polymeric pigments that aid in long-term colour stability. To achieve this, similar factorial experiments to those previously described in Setford et al. (2018) and Setford et al. (2019b) could be undertaken for both seed and skin tannin extraction, applying the same mass transfer model presented in Section 2.2.

A further refinement which would also expand the scope of utility of the presented model relates to the characterisation of hydrodynamic behaviour. In this model, a high external mass transfer rate is used to simulate vigorous mixing operations, leaving internal diffusion the rate limiting step for extraction. An improvement to this assumption for consideration in future work would be to directly measure or estimate average fluid velocities that occur during mixing operations. As an example, the average fluid velocity in the fermenter during pump-over operations could be estimated as a function of the volumetric flow rate. Hence, the rate of external mass transfer could be calculated through a system of dimensionless equations describing the fluid flow and properties of the system (Setford et al. 2017):

$$Sh = Sh_0 + CRe^m Sc^{1/3} \tag{15}$$

$$Re = \frac{\rho v d}{\eta},\ Sh = \frac{k_{c\gamma} L}{D_{s\gamma}},\ Sc = \frac{\eta}{\rho D_{s\gamma}} \tag{16}$$

Here, C and m are determined by the physical characteristics of the system, which for a pump-over operation could potentially be described as flow through a filter bed.

297 Wine extraction simulations using such models could be used to inform optimal mixing,
298 temperature, and initial fermentation parameters, to yield a desired extraction rate and final
299 liquid phase concentration. By uniting the proposed model with well-established predictive
300 fermentation models, such as that presented in Coleman et al. (2007), winemakers would be
301 able to predict not only the possible anthocyanin extraction pattern and final concentration, but
302 also control this process to a desired outcome (such as maximising the extraction potential or
303 providing consistency from vintage-to-vintage). Furthermore, simulations such as these that
304 account for mixing could be used to inform winemakers on the quality impact of mixing
305 operations at the later stages of fermentation by predicting the effect this may have on gaining
306 any improved extraction.

307 Because the phenolic content of wine is a significant driver of quality, it is therefore a
308 key parameter for winemakers to make processing decisions. Additional knowledge on
309 extraction during the early stages of fermentation would provide winemakers with enhanced
310 ability to appropriately plan downstream unit operations (such as pressing operations and tank
311 transfers) resulting in an increased overall winery efficiency and reduced production costs.

312 ## 4. Conclusions

313 Predictive simulations of M3G extraction from grape solids during red wine
314 fermentation were undertaken using a mass transfer model based on first principles that
315 incorporated surface response equations to determine mass transfer variables as a function of
316 fluid properties. These predictive simulations were compared with results from the analysis of
317 M3G in samples collected from commercial scale red wine fermentations. In most cases, the
318 simulated extraction exhibited similar behaviour to that shown by the measured extraction
319 curves. These commonalities included a fast initial release of M3G from grape solids within
320 the first few hours of contact, a lag phase following this initial release, and a subsequent

extraction period that varied with fermentation rate and temperature. Additionally, these simulations accounted for the effect of mixing operations by varying the rate of liquid phase mass transfer accordingly, resulting in a previously undescribed but not unexpected step-wise extraction pattern. Although the simulations presented here represent a significant advancement in the understanding of anthocyanin extraction and to a degree can be used to predict this process, future studies should seek to diminish some of the limitations presented above and build on the existing model to improve the fit with respect to experimentally determined concentrations.

5. Acknowledgments

The authors would like to thank the staff at Pernod Ricard Winemakers for provision of commercial fermentation samples and associated fermentation records.

References

Boulton, R., Singleton, V., Bisson, L., & Kunkee, R. (1996). *Principles and Practices of Winemaking*. New York: Chapman and Hall.

Coleman, M. C., Fish, R., & Block, D. E. (2007). Temperature-dependent kinetic model for nitrogen-limited wine fermentations. *Applied and Environmental Microbiology, 73*(18), 5875-5884, doi:https://10.1128/AEM.00670-07.

Cowey, G. (2016). Predicting alcohol levels. *Australian & New Zealand Grapegrower & Winemaker,* (626), 68.

Cozzolino, D., Kwiatkowski, M., Parker, M., Cynkar, W., Dambergs, R., Gishen, M., et al. (2004). Prediction of phenolic compounds in red wine fermentations by visible and near infrared spectroscopy. *Analytica Chimica Acta, 513*(1), 73-80, doi:https://doi.org/10.1016/j.aca.2003.08.066.

Espinoza-Pérez, J., Vargas, A., Robles-Olvera, V., Rodríguez-Jimenes, G., & García-Alvarado, M. (2007). Mathematical modeling of caffeine kinetic during solid–liquid extraction of coffee beans. *Journal of Food Engineering, 81*(1), 72-78, doi:https://doi.org/10.1016/j.jfoodeng.2006.10.011.

Jin, X., Wu, X., Liu, X., & Liao, M. (2017). Varietal heterogeneity of textural characteristics and their relationship with phenolic ripeness of wine grapes. *Scientia Horticulturae, 216*(Supplement C), 205-214, doi:https://doi.org/10.1016/j.scienta.2017.01.010.

Mercurio, M. D., Dambergs, R. G., Herderich, M. J., & Smith, P. A. (2007). High throughput analysis of red wine and grape phenolics adaptation and validation of methyl cellulose precipitable tannin assay and modified somers color assay to a rapid 96 well plate format. *Journal of Agricultural and Food Chemistry, 55*(12), 4651-4657, doi:https://doi.org/10.1021/jf063674n.

356 Rodríguez-Jimenes, G. C., Vargas-Garcia, A., Espinoza-Pérez, D. J., Salgado-Cervantes, M.
357 A., Robles-Olvera, V. J., & García-Alvarado, M. A. (2013). Mass transfer during
358 vanilla pods solid liquid extraction: Effect of extraction method. *Food and Bioprocess*
359 *Technology, 6*(10), 2640-2650, doi:https://doi.org/10.1007/s11947-012-0975-6.
360 Setford, P., Jeffery, D., Grbin, P., & Muhlack, R. (2019a). Mass transfer of anthocyanins
361 during extraction from pre-fermentative grape solids under simulated fermentation
362 conditions: effect of convective conditions. *Molecules, 24*(1), 73,
363 doi:https://doi.org/10.3390/molecules24010073.
364 Setford, P. C., Jeffery, D. W., Grbin, P. R., & Muhlack, R. A. (2017). Factors affecting
365 extraction and evolution of phenolic compounds during red wine maceration and the
366 role of process modelling. *Trends in Food Science & Technology, 69, Part A*, 106-
367 117, doi:https://doi.org/10.1016/j.tifs.2017.09.005.
368 Setford, P. C., Jeffery, D. W., Grbin, P. R., & Muhlack, R. A. (2019a). Modelling the mass
369 transfer process of malvidin-3-glucoside during simulated extraction from fresh grape
370 solids under wine-like conditions. *Molecules, 23*(9), 2159,
371 doi:https://doi.org/10.3390/molecules23092159.
372 Setford, P. C., Jeffery, D. W., Grbin, P. R., & Muhlack, R. A. (2019b). Mathematical
373 modelling of anthocyanin mass transfer to predict extraction in simulated red wine
374 fermentation scenarios. *Food Research International*, *121*, 705-713,
375 doi:https://doi.org/10.1016/j.foodres.2018.12.044.
376 Sparrow, A. M., Smart, R. E., Dambergs, R. G., & Close, D. C. (2015). Skin particle size
377 affects the phenolic attributes of Pinot Noir wine: Proof of concept. *American Journal*
378 *of Enology and Viticulture, 67*, 29-37, doi:https://doi.org/10.5344/ajev.2015.15055
379 Zanoni, B., Siliani, S., Canuti, V., Rosi, I., & Bertuccioli, M. (2010). A kinetic study on
380 extraction and transformation phenomena of phenolic compounds during red wine

381 fermentation. *International Journal of Food Science & Technology, 45*(10), 2080-
382 2088, doi:https://doi.org/10.1111/j.1365-2621.2010.02374.x.

Figures

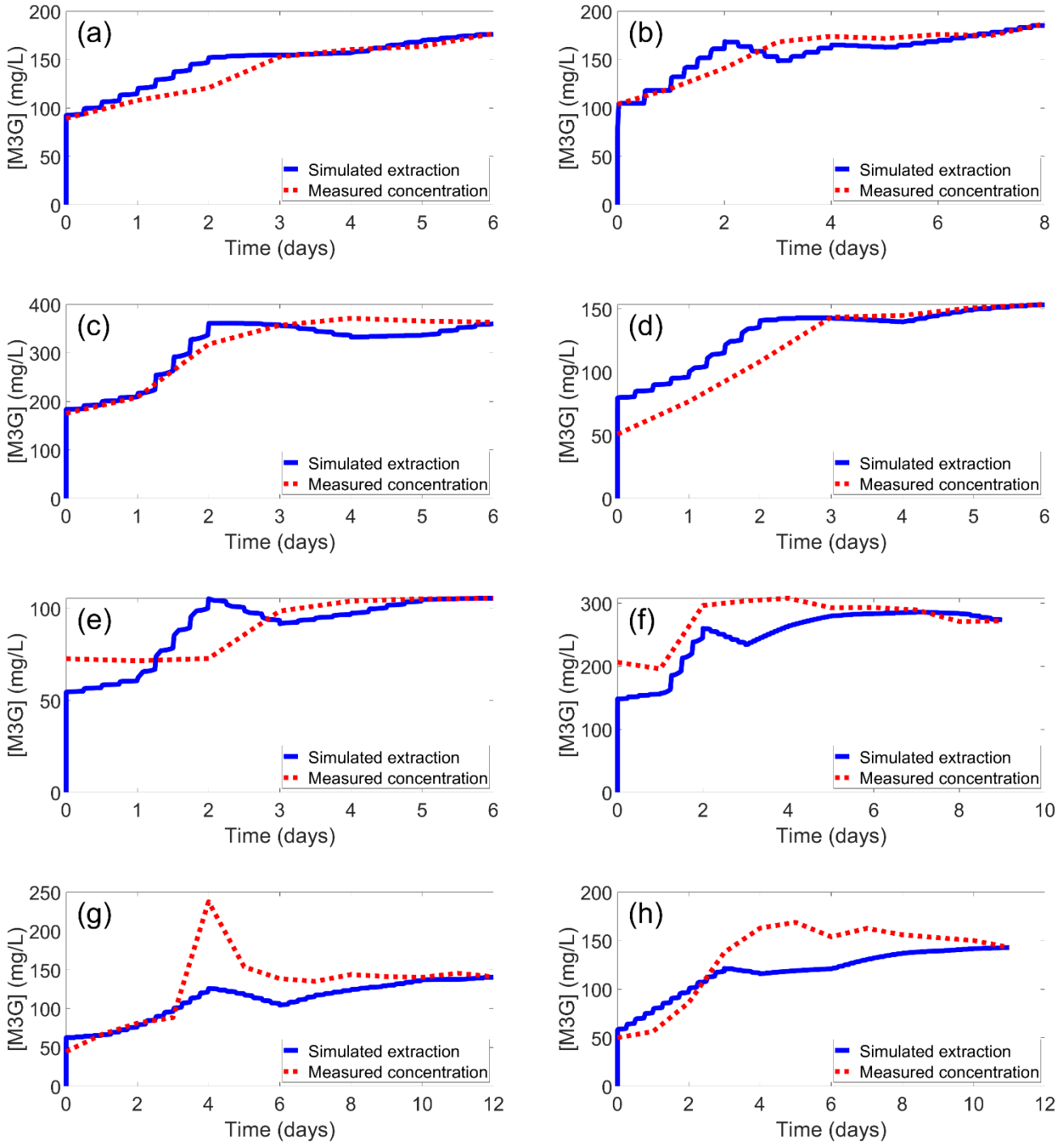

Figure 1. Predictive simulations of M3G extraction during commercial red wine fermentations compared with measured concentrations at daily intervals. Specific details including daily values for temperature, Baume and mixing regimes can be found in Tables S1 to S13

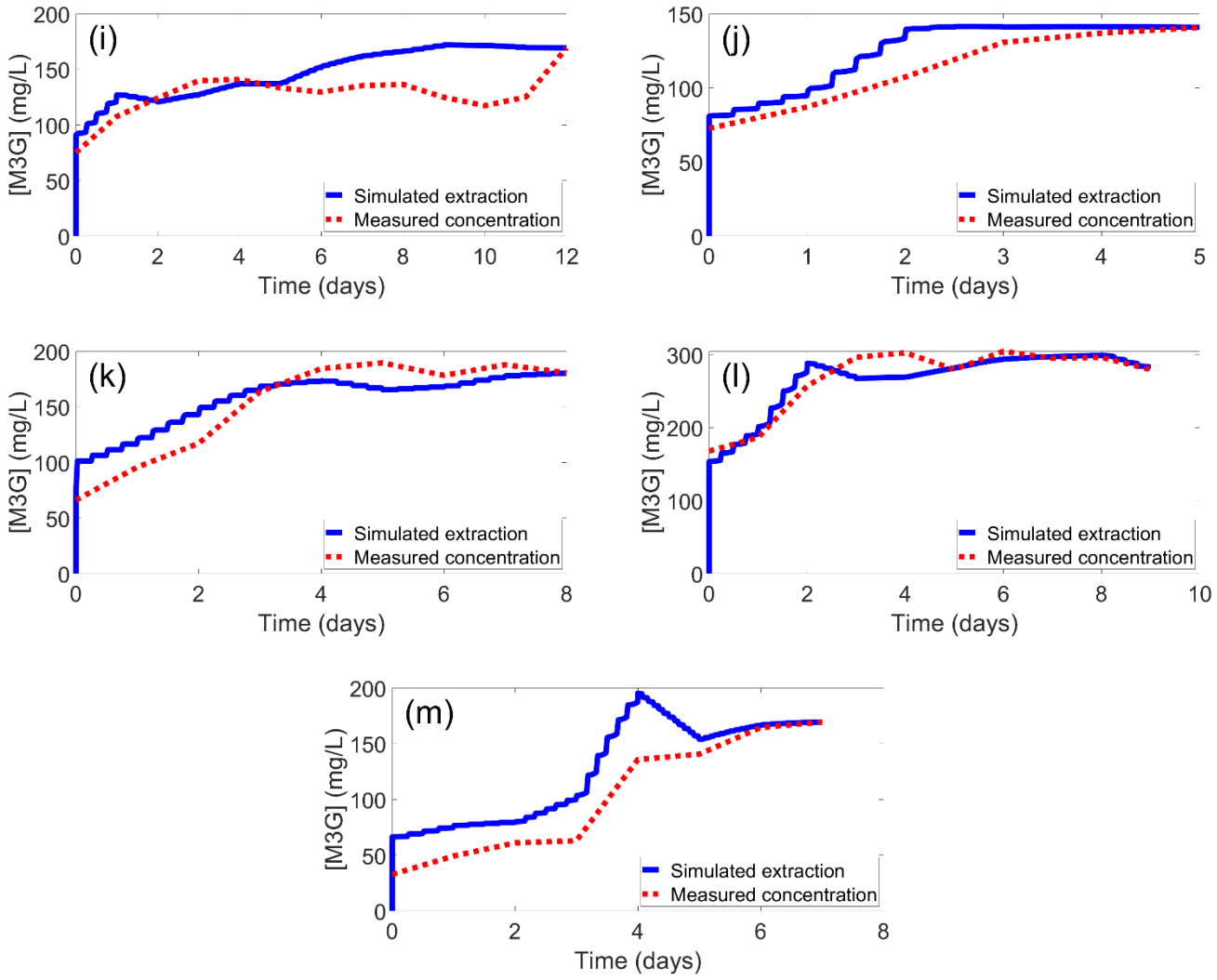

Figure 1 (continued): (caption on previous page)

Tables

Table 1. Statistical parameters (RMSE and R^2) for simulated extraction of M3G during active fermentation and additional information for respective industry fermentations (tank size, ferment size, tank type and grape variety).

Figure	Grape Variety	Tank size (kL)	Ferment size (kL)	Tank Type	RMSE	R^2
1a	Shiraz	227	125	Jet	10.64	0.88
1b	Cabernet Sauvignon	55	33	Potter	14.14	0.73
1c	Shiraz	55	33	Potter	19.11	0.94
1d	Cabernet Sauvignon	227	125	Jet	16.76	0.80
1e	Shiraz	92	60	Jet	13.52	0.24
1f	Shiraz	58	35	Static	38.08	-0.02
1g	Cabernet Sauvignon	55	33	Potter	36.28	0.40
1h	Shiraz	227	125	Jet	26.39	0.58
1i	Merlot	227	125	Jet	27.40	-0.76
1j	Shiraz	92	60	Jet	12.48	0.77
1k	Cabernet Sauvignon	55	33	Potter	15.02	0.88
1l	Shiraz	58	35	Static	15.95	0.88
1m	Pinot Noir	31	20	Static	28.74	0.70

Note: the initial simulated M3G concentrations used to calculate these parameters (at t = 0) were adjusted to account for the fast initial increase that occurs within the first 5 minutes of the simulations. This also accounts for, in part, the actual lag between when grapes are crushed and the first sample collected.

404 # Electronic Supplementary Material for

405 # A new method for predicting the extractive behaviour of anthocyanins

406 # during red wine fermentation

407 Patrick C. Setford[1], David W. Jeffery[1], Paul R. Grbin[1] and Richard A. Muhlack[1,*]

408 [1]Department of Wine and Food Science, School of Agriculture, Food and Wine, The University

409 of Adelaide (UA), PMB 1, Glen Osmond SA 5064, Australia

410 ## Table of Contents

	Page
Table S1. Winery data used for simulated M3G extraction in Figure 1a	S-2
Table S2. Winery data used for simulated M3G extraction in Figure 1b	S-2
Table S3. Winery data used for simulated M3G extraction in Figure 1c	S-2
Table S4. Winery data used for simulated M3G extraction in Figure 1d	S-3
Table S5. Winery data used for simulated M3G extraction in Figure 1e	S-3
Table S6. Winery data used for simulated M3G extraction in Figure 1f	S-4
Table S7. Winery data used for simulated M3G extraction in Figure 1g	S-4
Table S8. Winery data used for simulated M3G extraction in Figure 1h	S-5
Table S9. Winery data used for simulated M3G extraction in Figure 1i	S-5
Table S10. Winery data used for simulated M3G extraction in Figure 1j	S-6
Table S11. Winery data used for simulated M3G extraction in Figure 1k	S-6
Table S12. Winery data used for simulated M3G extraction in Figure 1l	S-7
Table S13. Winery data used for simulated M3G extraction in Figure 1m	S-7

411

412 **Table S1.** Winery data used for simulated M3G extraction in Figure 1a

Time (days)	Temperature (°C)	Baume	Mixing Regime
0	17.3	13.2	30 min / 6 hrs
1	20.6	11.6	30 min / 6 hrs
2	22.5	8.5	120 min / 6 hrs
3	19.6	5.3	120 min / 6 hrs
4	19.0	3.4	120 min / 6 hrs
5	22.0	1.7	120 min / 6 hrs
6	24.7	0.4	120 min / 6 hrs

413

414 **Table S2.** Winery data used for simulated M3G extraction in Figure 1b

Time (days)	Temperature (°C)	Baume	Mixing Regime
0	19.6	13.6	60 min / 12 hrs
1	22.6	12.2	60 min / 6 hrs
2	25.8	9.6	60 min / 6 hrs
3	18.0	7.1	60 min / 6 hrs
4	20.5	5.8	60 min / 6 hrs
5	19.0	4.6	60 min / 6 hrs
6	20.0	3.1	60 min / 6 hrs
7	22.0	2.1	20 min / 6 hrs
8	24.7	1.3	10 min / 6 hrs

415

416 **Table S3.** Winery data used for simulated M3G extraction in Figure 1c

Time (days)	Temperature (°C)	Baume	Mixing Regime
0	16.6	14.9	20 min / 6 hrs
1	18.6	14.1	20 min / 6 hrs
2	25.5	9.5	60 min / 6 hrs
3	22.3	6.9	60 min / 6 hrs
4	18.0	4.3	60 min / 6 hrs
5	18.2	3.7	30 min / 6 hrs
6	21.3	1.7	30 min / 6 hrs

417 **Table S4.** Winery data used for simulated M3G extraction in Figure 1d

Time (days)	Temperature (°C)	Baume	Mixing Regime
0	17.3	13.3	30 min / 6 hrs
1	19.8	11.8	120 min / 6 hrs
2	25.0	8.6	120 min / 6 hrs
3	22.0	5.2	120 min / 6 hrs
4	20.0	3.2	120 min / 4 hrs
5	23.0	1.6	120 min / 4 hrs
6	25.0	0.4	120 min / 6 hrs

418

419 **Table S5.** Winery data used for simulated M3G extraction in Figure 1e

Time (days)	Temperature (°C)	Baume	Mixing Regime
0	17.6	13.6	60 min / 6 hrs
1	18.4	12.6	120 min / 6 hrs
2	27.0	7.7	120 min / 6 hrs
3	19.0	4.6	120 min / 6 hrs
4	20.6	2.9	120 min / 6 hrs
5	24.5	1.0	30 min / 6 hrs
6	25.7	0.0	30 min / 6 hrs

420

421 **Table S6.** Winery data used for simulated M3G extraction in Figure 1f

Time (days)	Temperature (°C)	Baume	Mixing Regime
0	19.6	14.3	10 min / 6 hrs
1	16.1	12.4	10 min / 6 hrs
2	23.5	6.6	20 min / 4 hrs
3	18.4	5.0	20 min / 2 hrs
4	22.6	3.4	20 min / 2 hrs
5	25.7	1.9	20 min / 6 hrs
6	27.5	0.6	20 min / 6 hrs
7	28.2	0.5	20 min / 6 hrs
8	28.0	0.2	20 min / 6 hrs
9	25.2	0.2	20 min / 6 hrs

422

423 **Table S7.** Winery data used for simulated M3G extraction in Figure 1g

Time (days)	Temperature (°C)	Baume	Mixing Regime
0	13.0	13.0	10 min / 6 hrs
1	14.3	13.0	30 min / 6 hrs
2	16.6	12.2	60 min / 6 hrs
3	20.5	10.9	40 min / 6 hrs
4	24.6	9.0	60 min / 6 hrs
5	18.7	6.2	60 min / 6 hrs
6	13.6	5.0	60 min / 6 hrs
7	17.0	4.4	60 min / 6 hrs
8	18.9	3.9	60 min / 6 hrs
9	19.8	2.3	30 min / 6 hrs
10	22.4	1.9	30 min / 6 hrs
11	22.6	1.5	30 min / 6 hrs
12	24.0	0.9	30 min / 6 hrs

424

425 **Table S8.** Winery data used for simulated M3G extraction in Figure 1h

Time (days)	Temperature (°C)	Baume	Mixing Regime
0	13.0	13.8	60 min / 6 hrs
1	21.0	13.7	60 min / 6 hrs
2	23.7	12.1	60 min / 6 hrs
3	24.6	9.3	120 min / 6 hrs
4	20.4	7.3	120 min / 4 hrs
5	19.8	5.6	120 min / 4 hrs
6	19.6	4.4	120 min / 4 hrs
7	22.3	3.0	120 min / 4 hrs
8	24.8	1.7	120 min / 4 hrs
9	26.7	0.4	60 min / 4 hrs
10	28.1	0.2	60 min / 6 hrs
11	28.4	0.4	60 min / 6 hrs

426

427 **Table S9.** Winery data used for simulated M3G extraction in Figure 1i

Time (days)	Temperature (°C)	Baume	Mixing Regime
0	19.3	13.3	60 min / 6 hrs
1	24.0	11.2	60 min / 6 hrs
2	19.9	10.0	120 min / 4 hrs
3	18.7	8.1	120 min / 4 hrs
4	19.4	6.6	120 min / 4 hrs
5	18.2	5.3	120 min / 4 hrs
6	21.4	3.9	120 min / 4 hrs
7	23.7	2.6	120 min / 6 hrs
8	25.4	1.3	60 min / 6 hrs
9	27.7	0.8	60 min / 6 hrs
10	27.7	0.6	30 min / 6 hrs
11	27.7	0.0	30 min / 6 hrs
12	27.6	0.0	30 min / 6 hrs

428

429 **Table S10.** Winery data used for simulated M3G extraction in Figure 1j

Time (days)	Temperature (°C)	Baume	Mixing Regime
0	17.4	13.3	30 min / 6 hrs
1	19.8	12.2	60 min / 6 hrs
2	24.3	8.7	120 min / 6 hrs
3	21.0	5.2	120 min / 6 hrs
4	20.1	3.6	120 min / 6 hrs
5	19.2	1.6	60 min / 6 hrs

430

431 **Table S11.** Winery data used for simulated M3G extraction in Figure 1k

Time (days)	Temperature (°C)	Baume	Mixing Regime
0	19.0	13.4	30 min / 6 hrs
1	21.0	12.2	60 min / 6 hrs
2	23.5	10.4	60 min / 6 hrs
3	23.7	7.7	60 min / 6 hrs
4	22.7	5.4	60 min / 6 hrs
5	19.7	3.7	60 min / 6 hrs
6	20.0	2.4	60 min / 6 hrs
7	22.7	1.2	20 min / 6 hrs
8	24.0	0.2	20 min / 6 hrs

432

433 **Table S12.** Winery data used for simulated M3G extraction in Figure 1l

Time (days)	Temperature (°C)	Baume	Mixing Regime
0	18.2	14.3	10 min / 6 hrs
1	22.3	13.0	10 min / 6 hrs
2	25.4	7.9	20 min / 4 hrs
3	20.4	5.3	20 min / 4 hrs
4	19.9	3.8	20 min / 2 hrs
5	21.7	3.0	20 min / 2 hrs
6	24.0	1.4	20 min / 4 hrs
7	25.3	0.5	20 min / 6 hrs
8	26.0	0.2	20 min / 6 hrs
9	21.6	0.3	20 min / 6 hrs

434

435 **Table S13.** Winery data used for simulated M3G extraction in Figure 1m

Time (days)	Temperature (°C)	Baume	Mixing Regime
0	11.4	14.2	10 min / 6 hrs
1	13.6	13.8	10 min / 6 hrs
2	14.6	13.8	10 min / 4 hrs
3	18.4	12.7	10 min / 4 hrs
4	31.0	5.3	10 min / 2 hrs
5	20.0	4.1	10 min / 2 hrs
6	23.3	2.0	10 min / 2 hrs
7	25.0	0.4	10 min / 6 hrs

436

CHAPTER 6

Concluding remarks and future perspectives

6. Concluding remarks and future perspectives

6.1. Summary and conclusions

The ability to predict the effect that results from a change in operating conditions is a fundamental aspect of process control in any industry. Despite this, *quantitative* knowledge on the effect of fermentation process variables on red wine phenolic extraction (a process critical to wine product quality) is largely lacking. Additionally, mathematical models that provide quantitative insight into future fermentation scenarios by accounting for these change in process variables (such as the formation of ethanol during fermentation) are also scarce. The creation of such a model however would allow winemakers the ability to predict a wine's phenolic potential prior to fermentation and thereby optimise the process to a desired outcome, which in turn, would likely lead to economic benefits for the winery. The overarching goal of this project was to bridge this gap in knowledge, by developing a predictive mathematical model for the extraction of anthocyanins and in particular, malvidin-3-glucoside (M3G) during red wine fermentative maceration, which could in the future be extended to other red wine quality parameters and subsequently used in the development of real-time process control technologies.

6.1.1. Factors affecting extraction and evolution of phenolic compounds during red wine maceration and the role of process modelling

The first objective of this project was to identify and review the main factors that impact the rate and extent of phenolic extraction during red wine maceration. Chapter 1 summarises the current state of literature in this area, and the parameters identified in this study to most strongly influence phenolic extraction included temperature, liquid phase solvent (ethanol) concentration, and solid-liquid contact area. Additionally, mathematical models were identified throughout this study that could be used to describe the effects of various process variables (for

example, temperature) on the rate of phenolic extraction. Among these models, a system of dimensionless equations commonly used in chemical engineering to describe fluid flow was identified allowing for the calculation of liquid phase mass transfer of phenolic compounds, which was used to describe this process in Chapters 2 to 5 of this thesis.

6.1.2. Modelling the mass transfer process of malvidin-3-glucoside during simulated extraction from fresh grape solids under wine-like conditions

After identifying in Chapter 1 the main factors that influence phenolic (and in particular, anthocyanin) extraction during red winemaking, the second objective of this project, presented in Chapter 2, was to develop predictive models capable of describing this non-steady state process at conditions that change both naturally throughout fermentation or that can be manipulated by a winemaker. To accomplish this, a first-principles model based on macroscopic and microscopic solutions to Fick's second law of diffusion was developed for phenolic extraction from grape skins – a method employed previously in the extraction of solutes in other biological systems. A key feature of this new extraction model, distinguishing it from other mathematical models in the literature, is that it separates the effects of internal (solid phase) and external (liquid phase) mass transfer allowing the effects of each parameter on the overall rate of mass transfer to be independently studied. This feature was exploited in Chapter 2 to explore the influence of variables most dramatically impacting solid phase mass transfer of M3G (identified in Chapter 1) from pre-fermentative red grape solids, which were temperature and solvent concentration. The model developed in this chapter was applied to experimental extraction curves of M3G under forced convective conditions and at different liquid-phase conditions (temperature, ethanol concentration and sugar concentration), allowing for the rate of internal diffusion and extractability (represented by the distribution constant) to be calculated. Utilising the factorial design of the experiment, surface response equations for the internal diffusion and phase distribution constant were applied to the internal diffusion

coefficient and distribution constants, allowing the estimation of these parameters at conditions that would be observed in real-world fermentative macerations. In addition, analysis of variance showed temperature and ethanol to be most relevant for internal diffusion of M3G, whereas all investigated parameters (ethanol, sugar and temperature) as well as their combined interactions were significant in their effect on the distribution constant (which described the maximum extractability in the liquid phase).

6.1.3. Mass transfer of anthocyanins during extraction from pre-fermentative grape solids under simulated fermentation conditions: Effect of convective conditions

Whereas Chapter 2 investigated the effects of relevant extraction parameters on mass transfer of M3G within the solid phase (grape skins), Chapter 3 explored the impact of liquid phase convection (mixing) on the overall rate of extraction – another parameter identified in Chapter 1 as a strong influencer of phenolic extraction kinetics. Here, free convective (no mixing) rates of external mass transfer for M3G were quantified under conditions emulating different fermentation stages using the previously developed mathematical modelling of Chapter 2. This, combined with knowledge of external mass transfer rates gained in the study presented in Chapter 3 provided the additional ability to undertake predictive simulations of M3G extraction under dynamic liquid phase conditions simulating fermentation. These simulations provide new insight into anthocyanin extraction during fermentation: firstly, they showed that under low rates of liquid phase convection (such as that observed for the majority of a red wine fermentation), both solid phase diffusion and liquid phase mass transfer were rate limiting for the overall mass transfer of M3G. Additionally, and as was expected, at higher rates of liquid convection (such as that observed during red wine mixing operations), internal diffusion was the limiting step for mass transfer. It became clear that simulations undertaken in this study could be used as a basis for studying different mixing operations common in red winemaking that would address the shortcomings of other methods proposed in the literature.

Previous studies seeking to compare the effects of different mixing methods (e.g. liquid pump-over, mechanical punch-down of the solids, or rotating the fermentation vessel) have yielded conflicting results as to the efficacy of each method. However the extraction model used to accomplish the simulations in Chapter 3 is based on physical system properties that can be identified and defined (such as liquid phase velocity), rather than simply a comparison of mixing methods that would likely change from vessel to vessel and winery to winery.

6.1.4. Mathematical modelling of anthocyanin mass transfer to predict extraction in simulated red wine fermentation scenarios

The third objective of this project, which was to develop predictive models of anthocyanins during maceration at various process conditions, was addressed in Chapter 4. Here, predictive mass transfer models of anthocyanin extraction during maceration at various process conditions were evaluated using similar experimental methodology as developed in Chapter 2 together with predictive simulations of fermentative maceration scenarios from Chapter 3. However, Chapter 4 dealt with a different cultivar, Pinot noir – a grape variety that presents notorious difficulties for producing wines with long-term stable colour. Simulations of extraction during fermentation scenarios yielded several observations that could be exploited by winemakers. Chief among these is that the overall extraction rate under forced convective conditions is affected greatly by the concentration of ethanol in the liquid phase. This has implications for the commonly practiced winemaking technique of 'cold soaking', whereby unfermented must is held at a low temperature for several days prior to fermentation with the intent of improving the extraction of anthocyanins. Simulations presented in Chapter 4 suggest, however, that the maximum extractability of anthocyanins (assuming constant fermentation temperature) will not be achieved until the end of fermentation. This observation of ethanol limiting the rate and extractability of anthocyanins provides context for a previously undescribed extraction pattern, whereby a slower extraction period can be observed following

crushing until day two or three whereupon the rate of fermentation is increased and with it, the total ethanol concentration. In part, this observation challenges conventional understanding of phenolic extraction during red wine fermentation as a time-dependent concentration driven process and highlights the importance of understanding the effect of mixing and changing liquid conditions on internal and external mass transfer separately. Secondly, this study further supports conventional understanding that fermentation temperature drastically increases both the overall extraction rate and extractability of anthocyanins.

6.1.5. A new method for predicting the extraction of anthocyanins during red wine fermentation

The final objective of this project was to validate predictive mass transfer models in real-world scenarios. Accordingly, Chapter 5 sought to test the robustness of the mathematical modelling approach developed in Chapters 2 to 4 when applied to large-scale red wine fermentations typical of commercial winemaking practice. The extraction of M3G in industry fermentations at volumes ranging from 20-125 kL was measured and compared to predictive simulations based on temperature, fermentation (Baume) and mixing data (timing) for each respective ferment. In the majority of cases (8 out of 13), an R^2 value of ≥ 0.70 was observed for predictive simulations of M3G extraction using the mass transfer and response models developed in Chapters 2 and 3. In each extraction simulation, the positive impact of mixing operations on extraction could be observed as a feature of the model, whereby a stepped extraction curve during periods of mixing was clearly apparent as opposed to the smooth extraction curve described by simpler regression models. With the ability to predict, to a certain degree, the expected extraction profile of a given ferment based on easily measurable and controllable processing variables, the model developed in this project and employed for predictive simulations in Chapter 5 represents a significant step forward in both the

understanding of anthocyanin extraction during red winemaking as well as the potential for process control and automation of winemaking extraction phenomena.

6.2. Future perspectives

6.2.1. Extension of mass transfer model to include other red grape phenolic compounds

Although anthocyanins were the focus for this project (due to being an important class of objective quality compounds across all red wine grape varieties), the mass transfer model and experimental methodology developed in Chapters 2 to 4 could be readily adopted for other important qualitative compounds extracted during fermentation. In particular, the extraction of both skin and seed tannins responsible for the astringency and long term colour stability of red wines would be of particular value. Once developed, these models could potentially be unified with anthocyanin extraction models developed in this study and used to predict the rate and extent of polymeric pigment formation during fermentation and wine maturation.

6.2.2. Introducing post-extraction mathematical models for reactions of anthocyanins and other phenolic compounds

In Chapter 1, several chemical and physiochemical reactions were identified for anthocyanins (and proanthocyanidins) including but not limited to oxidation, derived pigment formation (such as polymeric pigments) and adsorption to yeast biomass that impact the observed concentration of these compounds during maceration and ageing. Further study on these reactions as affected by process variables (both controllable and uncontrollable such as temperature and fermentation extent) in conjunction with the development of response models for these processes would allow for incorporation with the mass transfer model presented in this study to better predict the extraction pattern and subsequent fate of anthocyanins.

One way to include post-extraction reaction phenomena in future iterations of the model proposed in this thesis would be to consider kinetic data from commercial scale studies that

model extraction data based on temperature and ethanol concentration and compare the effectiveness of the models. In doing so, any significant deviations from the predicted extraction curve and the extraction observed in real-time would be easily observed and allow for refinement of the model, which would ultimately improve it's predictive capabilities.

6.2.3. Rederivation and application of model for other non-grape extraction processes in winemaking

In this project, a model that concerns both solid and liquid phase mass transfer of phenolic compounds from grape solids to fermenting liquid was developed and applied for anthocyanin extraction. Despite this, a similar model could be readily derived for the extraction of hydrolysable tannins and other quality compounds extracted from oak during maturation and studied with a similar experimental design to those presented in Chapters 2 to 4. This would likely prove simpler and more consistent than modelling grape solid extraction given that the geometry of oak barrels and oak chips can be well defined and is potentially less variable than post-crush grape solids from batch-to-batch. Analogous to the results presented in this thesis, such studies on oak extraction could potentially minimise the time required for wine contact with oak by optimising process variables important to phenolic extraction, such as temperature and mixing operations. In turn this would likely see positive economic benefits in the winery by allowing winemakers the ability to predict, prior to oak addition, the contact time required for the desired outcome and thus plan for logistical operations within the winery.

6.2.4. Incorporation of mass transfer model with online process control

The work in this thesis focusses predominantly on one of three key elements required for integrated process control of phenolic extraction during fermentative maceration. In addition to the development of a robust mathematical model able to predict the impact of changing process variables for extraction, integrated process control would also require the design of on-line sensing tools able to accurately measure the concentration of anthocyanins

and other phenolic compounds as well as a control algorithm able to account for deviations from the model's prediction. The development of such models would not only allow winemakers the ability to predict the likely extraction outcome of a red wine fermentation, but also to direct this process to a specified outcome by automatically controlling process parameters identified within this thesis (temperature, fermentation rate and mixing rate and frequency). Such a tool would aid winemakers seeking to produce a consistent product from year-to-year despite changes in fruit quality and grape phenolic content from vintage-to-vintage. An integrated process control algorithm, whether designed as a feed-back or feed-forward process control, would also allow for reactions or pre-emptive corrections respectively to any deviations from the extraction pattern predicted by the mathematical model presented in this study, further improving the effectiveness of such an approach to winemaking.

6.2.5. Further developments for the current mathematical model

Finally, the model presented in this study considers mass transfer as a two-phase (solid-liquid) extraction process. Although this is a good description of the process during early maceration and especially during mixing operations, where the solids are well distributed within the liquid phase creating a relatively homogenous system, this description may be improved upon for periods of increased fermentation activity causing a compressed solids cap to form at the top of the fermenter. In this instance, the system could potentially be modelled as a two-interface (three-phase, solid-liquid-liquid) extraction system, whereby phenolic compounds pass from within the solid phase to the interstitial liquid within the grape solids and from here, diffuse from the interstitial liquid to the bulk of the liquid phase. In this case, the interstitial liquid holdup would present a further mass transfer step and potentially limit the overall extraction rate.

The addition of computational fluid dynamic (CFD) modelling to the current mathematical models developed here would aid in the simulation of spatial 3-dimensional fluid

and temperature profiles that naturally occur during red wine fermentation, and allow for the system to be easily separated into different sections where mass transfer rates would likely differ. Further investigation on the mass transfer of anthocyanins at increased temperatures such as those that may be observed in the cap of large commercial fermentations, which can be considerably hotter than the liquid depending on the management of the ferment, would also be a worthwhile study. This knowledge would remove the current necessity of extrapolating mass transfer parameters for anthocyanin extraction at temperature higher than those presented in Chapters 2-4. In addition, modelling the extraction of anthocyanins utilising other techniques (such as enzymatic pre-treatment) and the re-adsorption of anthocyanins onto skin cell walls as affected by temperature, ethanol concentration and other processing conditions during fermentative maceration, would be a significant advancement towards effective modelling of the entire process.

Such continued improvements to the model proposed in this thesis could lead to greater improvements in the timing and duration of mixing operations and other process variables associated with extraction, potentially leading to improved decision-making tools and economic benefits for wine producers.